ELECTROKINETIC SEPARATIONS IN FUSED SILICA CAPILLARIES

by

Henrik Torstholm Rasmussen

Dissertation submitted to the Faculty of the
Virginia Polytechnic Institute and State University
in partial fulfillment of the requirements for the degree of

DOCTOR OF PHILOSOPHY

in

CHEMISTRY

APPROVED:

H. M. McNair, Chairman

M. R. Anderson

H. W. Gibson

J. O. Glanville

L. T. Taylor

October, 1990

Blacksburg, Virginia

ELECTROKINETIC SEPARATIONS IN FUSED SILICA CAPILLARIES

by

Henrik Torstholm Rasmussen

Committee Chairman: Harold M. McNair
Chemistry

(ABSTRACT)

Methods of cooptimizing resolution and detection in Capillary Zone Electrophoresis (CZE) and Micellar Electrokinetic Chromatography (MEKC) are examined by deriving mathematical expressions which illustrate the relative importance of various experimental parameters.

For CZE, expressions are derived to show the interrelationship between efficiency, capillary dimensions and sample size. The interrelationship shows that resolution and detectability cannot be optimized simultaneously. Efficiency and, therefore, resolution are maximized when small sample sizes and capillaries with small internal diameters are employed. Detection is more favorable when large sample sizes and capillaries with large internal diameters are used.

To achieve a favorable compromise between resolution and detection, the influence of pH, electrolyte concentration and forced air convection are examined. A decrease in pH or an increase in electrolyte concentration reduces electroosmotic flow. This increases the relative velocity difference between two zones and, thereby, minimizes the efficiency required for unit resolution. Forced air convection minimizes the loss in

efficiency observed as capillaries with larger internal diameters are employed.

In MEKC, the importance of efficiency is minimized by employing a micellar phase which provides adequate selectivity for the separation. The separation of ASTM test mix LC-79-2 obtained in sodium dodecyl sulfate, sodium decyl sulfate, and sodium dodecyl sulfate modified with Brij 35 indicates that selectivity is governed by the nature of the surfactant's polar head group. Beyond selectivity optimization, resolution may be improved by increasing efficiency or decreasing electroosmotic flow. Of these approaches, increasing capillary length, to improve efficiency, is more time effective.

Using the guidelines described herein, several practical applications were developed. The methods are examined with respect to migration time and quantitative reproducibility.

ACKNOWLEDGEMENTS

I would like to express my sincere gratitude to the many people without whom this work would not have been possible.

Professor Harold M. McNair, served as my advisor, and provided direction throughout the course of this work. I have benefited from his guidance and friendship during the past four years, both as a scientist and as a person.

Professors M. R. Anderson, H. W. Gibson, J. O. Glanville, G. L. Long, and L. T. Taylor, helped in the preparation of this manuscript and provided valuable technical assistance. Bill Wilson, James Frazier, Lee Polite, George Reiner, Lisa Goebel, Nick Snow, Vince Remcho, Joe Hedrick, Leah Mulcahey, Greg Slack, Mike Berg, and Paul Engen all helped in ways too numerous to mention. Their insights and ideas were a prized asset during the course of this work.

I would also like to thank: Professor J. W. Jorgenson and his research group, at UNC, Chapel Hill, who provided a protocol for the instrumentation used in this work; Jim Hall of Virginia Tech, who assisted in constructing the apparatus; and Colgate-Palmolive, Ciba-Geigy, and Burroughs-Wellcome for providing samples.

Finally, I would like to thank my friends and family, who have provided timely distractions and support. Love and encouragement are valuable assets in any endeavor.

TABLE OF CONTENTS

PAGE

LIST OF FIGURES

PAGE

LIST OF TABLES

CHAPTER I

INTRODUCTION

1.1 High Performance Capillary Electrophoresis

While more than half of the scientific papers currently published in biochemistry depend on some use of electrophoresis [1], the methods have, to date, been largely ignored by chemists. This is perhaps attributable to the broad acceptance of chromatographic techniques in chemical and pharmaceutical applications, and to the perception that electrophoresis is slow, labor intensive and of limited quantitative capability [2]. For electrophoresis to gain widespread acceptance with chemists, advances must be made in instrumentation, and suitable applications, which cannot be readily performed by chromatography, must be developed.

The potential to achieve these goals is provided by the recent development of High Performance Capillary Electrophoresis (HPCE) [3-4]. HPCE typically uses short (50-100 cm) capillaries, with internal diameters of 50-100 μm, as separation compartments. The small diameter capillaries eliminate the convection problems encountered in conventional electrophoresis, and thereby allow for separations to be conducted in free solution, rather than on solid supports. Heat is more effectively dissipated from a small diameter capillary than from a solid support. As a consequence, large electric field strengths (30 kV/m) can be employed to provide fast analysis (less than 10 minutes) and very high separation efficiencies (1,000,000 theoretical plates). The use of capillaries

additionally allows for the use of real time detectors, analogous to those used in HPLC. As a result, HPCE can potentially be automated to the same level as modern chromatography.

In contrast to chromatography, in which separation is based on the distribution of solute between two dissimilar phases, electrophoretic separations are based on variabilities in the charge to size ratios of the sample components. The orthogonality of the techniques potentially provides a means of separating those samples not amenable to chromatography.

1.2 Research Objectives

As with chromatographic methods several modes of electrophoresis exist. The more important modes are moving boundary, zone (including molecular sieving), isoelectric focusing, and isotachophoresis [2]. This work focuses on free zone electrophoresis, the electrophoretic counterpart to elution chromatography, and on extending its general applicability to the analysis of neutral compounds via dynamic partitioning with charged micelles. The primary objectives are to study the influence of the experimental operating conditions on resolution, sensitivity and analysis time and, thereby, develop means for optimizing separations.

1.3 Capillary Zone Electrophoresis

Free zone electrophoresis in the capillary format has been termed Capillary Zone Electrophoresis (CZE) [5], although the technique is most frequently based on both electrophoresis and electroosmosis (or electroendosmosis).

CZE is best described by examining the apparatus used to effect the separations. As shown in Fig. 1, approximately 1 cm of polyimide coating is removed towards one end of a fused silica capillary, to produce an in-situ detector cell. The capillary is then placed in a detector, such that the cell is aligned in the detector's optical path and the capillary is filled with a buffer solution. To effect a separation, a small amount of sample is introduced into one end of the capillary, the capillary ends are immersed in reservoirs containing the operating buffer, and an electric field is applied between the two ends of the capillary.

In the electric field each ionic sample component experiences a force (F) of magnitude:

$$F = zeE \qquad (1)$$

where z is the charge of the species, e is the charge of an electron, and E is the electric field strength. The force accelerates each sample ion in the appropriate direction of the potential gradient. However, as an ion accelerates, it is retarded by viscous drag, and reaches only a limiting drift velocity (electrophoretic velocity), v_{el} [6].

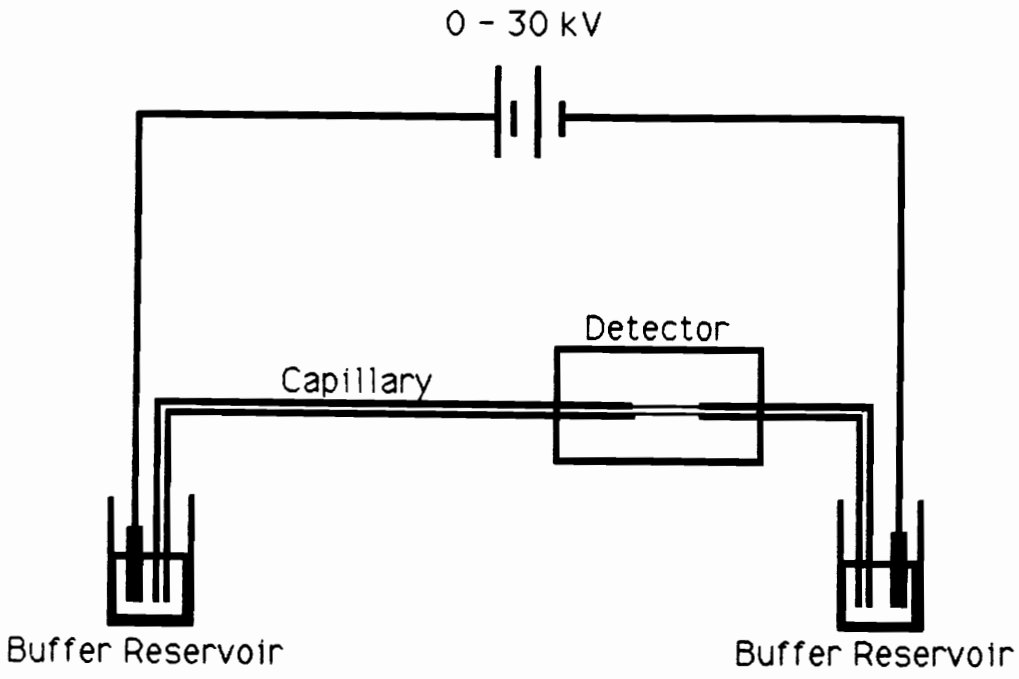

Figure 1. Schematic of the apparatus employed for Capillary Zone Electrophoresis.

The force provided by viscous drag is given by the Stokes relation as:

$$F = 6\pi\eta r_h v_{el} \qquad (2)$$

where η is the viscosity of the solvent medium and r_h is the hydrodynamic radius of the solvated ion. It follows from eqns. 1 and 2 that when the electrophoretic velocity is established:

$$6\pi\eta r_h v_{el} = zeE \qquad (3)$$

which may be rearranged to:

$$v_{el} = zeE/6\pi\eta r_h \qquad (4)$$

Cations, introduced into the positive end of the capillary, should accordingly be separated into discrete zones on the basis of their z/r_h ratios, and may be detected by the on-capillary detector placed towards the negative end of the electric field.

Under the outlined conditions, anionic sample components should migrate electrophoretically towards the positive end of the capillary, and a separation would not be predicted. Anions have, however, also been observed to move towards the cathode, as the result of a strong electroosmotic flow occurring inside the capillary [4].

Electroosmotic flow arises due to the surface charge of the fused silica capillary. As shown in Fig. 2, the fused silica surface is negatively charged

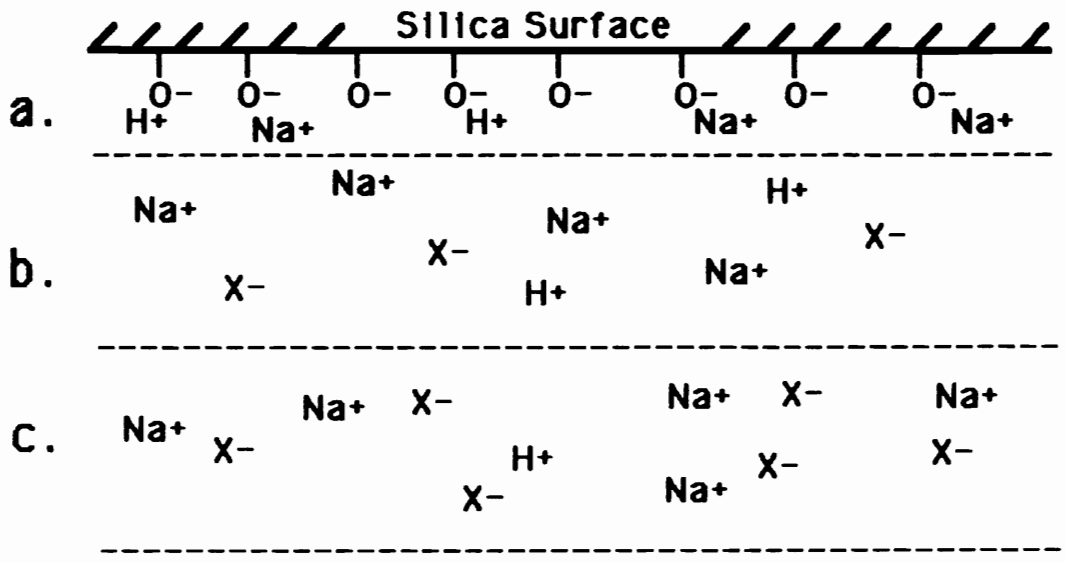

Figure 2. Illustration of the electrical double layer in a fused silica capillary. Region a) is the Stern plane, region b) is the diffuse layer and region c) is the bulk electrolyte.

at pH values above 2.0, due to the presence of ionized silanol groups [7]. To maintain electroneutrality, the surface charge is countered by a net excess of cations on the solution side of the capillary/buffer interface. These cations are arranged in an electrical double layer, consisting of a Stern plane, characterized by reversibly adsorbed counterions, and a diffuse layer, characterized by a net excess of counterions extending into solution as governed by a Boltzmann distribution [8]. When a potential is applied, the mobile cations in the double layer migrate, and due to momentum transfer, transport the bulk electrolyte towards the negative end of the electric field. In the presence of electroosmosis, the net velocity of a solute, v_{net}, becomes:

$$v_{net} = v_{el} + v_{eo} \qquad (5)$$

where v_{eo} is the electroosmotic flow velocity.

It is seen from eqn. 5 that as long as v_{eo} is either 1). in the same direction as the electrophoretic velocity or 2). of opposite direction and larger magnitude, than the electrophoretic velocity, the net direction of solute transport is towards the negative end of an electric field. It is, therefore, possible to analyze cations and anions in the same run. Neutral compounds are transported by electroosmosis, but are not separated since their z/r_h ratio is zero.

To illustrate the foregoing discussion and to demonstrate the potential of CZE as a separation technique, the separation of phenol, 4-hydroxy-3-methoxy-mandelic acid and 3,4-dihydroxymandelic acid is shown in Fig. 3.

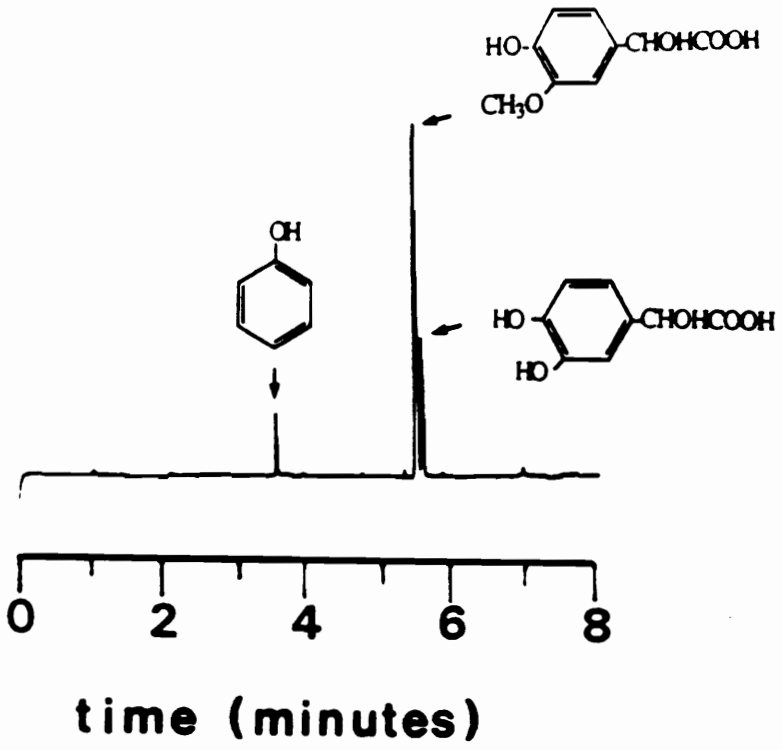

Figure 3. CZE separation of phenol, 4-hydroxy-3-methoxymandelic acid and 3,4-dihydroxymandelic acid. Conditions: Capillary: 100 µm (i. d.) x 55 cm (effective length). Buffer: 0.01 M Na_2HPO_4, pH 7.00. Electric field strength: 267 V cm^{-1}. Sample introduction: Siphoning at 3.8 cm for 7 s. Detection Wavelength: 230 nm.

At the buffer pH of 7.00, phenol (pKa = 10.0 at 25 °C) is essentially unionized and is transported exclusively by electroosmotic flow. The mandelic acids are partially ionized and migrate as anions. Their net migration velocity is, therefore, the vector sum of their electrophoretic velocity and the electroosmotic flow ($v_{el} + v_{eo}$). Since the magnitude of the electroosmotic flow is greater than the electrophoretic velocity ($v_{eo} > v_{el}$), the negative ions are transported towards the negative end of the capillary. The electrophoretic velocity of each mandelic acid is different and consequently the species are separated. In the electropherogram shown, the difference in the migration times of the two ions is approximately 4 seconds. Baseline resolution is, nevertheless, achieved due to a separation efficiency of 150,000 theoretical plates.

The high efficiency obtained in CZE is attributable to the nondispersive mass transfer provided by both electrophoresis and electroosmosis. An equation describing the electroosmotic flow velocity in a round capillary has been derived by Rice and Whitehead [9] as:

$$v_{eo}(r) = -\varepsilon\zeta E/4\pi\eta \cdot (1 - I_0(\kappa_d a)/I_0(\kappa_d r)) \qquad (6)$$

where ε is the dielectric constant of the buffer, ζ is the zeta potential at the capillary/buffer interface, κ_d is the reciprocal of the double layer thickness, a is the distance from the capillary axis, r is the capillary radius, and I_0 is a zero order Bessel function of the first kind. The double layer thickness is typically small with respect to capillary internal radius.

As a result, eqn. 6 may be rewritten as [9]:

$$v_{eo} = -\varepsilon\zeta E / 4\pi\eta \qquad (7)$$

Eqn. 7 indicates that there is no radial velocity dependence for electroosmotic flow. i.e., as shown in Fig. 4a, the flow profile provided by electroosmosis is flat, in contrast to the bullet shaped profile of laminar flow (Fig. 4b). As a consequence, no zone dispersion is incurred as a result of the sample's radial position in the capillary [10].

1.4. Micellar Electrokinetic Chromatography

To extend the high efficiency provided by electrokinetic transport to the analysis of neutral compounds, Terabe et al. [11-12] have introduced Micellar Electrokinetic Chromatography (MEKC). In MEKC, separation is achieved by adding a charged surfactant, at a concentration above the critical micelle concentration (CMC), to the separation buffer. Separation of neutral compounds is effected on the basis of variability in distribution coefficients of solutes between the aqueous and micellar phases, and on differences in the migration velocities of each phase.

As shown in Fig. 5, for MEKC employing an anionic surfactant, the aqueous phase assumes a linear velocity dictated by electroosmotic flow and the micellar pseudophase assumes a velocity which is the vector sum of the electroosmotic flow and the micelle's electrophoretic mobility. The electrophoretic mobility of the micellar phase causes it to move at a slower

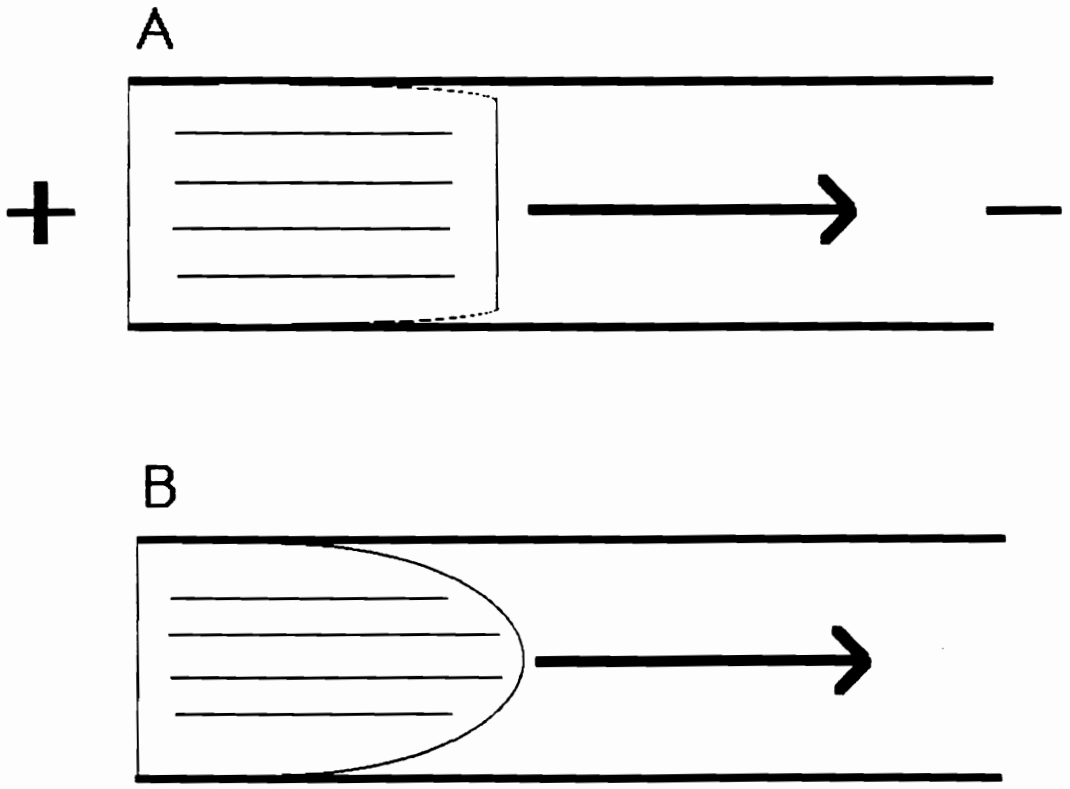

Figure 4. Profiles resulting from A) electroosmotic and B) laminar flow.

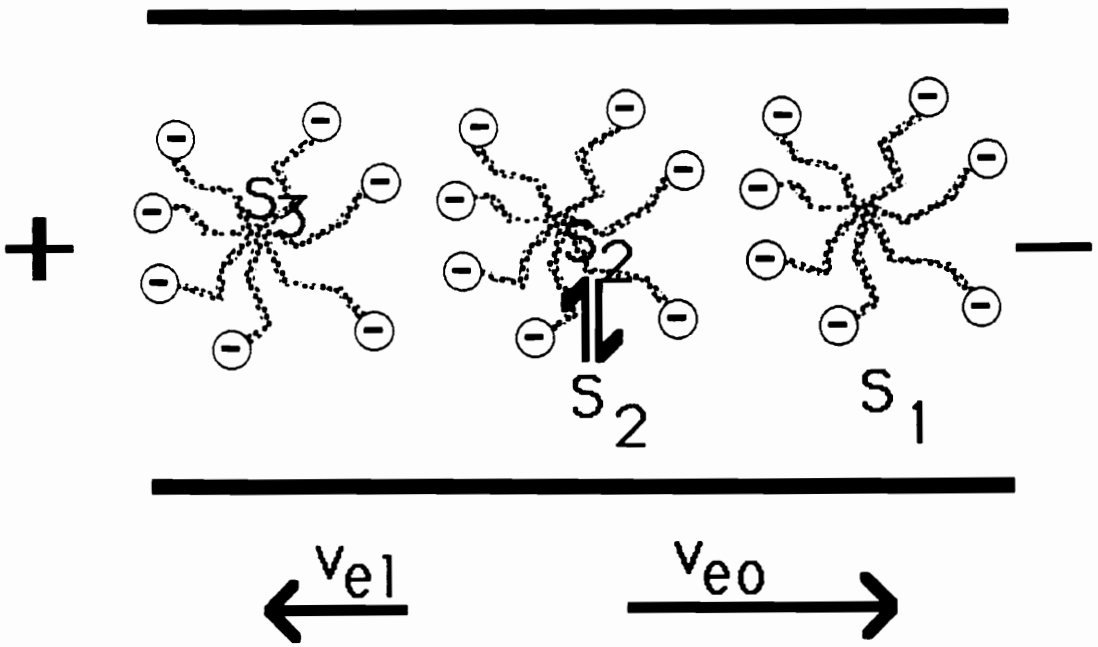

Figure 5. Schematic representation of MEKC. When an anionic micellar phase is added to the separation buffer, solutes with a larger affinity for the micellar phase (S_3) are selectively retarded due to the relative magnitudes of electrophoresis and electroosmosis.

linear velocity than the aqueous phase. Solutes with larger affinities for the micellar phase are, accordingly, selectively retarded.

MEKC may also be used for the analysis of ions [13-16]. When charged species are analyzed in micellar solution, the elution behavior is influenced by both electrophoresis and by the distribution coefficient between the two phases. The dual retention mechanism complicates theoretical predictions of elution behavior, but has been used to improve separation beyond that obtained in CZE [17].

CHAPTER II
HISTORICAL

2.1 Zone Electrophoresis

While the term electrophoresis was first used by Michaelis in 1909 to describe the migration of colloids in an electric field [18], the first form of electrophoresis that found application on a large scale was the moving boundary method introduced by Tiselius in 1937 [19].

In moving boundary electrophoresis, a long band of sample is placed in a U-tube between two buffer solutions. When an electrical field is applied, the most mobile cations and anions in the sample migrate rapidly towards the cathodic and anodic ends of the field, forming pure bands. Later, the next most mobile ions reach each electrode. However, since traces of the most mobile ions still exist in the bulk of the separation tube, due to the large initial sample band, the less mobile components are usually not completely resolved. The method is therefore generally limited to the measurement of electrophoretic mobilities, and is not widely used today [2].

Moving boundary electrophoresis does, however, provide the basis for free zone electrophoresis. The only difference between the two techniques is that in free zone electrophoresis, the sample is introduced as a narrow zone, instead of as a large band. Under this constraint, it is logical that the more mobile ions should not interfere with the separation of the additional sample components, and that separations analogous to Fig. 3 should be possible. The application of an electric field to an aqueous buffer, however,

results in Joule heating of the medium and since the heat is dissipated only at the boundaries of the separation chamber, a temperature, and therefore a density gradient is established [20]. This leads to the formation of convection currents which disrupt the separation by mixing the zones [2].

For zone electrophoresis to become a viable method of analysis, means of counteracting the convective currents had to developed. This goal was achieved in 1950 when Wieland and Fischer and others [1], performed zone electrophoresis on filter paper. Subsequently, starch, cellulose acetate, polyacrylamide and agarose [1] were introduced as supporting media, and remain popular today. However, several detrimental effects are associated with the use of such supports. While polyacrylamide, in particular, may provide a desirable orthogonal separation mechanism due to molecular sieving, adsorptive interaction may occur between sample components and the support. Additionally, nonuniformity in the pores of the support can result in eddy migration of the sample zones, and, consequently, zone broadening [2]. It is therefore generally desirable to find a means of performing zone electrophoresis in free solution.

Addressing this goal, Hjerten [20] used a rotating tube as the separation compartment to time-average the radial position of the liquid elements. His apparatus was complex, however, and did not gain widespread acceptance. As an additional possibility, zone electrophoresis has been performed in gravity-free environments on Skylab and the space shuttle [21]. In the gravity free environment, convection is eliminated since the radial distribution of liquid elements is not influenced by density.

A recent, more practical approach to the problem of convection has been to use separation compartments with narrow internal diameters. For isotachophoresis, Everaerts et al. [22] showed that when 0.4 mm internal diameter tubing is employed as the separation chamber, currents of up to 130 μAmps can be used without convective disturbance. As is the case when stabilizers are employed, the reduction in convection is the result of an increase in surface area to flow path cross sectional diameter. In agreement with Poiseuille's law, convection is suppressed due to frictional drag at the wall of the separation compartment.

2.2. Capillary Zone Electrophoresis

Free Zone Electrophoresis in the capillary format was first introduced in 1979 [3]. Using 200 μm Teflon capillaries and UV and conductimetric detection, Everaerts et al. were able to effect the separation of a sixteen component mixture in less than 10 minutes. Using 75 μm glass capillaries, Jorgenson and Lukacs [4] (1981) extended the initial work and named the technique Capillary Zone Electrophoresis (CZE) [5]. Since its introduction, CZE has grown exponentially. Advances in theory, instrumentation, and published applications are summarized below to convey the current status of CZE. MEKC is, for the purposes of this discussion, treated as a separate field although many of the developments in CZE are applicable to both methods.

2.2.1. Developments in the theory of CZE

The flat flow profile created by electroosmosis ideally limits band broadening in CZE to axial diffusion [4]. The spatial variance, σ_X^2, of a band after a time, t, may therefore, be written in accordance with the Einstein equation as:

$$\sigma_X^2 = 2D_a t \qquad (8)$$

where D_a is the diffusion coefficient of the solute in the aqueous buffer. Spatial variance may, in turn, be described in terms of theoretical plates, N, to give a measure of separation efficiency. By Giddings' [23] definition:

$$N = L^2/\sigma_X^2 \qquad (9)$$

where L is the distance of migration. Combination of eqns. 8 and 9 yields:

$$N = L^2/2D_a t \qquad (10)$$

Eqn. 10 may be related to the electrophoretic and electroosmotic velocities through the net migration velocity, v_{net}.

$$v_{net} = v_{eo} + v_{el} = L/t \qquad (11)$$

Accordingly N becomes:

$$N = (v_{eo} + v_{el})L/2D_a \qquad (12)$$

Expressing v_{eo} and v_{el}, through eqns. 7 and 4 as:

$$v_{eo} = -\varepsilon\zeta E/4\pi\eta = \mu_{eo}E \qquad (13)$$

and

$$v_{el} = zeE/6\pi\eta r_h = \mu_{el}E \qquad (14)$$

where μ_{el} and μ_{eo} are the coefficients of electrophoretic mobility and electroosmotic flow, respectively; and combining eqns. 12-14, allows N to be expressed as [4]:

$$N = (\mu_{eo} + \mu_{el})EL/2D_a \qquad (15)$$

Eqn. 15 suggests that maximum efficiency in CZE is achieved at high electric field strengths. However, as discussed, the application of an electric field to an aqueous buffer leads to Joule heating [20], and as a consequence a radial temperature gradient is established inside the capillary. Since a temperature increase is accompanied by a decrease in buffer viscosity [5], a direct result is that ions in the centre of the capillary migrate more rapidly than ions near the wall (eqns. 13 and 14). This variability in migration rates causes additional band broadening.

To add the dispersive influence of Joule heating to the band broadening arising from diffusion, N may be rewritten as:

$$N = L/H \qquad (16)$$

where H, the height equivalent of a theoretical plate, is the summation of independent sources of dispersion. i.e.

$$H_A = \Sigma H_i \qquad (17)$$

where H_A is the total height equivalent of a theoretical plate, and H_i is the independent contributions. Expressed in terms of H, eqn. 15 becomes:

$$H_D = 2D_a/(\mu_{eo} + \mu_{el})E \qquad (18)$$

where the subscript D denotes band broadening resulting from diffusion.

The height equivalent of a theoretical plate contribution stemming from Joule heating, H_T, has been addressed by several authors [24-26]. In simplest form it may be written may as:

$$H_T = 10^{-5}\phi^2E^5\lambda^2C^2d_c^6(\mu_{el} + \mu_{eo})/D_a\kappa^2 \qquad (19)$$

where ϕ is the fractional change in the net migration velocity per Kelvin; λ the molar conductivity of the medium; C the electrolyte concentration; d_c the capillary internal diameter; and κ the thermal conductivity of the

electrolyte solution. The additional parameters have been previously defined, and are summarized in the appendix.

It is seen from eqn. 19, that to obtain the high efficiency predicted at high electric field strengths (eqn. 15), the capillary internal diameter must be kept small. Unfortunately, this reduces the pathlength of the on-capillary cell, and in turn limits concentration detectability in optical detectors.

The latter limitation is magnified by the small sample volume which may be used in CZE. According to Sternberg [27], the height equivalent of a theoretical plate contribution from introduction of sample, H_S, is:

$$H_S = x^2/12L \qquad (20)$$

where x is the length of the sample plug introduced. Expressing the volume of sample, S, introduced into a cylindrical capillary as:

$$S = \pi(d_c/2)^2x \qquad (21)$$

allows for eqn. 20 to be expressed as:

$$H_S = 4S^2/3\pi^2d_c^4L \qquad (22)$$

Eqn. 22, implies that for H_S to provide a minimal contribution to the total height equivalent of a theoretical plate, the sample volume must be

minimized; especially when capillaries with small internal diameters, as prescribed by eqn. 19, are employed.

In light of the small sample size limitation, it seems logical to use optical detectors with large slit widths to maximize light throughput. However, "apparent" band broadening may be observed if the spatial resolution of the detection system is inadequate [28]. To avoid adverse detector effects, the slit width, W, of the detector should be much smaller than the width of the peak (4σ) being detected. For example, to maintain the plate height contribution stemming from the detector below 5% of the total height equivalent of a theoretical plate, the equation:

$$W < 0.05 \times 4\sigma \qquad (23)$$

must be satisfied.

In accordance with the above, it appears that CZE is not amenable to the high efficiency, trace analysis, of typical analytes. Instead, it may frequently be necessary to introduce fairly concentrated samples. Ionic solutes, introduced into the capillary as samples, however, alter the conductivity of the separation media in their vicinity. Since migration velocity is proportional to electric field strength, this can lead to uneven migration of such species [29]. Specifically, when the solute introduced decreases the local conductivity of the medium, tailing of the zones results; when the solute increases the local conductivity, peaks with appreciable leading edges are observed. In both instances efficiency is decreased [5, 30].

To minimize these solute effects, an operating buffer with with a large electrolyte concentration (approximately 100 times that of the sample) may be employed [30], but at the expense of an increase in H_T (eqn. 19). It follows that diffusion limited efficiency may not be feasible, even for relatively concentrated samples where the constraints of eqns. 22-23 are not prohibitive.

A final source of band broadening in CZE stems from adsorption of solute onto the wall of the fused silica capillary, which introduces mass transfer terms into the height equivalent of a theoretical plate equation. The contribution of mass tranfer terms, H_M, has been determined by Walbroehl [28] and Giddings [31-32] as:

$$H_M = H_L + H_C \qquad (24)$$

where H_L, is the contribution from mass transfer in the aqueous phase, and H_C the contribution from mass transfer at the capillary wall. H_L and H_C may be expressed as:

$$H_L = k'^2(\mu_{eo} + \mu_{el})E^2 d_c^2 / 16(1+k')^2 D_a \qquad (25)$$

and

$$H_C = 2k' t_d(\mu_{eo} + \mu_{el})E^2/(1+k')^2 \qquad (26)$$

where t_d is the mean adsorption time of an analyte on the capillary wall. The capacity factor, k', may be defined as the ratio of the time the solute

spends adsorbed to the capillary wall, t_c, to the time spent in the aqueous buffer, t_a.

$$k' = t_c/t_a \qquad (27)$$

Walbroehl [28] has demonstrated that even for a k' as low as 0.05 (which represents very little adsorption), the plate height is about 20 times greater than if there were no adsorption. Consequently, to obtain the high separation efficiencies predicted by eqn. 15, adsorption must be eliminated.

Adsorption is solute dependent and for most analytes is not a problem. However, some analytes, particularly proteins [5], adsorb strongly onto the surface of fused silica, necessitating surface modification. Such modification has been achieved by coating the capillary with Polyacrylamide [33], poly(ethylene glycol) [34], Dextran, and poly(vinyl alcohol) [35], or by deactivating the surface with a functional silane [35-36]. Alternatively, the surface has been changed dynamically by altering the pH of the buffer [37] (to reduce the surface charge), increasing buffer concentration [38] or by introducing a modifier into the buffer [39]. It should be noted, however, that surface modification changes the electroosmotic flow, and that none of the techniques described to date has completely eliminated adsorption of proteins.

Despite the dispersive effects outlined, efficiencies approaching 1,000,000 theoretical plates [37] have been reported for model proteins. This represents an improvement in efficiency of 1-2 orders of magnitude compared to GC and HPLC, and has provided a major impetus for the

development of CZE. It should be emphasized, however, that the purpose of a chemical separation is not merely to effect the efficient transport of sample components. The purpose is to resolve the components into discrete bands. Accordingly, it is the overall resolution, and not strictly the efficiency which should be optimized.

The resolution (R_s) obtained for a chemical separation which is based on the variability of solute velocities is, by Giddings' definition [23], given as:

$$R_s = \frac{N^{1/2}}{4} \quad \frac{\Delta V}{V_{avg}} \qquad (28)$$

where $\Delta v/v_{avg}$ is the relative velocity difference between two zones. In accordance with eqns. 11-13, resolution in CZE may be expressed as [4]:

$$R_s = \frac{N^{1/2}}{4} \quad \frac{\mu_{el.1} - \mu_{el.2}}{\mu_{el.avg} + \mu_{eo}} \qquad (29)$$

where the subscripts 1, 2 and avg denote the electrophoretic mobilities of two species, and their average electrophoretic mobility.

Optimization of CZE is, under the outlined efficiency and sensitivity criteria, contingent on optimizing eqn. 29. Means of achieving this are discussed in Chapter IV.

2.2.2. Instrumentation for CZE

To accompany the advances in the theory of CZE, rapid developments have been made in instrumentation. Despite the stringent criteria placed on detection in CZE, UV [40-42], fluorescence (including laser induced fluorescence) [43-47], conductivity [48-49], electrochemical [50-52], radioisotopic [53] and MS [54-56] detectors have been used sucessfully.

Using UV detection and typical analytes, concentration detection limits are typically to the order of $1 \times 10^{-5} - 3 \times 10^{-7}$ M [40-41]. For many analyses this is considered prohibitively high, and consequently numerous authors have discussed means for improvement. Jansson et al. [57], for example, have suggested that a longer pathlength, but equal heat dissipation may be possible in rectangular capillaries. Wilson et al. [58] have addressed the feasibility of dynamically coupling micro HPLC to CZE. In this arrangement, the HPLC column serves as a sample concentrator and effectively introduces a more concentrated sample onto the CZE capillary. As noted by Bushey and Jorgenson [59], dynamically coupled HPLC-CZE also provides an orthogonal degree of selectivity, and may therefore additionally be used to improve separation.

A more straightforward approach to improving sensitivity, however, has been to use more sensitive detection methods. Using laser induced fluorescence, Dovichi et al. [45] have reported concentration detection limits of 5×10^{-12} M for the fluorescein isothiocyanate derivative of aniline (3 times signal to noise). By virtue of the 1 nL sample volume, this corresponds to a mass detection limit of less than 6000 molecules.

It should be noted, however, that laser induced fluorescence is more selective than UV detection and therefore does not have the same general applicability. Furthermore, when solutes are derivatized they assume different electrophoretic behavior than their underivatized counterparts, and are, in some instances, not separated. Addressing this problem, Rose and Jorgenson [60] and Zare et al. [61] have developed post capillary reactors for CZE, which allow for species to migrate in their native state and subsequently be derivatized for fluorescence detection. Nevertheless, due to the limited number of suitable derivitization reagents, fluorescence detection remains fairly selective.

Analogous conclusions may be made about the selectivity of electrochemical and radioisotope detectors. In this light, conductivity and MS detection seem desirable due to their universal response. Using conductivity detection Zare et al [48] have reported detection limits of approximately 10^{-7} M (2 times signal to noise) for lithium; less conductive ions such as arginine were analyzed at the 4×10^{-5} M level using inverse conductivity detection. Although these detection limits are poor in comparison to HPLC, online detection provides a potential for automation not possible in conventional electrophoresis, where detection is typically performed post run by staining the supporting media. As a consequence improved reproducibility should be possible.

To automate CZE, autosamplers [62-65], fraction collectors [66-67] and capillary thermostats [64-65, 68] have been developed. The use of autosamplers has been noted to improve quantitative reproducibility;

thermostatting the capillary provides more reproducible buffer viscosities and, therefore, more reproducible migration times.

2.2.3. Applications of CZE

Using the outlined instrumentation, CZE has been shown to be applicable to the analyses of charged species ranging in size from Group I cations [48] to polystyrene nanospheres with diameters of up to 683 nm [69]. Specific applications have included the analysis of amino acids and peptides [4, 45, 70-71], proteins [34, 36-38, 72-73], polyamines [74], low molecular weight carboxylic acids [49], marine toxins [47], red blood cells [75] and pharmaceuticals [46, 56, 76].

It has also been demonstrated that CZE is not limited to strictly aqueous buffers. Wahlbroehl and Jorgenson [40] and Fujiwara and Honda [77], have shown that methanol and acetonitrile, in addition to improving solute solubility, improve the separation of positional isomers. Zare et al. [78-79] and Fanali et al. [80] have used CZE to effect the separation of enantiomers, by adding chiral complexes to the operating buffers. In analogy to MEKC, such separation is achieved because of secondary equilibria between the enantiomers and the complex which, due to electrophoresis and electroosmosis, migrate at different rates. Both of these latter applications are important, since they demonstrate that improving selectivity, i.e. increasing the relative velocity difference (eqn. 28), is possible in CZE.

2.3. Developments in MEKC

From the discussion presented in section 1.4, MEKC may be considered analogous to conventional chromatography, with the exception that the conventional stationary phase is replaced by a micellar phase which is itself mobile. As a result of the mobility of the secondary phase, modifications must be made to some of the conventional definitions of chromatographic parameters.

As noted by Terabe et al. [11], if the capacity factor of a given solute, k', is defined as:

$$k' = n_{mc}/n_{aq} \qquad (30)$$

where n_{mc} is the number of moles of solute in the micellar phase and n_{aq} is the number of moles of solute in the aqueous phase; k' of a neutral solute may for MEKC be expressed as :

$$k' = \frac{t_R - t_0}{t_0(1 - t_R/t_{mc})} \qquad (31)$$

where t_R is the retention time of an analyte, t_0 the retention time of a solute which distributes exclusively into the aqueous phase, and t_{mc} the retention time of a solute which distributes exclusively into the micellar

phase. It follows that the retention time of the solute may be expressed as:

$$t_R = \frac{(1 + k')t_0}{1 + (t_0/t_{mc})k'} \qquad (32)$$

and that the master resolution equation for MEKC becomes [12]:

$$R_s = \frac{N^{1/2}}{4}\left(\frac{\alpha - 1}{\alpha}\right)\left(\frac{k_2'}{1 + k_2'}\right)\left(\frac{1 - t_0/t_{mc}}{1 + (t_0/t_{mc})k_1'}\right) \qquad (33)$$

where k'_2 and k'_1 are the capacity factors of solutes 2 and 1, respectively, and α is the selectivity ($\alpha = k'_2/k'_1$).

Assuming a value of infinity for t_{mc} (i.e. a stationary secondary phase), eqns. 31-33 reduce to the forms used in conventional chromatography. It is therefore logical that, as for conventional chromatography, optimization of MEKC is contingent on optimizing each of the terms in the master resolution equation. However, as is evident from the last term in eqn. 33, the capacity factor dependent terms are more complicated in MEKC.

Assuming $k'_1 = k'_2$, resolution in MEKC may be expressed as a function of the capacity factor dependent terms as [12]:

$$f(k') = \left(\frac{k'}{1 + k'}\right)\left(\frac{1 - t_0/t_{mc}}{1 + (t_0/t_{mc})k'}\right) \qquad (34)$$

f(k') is plotted as a function of k' in Fig. 6. Curve (a). depicts a situation where t_0/t_{mc} is zero and corresponds to conventional chromatography. When

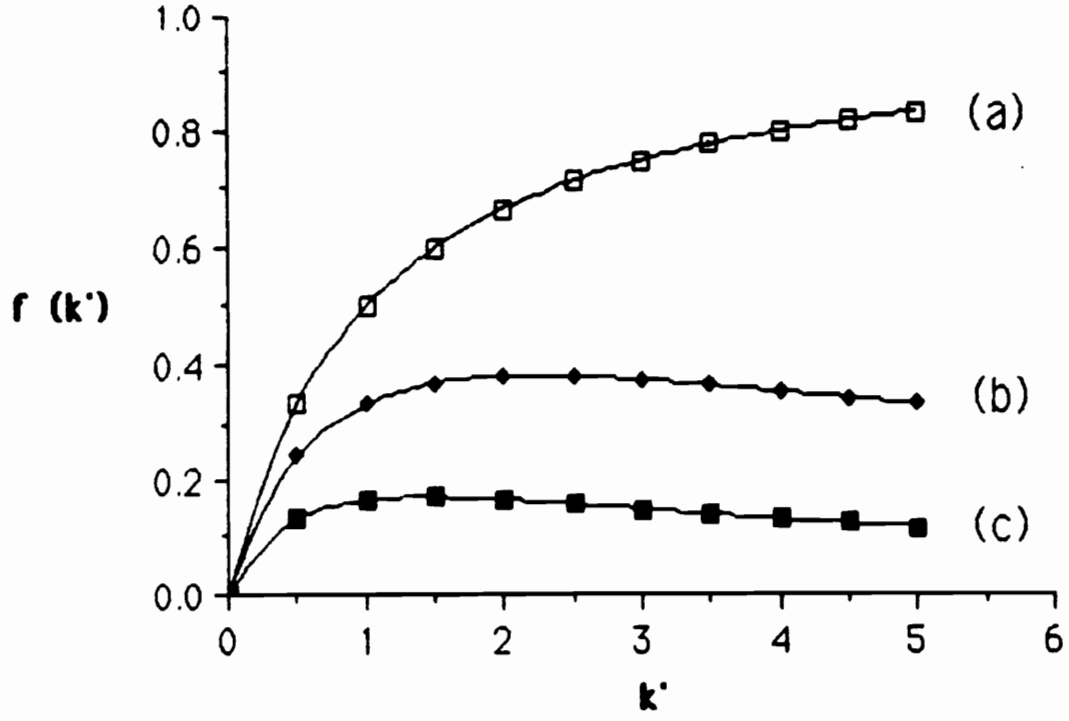

Figure 6. f(k') as a function of k' for t_0/t_{mc} ratios of: (a) 0 (b) 0.2 and (c) 0.5.

t_0/t_{mc} is increased (curves b and c), the maximum of f(k') is reduced and occurs at a lower k'. Accordingly, to optimize resolution in MEKC t_0/t_{mc}, as well as N, α, and k' must be optimized.

As shown in Fig. 6, maximizing resolution is contingent on minimizing t_0/t_{mc}. As implied in Fig. 5, this may be achieved by decreasing the magnitude of electroosmotic flow. As for CZE, electroosmotic flow may be decreased by reducing pH [81-82] or by using surface modified capillaries [83-85]. It is additionally notable from Fig. 6, however, that the capacity factor must also be optimized in accordance with t_0/t_{mc}, and that the optimum capacity factor does not occur at infinite retention unless $t_0/t_{mc} = 0$.

Fortunately k' is readily adjusted. Relating k' to the partition coefficient, K, as:

$$K = k'B \qquad (35)$$

where B is the ratio of the volume of aqueous phase to the volume of the micellar phase; it is seen that k' may be changed by simply changing the concentration of the surfactant comprising the micellar phase [12].

Optimization of selectivity, in turn, is contingent on choosing a micellar phase which provides different partition coefficients for the solutes to be separated. To date, most applications of MEKC have employed sodium dodecyl sulfate (SDS) as the micellar phase [86-91]. The use of sodium decyl sulfate, sodium tetradecyl sulfate, sodium dodecanesulfonate, cetyl, dodecyl and hexadecyl trimethylammonium salts, sodium n-dodecanoyl-L-

valinate, and sodium lauroylmethyl taurate have, however, also been briefly explored [12-15, 92-94]. Notably, selectivity appears to be governed primarily by the nature of the surfactant's polar head group. Addition of tetraalkyl ammonium salts [95], methanol [96-97], metal ions [98], sodium octyl sulfate alcohols [99], and Brij 35 [100] to SDS micelles has similarly been shown to alter selectivity.

From the foregoing, it is seen that three of the four parameters governing resolution are readily manipulated. However, numerous terms contribute to the total height equivalent of a theoretical plate in MEKC. It may therefore be necessary to, additionally, consider the effect on efficiency of optimizing each of these parameters. The specific causes of band broadening in MEKC have been addressed by several authors [101-103], and are in many respects similar to those outlined for CZE (eqns. 18-26). Slight modifications, and additional terms are, however, required due to the presence of a secondary phase.

According to Terabe et. al, [101] the total height equivalent of a theoretical plate, H_A, is, for MEKC, the sum of 6 primary contributions: longitudinal diffussion (H_D), micelle sorption-desorption kinetics (H_{mc}), intermicelle mass transfer (H_I), micelle polydispersity (H_P), Joule heating (H_T) and sample volume (H_S). I.e:

$$H_A = H_D + H_{mc} + H_I + H_P + H_T + H_S \qquad (36)$$

In contrast to eqn. 18, H_D must, for MEKC, be expressed in terms of solute diffusion coefficients in both the micellar and aqueous phases, and must

take into account the fractional time the solute spends in each phase. Accordingly, [101]:

$$H_D = \frac{2\,(D_a + k'\,D_{mc})}{1 + (t_0/t_{mc})k'} \quad \frac{1}{v_{eo}} \qquad (37)$$

where D_{mc} is the diffussion coefficient of the solute in the micellar phase.

H_{mc} and H_l, result from the statistical distributions created as molecules of a given species travel through the capillary. Specifically, H_{mc} describes the variability in the number of interactions the molecules have with the micellar phase, and H_l the variability in the time the molecules spend diffusing from micelle to micelle. Using Giddings' [32] nonequilibrium theory, Terabe et al. [101] have shown that for MEKC, H_{mc} may be expressed as:

$$H_{mc} = \frac{2\,(1 - t_0/t_{mc})^2\,k'}{[1 + (t_0/t_{mc})k'](1 + k')^2} \quad \frac{v_{eo}}{k_d} \qquad (38)$$

where k_d is solute desorption rate constant from the micellar phase. H_l, can derived from the random walk theory [32, 101] as:

$$H_l = \left(\frac{k'}{k' + 1}\right)^2 \frac{(1 - t_0/t_{mc})^2}{1 + (t_0/t_{mc})k'} \quad \frac{d^2\,v_{eo}}{4D_a} \qquad (39)$$

where d is the intermicelle distance. It is notable that for 0.05 M SDS, d is approximately 10 nm [101]. As a consequence, the variance stemming from

intermicelle mass transfer, is considerably less than for the comparable effect in HPLC.

H_P, the contribution stemming from micelle polydispersity, arises as as a consequence of the distribution in the number of surfactant molecules which form a given micelle (aggregation number). Terabe et al. [101] have derived this contribution to be:

$$H_P = \frac{\omega (1 - t_0/t_{mc})^2 k'}{1 + (t_0/t_{mc})k'} \frac{v_{eo}}{k_d} \qquad (40)$$

where ω is a constant, dependent on the average micelle diameter, the average aggregation number, the standard deviation of the average aggregation number and the thickness of the micelle's electrical double layer. For SDS, ω is approximately 0.26 [101].

H_T and H_S are considered here to be analogous to the expressions derived for CZE, although it must be noted that the presence of charged surfactants will increase the conductivity of the separation media and therefore, increase the degree of Joule heating. As a consequence, the surfactant concentration influences not only solute capacity factors (eqn. 35), but also separation efficiency. This effectively places a limit on the surfactant concentration which can be employed to achieve a given k'.

The elution range, t_0/t_{mc}, and k' are similarly seen to directly influence H_A through eqns. 36-40. The chemical nature of the micelle in turn determines k_d, and as a result selectivity must also be considered with

respect to efficiency. These considerations are examined further in Chapter IV, to provide additional insight into optimizing resolution in MEKC.

CHAPTER III

INSTRUMENTATION AND METHODS

3.1. Instrumentation

The instrumentation used for this work was constructed in-house from commercially available components. As shown in Fig. 7, a fused silica capillary (50 or 100 μm i. d. x 50-100 cm in length) was filled with a buffer solution and placed such that each end was immersed in a buffer reservoir (typically a 4 mL vial). To provide an electrical circuit, one reservoir was connected to a Spellman model RHR 30 high voltage power supply (Spellman, Plainview, NY) and the other was connected to ground. Electrical connections were made with 4 cm x 0.5 mm diameter platinum electrodes (Aldrich Chemical Co, Milwaukee, WI) and 30 kV electrical cable. To protect the operator, the live electrode was placed in an 18" x 18" x 18" plexiglass box equipped with an interlock. Opening the box automatically turned off the power supply in the event that the operator had neglected to do so manually. Detection and data handling were performed by an ISCO model CV4 Capillary Electrophoresis Absorbance detector (ISCO, Lincoln, NE) connected to a Hewlett-Packard model 3390 A Integrator (Hewlett-Packard, Avondale, PA).

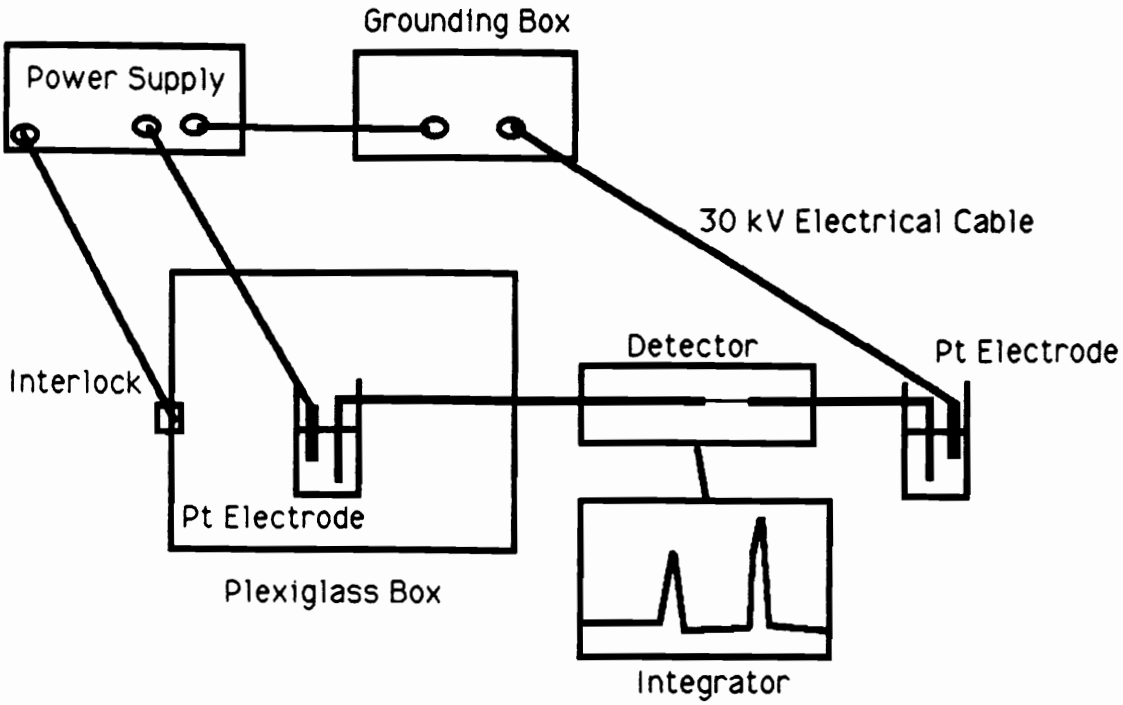

Figure 7. Schematic of the instrumentation used in this work.

3.2. Methods

The basis of operation, for the outlined instrumentation, was briefly discussed in section 1.3. A more detailed explanation of general operating procedures is given below. Details of the specific operating conditions employed for the experimental parts of this work are, for organizational purposes, presented in section 3.3.

3.2.1. Preparation of Capillaries

To prepare fused silica capillaries for use, approximately 1 cm of polyimide coating was burned off the capillary with a butane lighter to provide an on-capillary UV flow cell. The capillary was then inserted into the detector, and the detector's aperture adjusted to align the cell in the optical path. Following installation, the capillary was conditioned, using a modification of the procedure suggested by Lauer and McManigill [37]. Specifically, the capillary was washed successively with 1 M NaOH (15 minutes), 0.1 M NaOH (15 minutes) and deionized water (15 minutes). On the basis of ion exchange, such conditioning should remove any adsorbed ions on the fused silica surface and provide improved capillary to capillary reproducibility.

After conditioning, the capillary was filled with the appropriate buffer. To minimize the formation of air bubbles during separations and to insure equilibration, buffers were degassed in a sonicator and passed through the capillary for 15 minutes. Washing and filling the capillary was achieved by

immersing one end of the capillary into the appropriate solution, and applying a gentle vacuum to the other end.

It was generally not necessary to clean the capillary during a series of runs. However, cleaning, was performed when a new buffer was employed, or when the capillary was stored overnight. The cleaning procedure consisted of washing with 0.1 N NaOH (15 minutes) and with deionized water (15 minutes). Using this procedure, capillary lifetimes were generally in excess of 100 runs.

3.2.3. Methods of Operation

Once filled with the appropriate buffer, the capillaries were ready for use. As discussed, operation consists of introducing sample into the appropriate end of the capillary, immersing the capillary between the two buffer reservoirs, and applying an electric field.

Several methods of sample introduction for CZE have been reported and are available on commercial systems. These include the use of sample valves [104], split-flow introduction methods [64, 105], electrokinetic sampling [4-5, 63, 106] and siphoning/hydrodynamic sampling [62-63, 65, 107]. Due to ease of operation the latter two methods were employed throughout this work.

Electrokinetic sampling was achieved by replacing the appropriate buffer reservoir with a vial containing the sample and applying an electric field, E,

for a time, t_s. The electric field strength is defined here as:

$$E = V/L_T \qquad (41)$$

where V is the applied voltage and L_T, the total capillary length. L as used in previous equations is the effective distance of migration and does not take into account the length of capillary extending from the detector to the buffer reservoir.

The sample volume, S, introduced by electrokinetic sampling is given as:

$$S = (\mu_{el} + \mu_{eo})Et_s\pi r^2 \qquad (42)$$

Eqn. 42, dictates which end of the capillary must be used for sampling. The term, $(\mu_{el} + \mu_{eo})$, must be such that sample components migrate onto the capillary towards the detector. Due to the relative magnitude of μ_{eo} and μ_{el}, and since electroosmotic flow is towards the cathode, sample is typically introduced at the anodic (positive voltage) end of the capillary. Eqn. 42 further shows that a suitable injection volume may be introduced by choosing an appropriate sampling time and applied field strength. However, due to the dependence of sample volume on electrophoretic mobility, S will differ for each sample component.

To prevent sample volume discrimination, siphoning was employed as the primary method of sample introduction. Siphoning is based on the flow induced when the ends of the capillary are subjected to different pressures. Differential pressure may be created by applying a vacuum or head pressure

to one end of the capillary, or more simply by varying the relative heights of two reservoirs. To effect such sampling, a block, as shown in Fig. 8 was constructed. Sample introduction was achieved by replacing the appropriate buffer reservoir with a vial containing the sample, and raising the sample onto the block for a specified time.

Assuming that hydrodynamic flow can be described by the Poiseuille equation for flow in a circular tube, the flow velocity, v_{sf}, resulting from a height difference, Δh, is given as [63]:

$$v_{sf} = \rho g r^2 \Delta h / 8\eta L_T \qquad (43)$$

where ρ is the density of the sample solution and g the gravitational acceleration. Eqn. 43, may be expressed in terms of the volume, S, introduced after siphoning for a time, t_s, as:

$$S = \rho g \pi r^4 \Delta h t_s / 8\eta L_T \qquad (44)$$

The choice of suitable Δh and t_s values will be discussed in section 4.2. It is noted here that siphoning must not be superimposed on electrokinetic transport during an analysis. It was therefore important to ensure that both buffer reservoirs were filled to the same level during all analyses.

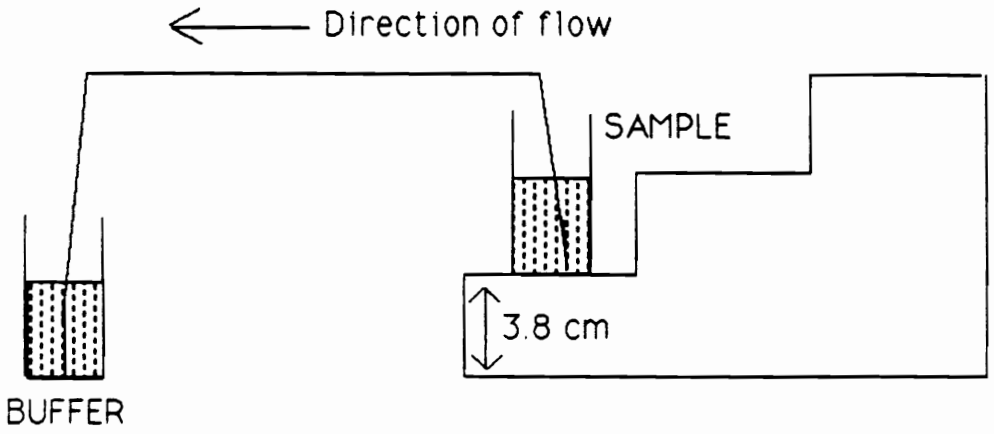

Figure 8. Illustration of hydrodynamic sample introduction (siphoning).

3.3. Experimental Conditions Employed

3.3.1. Conditions for the Evaluation of System Performance

Initial experiments were directed towards evaluating system performance by examining reproducibility. Long term performance was evaluated from the reproducibility in the analysis times of caffeine, run in triplicate, on four successive days. Short term performance, with respect to retention time and quantitation, was evaluated from five replicate analyses of caffeine (0.4 mg/mL) and theophylline (0.2 mg/mL). Both sets of analyses were performed in a 100 μm i. d. x 100 cm (total length, L_T) fused silica capillary (Chrompack, Raritan, NJ) with a migration distance (L) of 75 cm. The sample solvent and operating buffer was 0.01 M Na_2HPO_4, adjusted to a pH of 7.00; the applied voltage was +30 kV. Samples were introduced electrokinetically at +3 kV for 5 seconds and detected at a wavelength of 220 nm.

To obtain comparable quantitative data, using siphoning as the method of sample introduction, replicate determinations were performed on samples of 4-hydroxy-3-methoxymandelic acid and phenol. Analyses were performed in a 100 μm x 75 cm capillary (Polymicro, Phoenix, AZ) with a migration length of 50 cm, using 0.01 M Na_2HPO_4, pH 7.00. Samples were introduced by siphoning for 10 seconds at an elevation of 3.8 cm, run at 20 kV, and monitored at 254 nm.

3.3.2. Conditions for the Determination of Suitable Sampling Procedures

To determine a suitable introduction time for siphoning at an elevation of 3.8 cm, a solution of 4-hydroxy-3-methoxymandelic acid, dissolved in 0.01 M Na_2HPO_4 (pH 7.00), was introduced into a 100 µm x 68 cm capillary (Polymicro) with an effective migration distance of 48 cm. Measurement of the time required for the sample to reach the detector (breakthrough time) allows for calculation of the volume of sample introduced per unit time, and, therefore, the contribution to the height equivalent of a theoretical plate resulting from different introduction times.

To determine the influence of sample concentration on efficiency, serial dilutions were made of a 2.0 mg/mL stock solution of 3,4-dihydroxy-mandelic acid. The resulting solutions were analysed using: a 100 µm x 75 cm capillary (Polymicro), with a migration distance of 50 cm; a 0.01 M Na_2HPO_4 (pH 7.00) buffer; and an operating voltage of +20 kV. Sample introduction was by siphoning at 3.8 cm for 7 seconds and detection was performed at 230 nm.

Efficiency was calculated using the equation [27]:

$$N = 2\pi(t_R h/A)^2 \qquad (45)$$

where h is the peak height and A the peak area. Migration times and area to height ratios were provided by the integrator.

3.3.3 Conditions Employed for Determining the Influence of pH on the Coefficient of Electroosmotic Flow

Equation 29 shows electroosmotic flow to be an important parameter for optimizing the relative velocity difference between two zones, and therefore, in optimizing resolution. It is desirable to adjust electroosmotic flow so that it is of equal magnitude, but of opposite direction to the electrophoretic migration of charged sample components. To study the influence of pH on the coefficient of electroosmotic flow, the migration time of phenol was determined in 0.01 M Na_2HPO_4, adjusted to pH 7.00, 5.96, 5.11, and 3.00. All analyses were performed in a 100 µm x 97 cm capillary (Chrompack) with an effective length of 75 cm, using an operating voltage of +30 kV. Sample introduction was achieved electrokinetically at +3 kV for 7 seconds and detection was effected at 254 nm.

Phenol (pKa = 10.0 at 25 °C) is essentially unionized at each pH employed and μ_{eo} may, therefore, be determined directly from migration time as:

$$\mu_{eo} = LL_T/t_{R(phenol)}V \qquad (46)$$

3.3.4. Conditions for Determining the Influence of Buffer Concentration, Capillary Internal Diameter and Forced Convection on Resolution in CZE

To examine the influence of buffer concentration, capillary internal diameter, and electric field strength on resolution, analyses of phenol and

sodium toluenesulfonate were conducted in 0.01, 0.02 and 0.05 M Na_2HPO_4, pH 7.00, using 1 m x 100 µm i. d. (Chrompack, Raritan, NJ) and 1 m x 50 µm i. d. (Polymicro, Phoenix, AZ) fused silica capillaries, and voltages ranging from +10 to +25 kV. The variance stemming from sample introduction was minimized by preparing the capillaries with effective migration lengths of 80 cm, and introducing the samples electrokinetically at +3kV for 5 seconds. All separations were monitored at 254 nm.

To determine resolution under each set of operating conditions, the relative velocity difference between the two zones and separation efficiency were determined from each analysis. The individual terms in the relative velocity difference expression $(\mu_{el.1} - \mu_{el.2})/(\mu_{el.avg} + \mu_{eo})$, were calculated from the migration times of the test solutes. Specifically, μ_{eo} was determined using eqn. 46; $\mu_{el.1}$ was taken to be the electrophoretic mobility of phenol, and was assumed to be zero.

$\mu_{el.2}$ was determined from the migration time of sodium toluenesulfonate. The total linear velocity (v_{net}) of sodium toluenesulfonate is governed by both electrophoresis and electroosmosis and its migration time, t_R, may, therefore, be written as:

$$t_R = L/v_{net} = L/(-\mu_{el.2} + \mu_{eo})E \qquad (47)$$

Rearrangement allows for $\mu_{el.2}$ to be expressed in terms of experimentally measurable parameters as:

$$\mu_{el.2} = \mu_{eo} - L/t_R E \qquad (48)$$

$\mu_{el,avg}$ is the average electrophoretic mobility of phenol and sodium toluenesulfonate, or in this case, one half of $\mu_{el,2}$. Separation efficiency was determined using eqn. 45.

To evaluate the effect of forced air convection on the coefficient of electroosmotic flow, and on separation efficiency, the capillary was inserted into a 50 cm x 8 mm i. d. glass tube, and air was introduced through a sidearm in the tube at 3.5 L/min. (Fig. 9).

3.3.5. Conditions for the Evaluation of Alkyl Sulfates as Micellar Phases

To evaluate the suitability of several alkyl sulfates for MEKC, 0.025, 0.05 and 0.075 M solutions of sodium octyl, decyl, dodecyl and tetradecyl sulfate (Aldrich Chemical Co., Milwaukee, WI) were prepared in 0.01 M Na_2HPO_4, pH 7.00. ASTM test mix LC-79-2 [108-109], dissolved in each of the surfactant solutions under investigation, was used as the sample. This test mix contains 1.5 mg/mL benzyl alcohol, 0.02 mg/mL benzaldehyde, 0.025 mg/mL acetophenone, 1.04 mg/mL benzene, 0.4 mg/mL methyl benzoate, and 0.054 mg/mL dimethyl terephthalate. To calculate thermodynamic parameters, 1% (v/v) methanol and a small amount of Sudan III were added to the conventional test mix, to mark, respectively, the elution times of completely unretained and completely retained solutes (i.e. t_0 and t_{mc}) [12]. Analyses were performed, at ambient temperature, in an 80 cm x 100 µm i. d. fused silica capillary (Polymicro, Phoenix, AZ) with an effective length of 50 cm. Separations were performed at +15 kV and monitored at 254 nm.

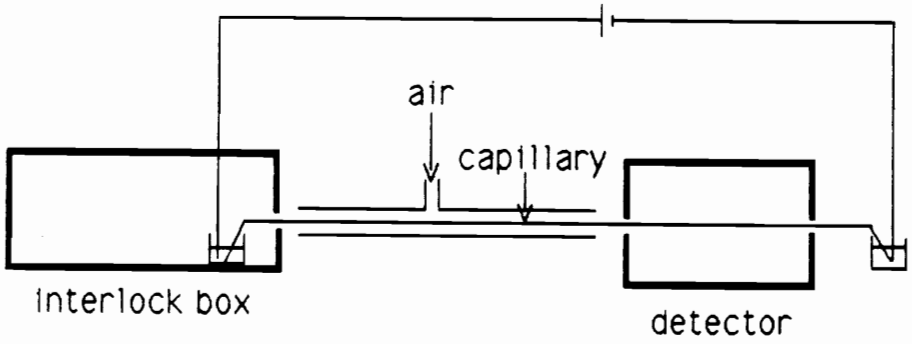

Figure 9. Schematic of the apparatus employed for CZE with forced air convection.

Sample introduction was by siphoning for 10 seconds at an elevation of 3.8 cm.

3.3.6. Conditions for the Evaluation of Brij 35 ® as a Micellar Phase Modifier

ASTM test mix LC-79-2 was additionally analyzed using 0.025 M SDS, modified with 0.01, 0.03 and 0.05 M Brij 35 (registered trademark of ICI Americas, Wilmington, DE). The experimental conditions, using the modified micellar phases, were as described above except for the capillary and applied voltage. Analyses, using the modified micellar phase, were conducted at +20 kV, in a 70 cm x 100 µm fused silica capillary (Polymicro) with an effective length of 48 cm.

3.3.7. Conditions for Studying the Influence of pH on Elution Behavior in MEKC

The influence of buffer pH on the MEKC separation of methyl, ethyl, propyl and butyl paraben (Aldrich, Milwaukee, WI) was investigated using 0.01 M Na_2HPO_4/0.05 M SDS, pH 6.75 and pH 3.37. Samples containing 0.8 mg/mL of each component were introduced into the appropriate end of a 100 cm x 100 µm i. d. fused silica capillary (Chrompack, Raritan, NJ), and analyzed using an applied voltage of 25 kV and a detection wavelength of 254 nm. To provide a direct comparison of solute migration times, regardless of which end of the capillary was used for sampling, detection was effected 50 cm from either end of the capillary. Samples were introduced

electrokinetically, at voltages and voltage durations required to provide reasonable peak heights. Peak identities were confirmed by spiking.

3.3.8. Conditions Employed for Practical Applications.

Several practical applications of CZE and MEKC, including analyses of pharmaceuticals (Burroughs-Wellcome, Research Triangle Park, NC), surfactant hydrotopes (Colgate-Palmolive, Piscaway, NJ), and bipyridinium salts, were developed during the course of this work. The choice of suitable conditions are discussed in section 4.4, to examine experimental considerations necessary for developing methods.

CHAPTER IV

RESULTS AND DISCUSSION

4.1. Evaluation of System Performance

To evaluate the reproducibility of the outlined apparatus and the general operating conditions, five replicate analyses of a mixture of caffeine and theophylline (Fig. 10) were performed using electrokinetic migration as the method of sample introduction. As shown in Table I, migration time reproducibility was less than 0.5 % Relative Standard Deviation (RSD). Quantitative reproducibility, as measured from the area counts exceeded 20 % RSD, indicating that the sampling technique was not reproducible. However, if a ratio of the peak areas of each analyte is calculated, to simulate employment of an internal standard, reproducibility was drastically improved (2.7 % RSD).

For comparison, the quantitative reproducibility of siphoning as a means of sample introduction was evaluated using 3,4-dihydroxymandelic acid as the analyte. For three sets of five replicate determinations, with each set using different analyte concentrations, the area count reproducibilities were 5.7, 9.4 and 8.0 % RSD. Using phenol as an internal standard, reproducibilities were improved to 1.4, 3.7 and 2.6 % RSD, respectively.

Day to day migration time reproducibility, as measured from the migration times of caffeine, was also evaluated (Table II). Analysis of variance (ANOVA) and Least Significant Difference (LSD) tests at the 95% confidence level showed all data sets to be statistically different, although

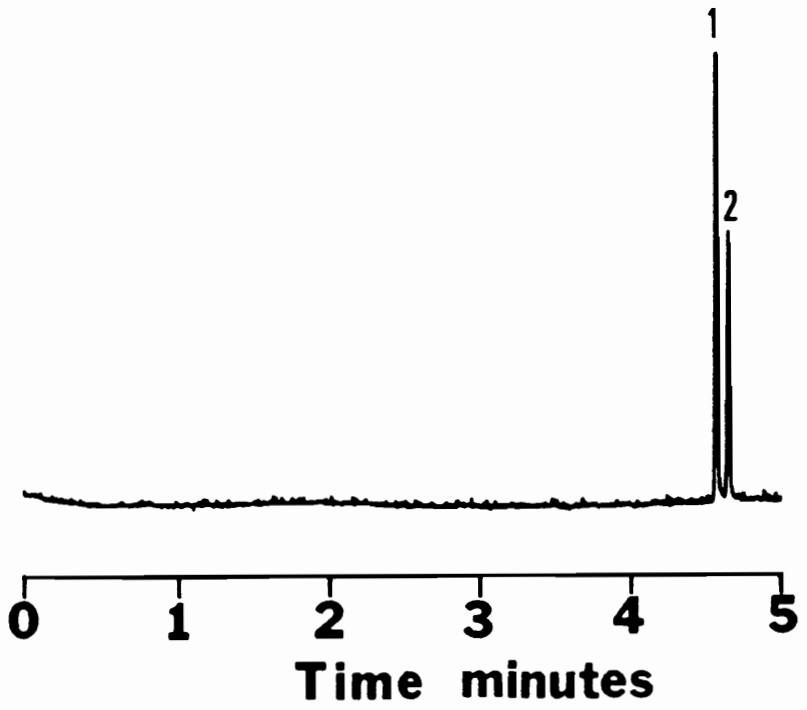

Figure 10. Separation of caffeine and theophylline.
Conditions: 100 µm x 100 cm capillary (L = 75 cm); 0.01 M Na_2HPO_4, pH 7.00, buffer; + 30 kV applied voltage. 3 kV/ 5s. electrokinetic injection; detection wavelength = 220 nm. Order of elution: 1. caffeine 2. theophylline.

Table I. Short term migration time and quantitative reproducibility in CZE*.

	Caffeine		Theophylline		Area Caffeine/
Run	tR (min)	Area (x105)	tR (min)	Area (x105)	Area Theophylline
1	5.66	385	5.74	170	2.27
2	5.61	445	5.69	198	2.24
3	5.60	338	5.68	155	2.18
4	5.61	263	5.69	112	2.35
5	5.64	262	5.71	114	2.29
avg.	5.63	339	5.70	150	2.27
s	0.02	79	0.02	37	0.06
%rsd	0.45	23.3	0.42	24.7	2.73

* Electromigration: +3kV/5 s.

Table II. Day to day reproducibility in the migration times of caffeine.

	t_R Caffeine (min.)			
Day	run 1	run 2	run 3	average
A	5.98	5.95	5.92	5.95
B	5.64	5.60	5.65	5.63
C	5.36	5.33	5.31	5.33
D	4.61	4.63	4.56	4.60

excellent run to run reproducibility was maintained. The day to day variability is attributed to changes in ambient temperature.

The above results are in good agreement with results reported elsewhere for manual injections. Jorgenson and Rose [63] obtained 13.4 % RSD for electrokinetic introduction, and 11.8% RSD for siphoning. Zare et al. [49] have reported peak area reproducibilities of 6.1-8.3 % RSD for siphoning; 2.3-4.6 % RSD when an internal standard was employed. Run to run migration time reproducibility, as reported by Zare et al. [49], was to the order of 0.9-1.4 % RSD. To minimize the variability in sampling time stemming from manual introduction, Jorgenson and Rose [63] have automated electrokinetic introduction by bringing the sampling time under computer control. As a result, peak area reproducibilities were reduced to 4.1% RSD. The use of a stepping motor to effect siphoning has similarly been shown to reduce peak area reproducibilities to 2.9 [63] and 0.92-2.3 [62] % RSD. Using a temperature controlled system, Tehrani et al. [64] have reported day to day migration time reproducibilities of 1.2 - 1.9% RSD. In contrast, the RSD of all the migration times shown in Table 4.2 is 9.6 %.

It is thus seen that a potential for improved reproducibility exists through automation of the sampling process and through more stringent temperature control. The analytical capabilities of the system used for this work are, however, superior to those of conventional electrophoresis, and were considered adequate.

4.2 Optimization of Resolution in CZE

The parameters governing resolution in CZE were addressed in section 2.2.1. As noted, optimization of resolution is contingent on optimization of both separation efficiency and the relative velocity difference between two zones. These terms show some interdependence, and are complicated by detectability considerations. Development of an approach to CZE is therefore, necessarily general, rather than universal.

This work focuses on developing considerations for a general approach. To achieve this goal, methods of maximizing efficiency and the relative velocity difference are first examined independently. Means of cooptimization, taking into account detection criteria, are then evaluated.

4.2.1 Optimization of Sample Size

Efficiency may be expressed through the height equivalent of a theoretical plate as the summation of independent terms (section 2.2.1). As noted, the contribution to the total height equivalent of a theoretical plate, stemming from sample volume and sample concentration, is contingent on the required detectability. If this constraint is eliminated, however, these contributions may be optimized independently from the relative velocity difference. Experimental means of controlling sample volume and sample concentration effects, therefore, serve as good starting points for optimizing resolution.

The volume of sample introduced as a function of sampling time (S/t_s) may, for siphoning, be calculated from breakthrough curves (section 3.3.2)

as:

$$S/t_s = \pi d_c^2 L/4t_b \qquad (49)$$

where t_b, the breakthrough time, is the time taken for sample to flow hydrodynamically from the point of sample introduction to the detector. The contribution to the total height equivalent of a theoretical plate stemming from sample volume, H_S, has been written as:

$$H_s = 4S^2/3\pi^2 d_c^4 L \qquad (22)$$

Combination eqns. 49 and 22 allows for t_s to be expressed as:

$$t_s = 3.46 H_s^{1/2} t_b/L^{1/2} \qquad (50)$$

Assuming that H_S should be less than a fraction, y, of the of the total height equivalent of a theoretical plate, H_A, eqn. 50 may be rewritten as:

$$t_s < 3.46 H_A^{1/2} y^{1/2} t_b/L^{1/2} \qquad (51)$$

If H_A, is expressed through eqn. 16 as:

$$H_A = L/N \qquad (52)$$

eqn. 51 may be reexpressed as:

$$t_s < 3.46y^{1/2}t_b/N^{1/2} \qquad (53)$$

which allows for calculation of a suitable t_s.

Using a 100 μm x 68 cm capillary with an effective migration distance of 48 cm, 0.01 M Na_2HPO_4 (pH 7.00) as the operating buffer, and a siphoning elevation of 3.8 cm, t_b was determined to be 74.9 +/- 0.3 minutes (n = 3). Using this value of t_b, limiting y to 0.1, and assuming that N for an infinitely small sample volume is 500,000 theoretical plates, eqn. 53 suggests that the sampling time should not exceed 7 seconds. Calculating S as:

$$S = t_s\pi d_C^2 L/4t_b \qquad (54)$$

this effectively limits the sample volume to 6 nL.

For a more general solution to the limiting sampling time and sample volume, eqn. 44 may be written as:

$$S/t_s = \rho g\pi d_c^4 \Delta h/128\eta L_T \qquad (55)$$

and combined with eqn. 49, to yield (on rearrangement):

$$t_b = 32L\eta L_T/\rho g d_c^2 \Delta h \qquad (56)$$

Eqn. 56 may be used to calculate values of t_b, under different operating conditions by ratioing the value of each parameter with those employed to determine t_b experimentally. If for example L is doubled, and the remaining parameters kept constant, t_b is doubled, allowing for twice the sampling time (eqn. 53). Ratioing of each parameter, and judicious choice of numerical values for N and y was used throughout this work to determine suitable sampling times for siphoning. A priori determinations of suitable values for N were approximated from eqn. 15. Specifically, efficiencies were calculated at low electric field strengths and the diffusion limited efficiency expected at the higher employed electric field strength obtained by linear extrapolation.

For electrokinetic sampling, the volume of sample introduced as a function of sampling time (S/t_s) is given as:

$$S/t_s = \pi d_c^2(\mu_{eo} + \mu_{el})V_s/4L_T \qquad (57)$$

where V_s is the sampling voltage. Eqn. 57 may be combined with eqn. 22, to yield:

$$H_s = (\mu_{eo} + \mu_{el})^2V_s^2t_s^2/12L_T^2L \qquad (58)$$

Under the approximation that μ_{eo} and μ_{el} are unaffected by electric field strength (the limitations of this approximation are shown in section 4.2.4),

$(\mu_{eo} + \mu_{el})$ may be calculated from the migration time of a solute as:

$$(\mu_{eo} + \mu_{el}) = LL_T/t_R V_0 \qquad (59)$$

where V_0 is the voltage used to effect the separation. Eqns. 58 and 59 may be combined to yield:

$$H_s = LV_s^2 t_s^2 / 12 V_0^2 t_R^2 \qquad (60)$$

which, on rearrangement, allows for t_s to be expressed as:

$$t_s = 3.46 H_S^{1/2} V_0 t_R / L^{1/2} V_s \qquad (61)$$

Invoking again that H_S should be less than a fraction, y, of H_A, and expressing H_A in terms of N, eqn. 61 becomes:

$$t_s < 3.46 y^{1/2} V_0 t_R / N^{1/2} V_s \qquad (62)$$

The migration time, t_R, in eqn. 62, may be obtained experimentally by analyzing a sample at an operating voltage of V_0. For a multicomponent sample the component with the smallest migration time becomes the governing solute. As for siphoning, a judicious choice of numerical values for N and y was used throughout this work to determine suitable sampling times and sampling voltages.

The influence of solute concentration was also explored in order to establish additional guidelines for the sampling procedure. The influence of 3,4-dihydroxymandelic acid (MW = 184.15) concentration on peak shape is shown in Fig. 11. At the higher solute concentrations the peaks show appreciable leading edges which result in reduced resolution. To determine the concentration required for maximum efficiency, resolution as a function of N is plotted against the $\log_{10}$ of concentration in Fig. 12. As shown, a solute concentration of less than 0.1 mM is required for maximum efficiency. This corresponds to a solute to buffer concentration ratio of less than 1:100. The latter concentration ratio is solute dependent, but is illustrative of the large influence solute concentration has on separation efficiency, and is good agreement with results reported previously by Lukacs and Jorgenson [30]. Invoking the 6 nL sample volume limit prescribed for 100 mm i. d. capillaries under typical operating conditions, the 0.1 mM concentration limit dictates that the total amount of sample for CZE should be less than approximately 6×10^{-13} moles.

The limits imposed by both the sample volume and the sample concentration were adhered to in subsequent theoretical studies, where it was of interest to examine the influence of the additional sources of band broadening independently. In practical applications, sample volume and sample concentration were limited only to conditions whereby sufficient resolution was obtained.

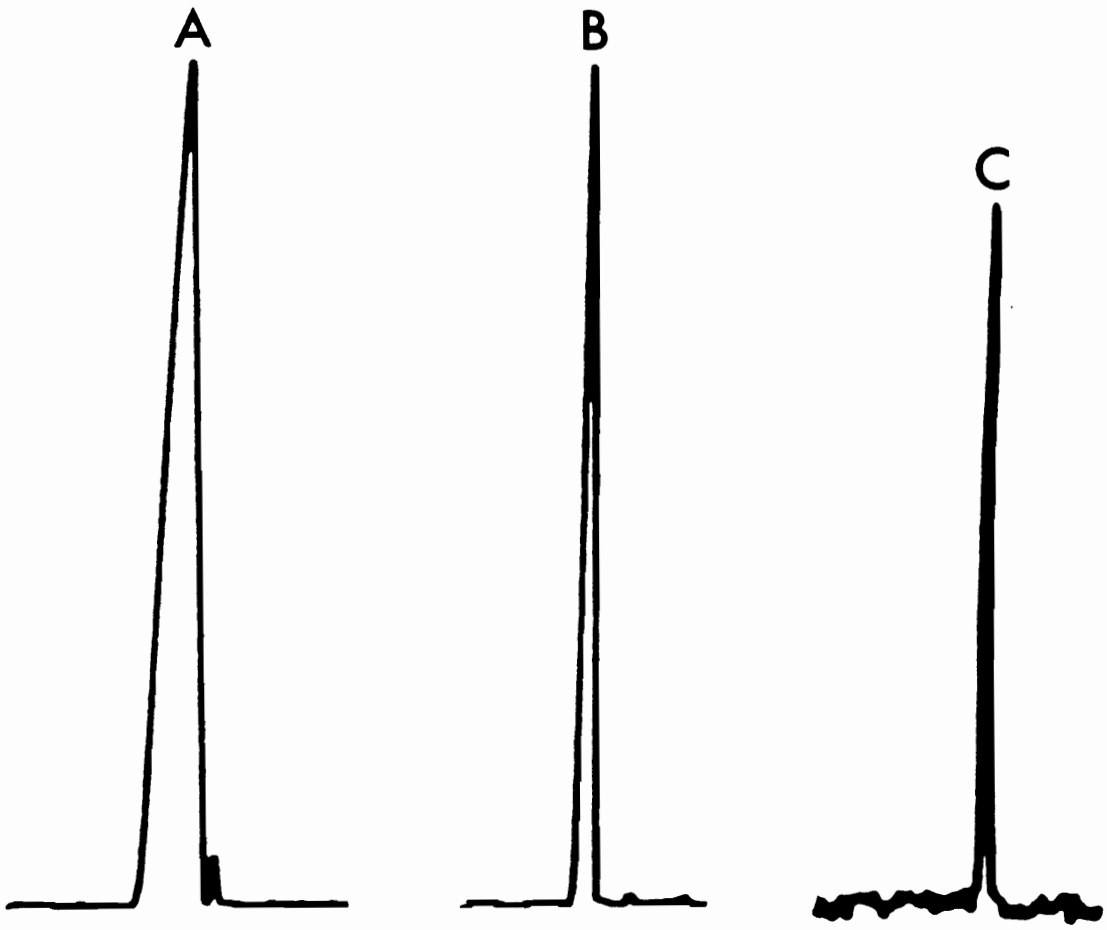

Figure 11. Influence of 3,4-dihydroxymandelic acid concentration on peak shape. Concentrations: A. 2 mg/mL B. 0.2 mg/mL C. 0.02 mg/mL.

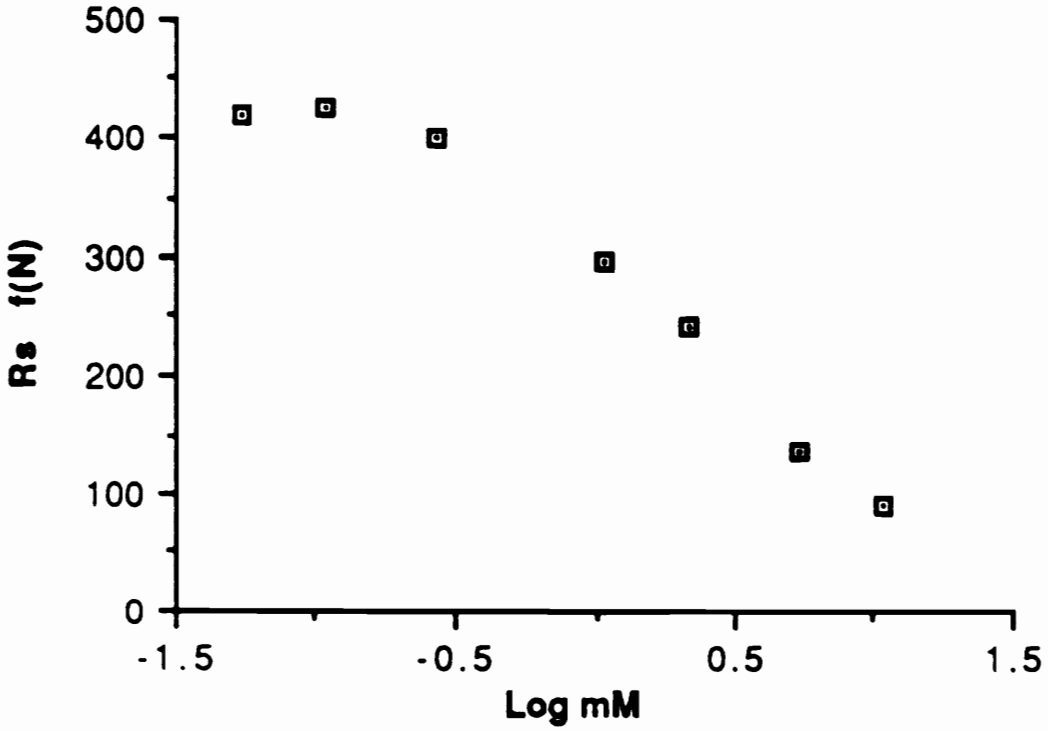

Figure 12. Resolution as a function of N vs. the Log_{10} of 3,4-dihydroxy-mandelic acid concentration.

4.2.2. Influence of pH on the Coefficient of Electroosmotic Flow

In addition to increasing resolution by maximizing efficiency, methods may by found to increase the relative velocity difference between sample components. As indicated by eqn. 29, the relative velocity difference of two zones is determined by the magnitude of electroosmotic flow, which is, in turn, dependent on the zeta potential at the buffer/capillary interface (eqn. 7). Surface charge is determined by the degree of protonation of surface silanol groups. Accordingly, electroosmotic flow should be suppressed by decreasing buffer pH [30, 110].

The influence of pH on μ_{eo} is, as shown in Table III, quite appreciable. The magnitude of the coefficient of electroosmotic flow is reduced by approximately a factor of four at pH 3.00 vs pH 7.00. At pH 5.11, μ_{eo} decreases from run to run, indicating that surface equilibration may be slow in weakly acidic media. The latter results are supported by the work of Lambert and Middleton [111], who note that at pH 4.00, surface equilibration may take in excess of 14 days.

The choice of buffer pH is, additionally, frequently mandated by the pKas of sample components. Controlling μ_{eo} via pH is, therefore, not always a practical option in CZE. As an alternative, coated capillaries [33-34] have been used to establish a different zeta potential at the buffer/capillary interface. Such a procedure is, however, not dynamic since different coatings are required to provide different zeta potentials. It is therefore desirable to find additional methods of controlling μ_{eo}.

Table III. Influence of pH on the coefficient of electroosmotic flow.

pH	μ_{eo} (cm^2/KV-min)	avg.	s	%rsd
7.00	56.25, 57.45, 57.58, 57.72	57.3	0.7	1.2
5.96	48.31, 48.70, 48.50	48.5	0.2	0.40
5.11	39.64, 39.19, 37.91, 34.08 28.09, 23.96, 20.70, 18.94 17.46, 16.56	28	9	34
3.00	13.99, 14.41, 13.56, 14.44	14.1	0.4	2.9

4.2.3. Influence of Buffer Concentration, Capillary Internal Diameter, and Forced Convection on Resolution.

Fig. 13 shows the influence of buffer concentration on μ_{eo} in a 50 μm capillary. Electroosmotic flow is suppressed in the more concentrated Na_2HPO_4 buffers [25, 34, 112] and increases slightly as larger electric field strengths are employed. The decrease in μ_{eo} with increasing buffer concentration is attributed to a decrease in the zeta potential. The zeta potential is reduced since the capillary surface is more effectively neutralized by higher salt concentrations. The increase in μ_{eo} with increasing electric field strength is caused by increased Joule heating. Joule heating raises the temperature of the buffer and as a result decreases viscosity. As shown by eqn. 13, μ_{eo} is increased in lower viscosity buffers.

In 100 μm capillaries (Fig. 14) the same relationship between buffer concentration and μ_{eo} was observed at low electric field strengths. However, as expected (eqn. 19), Joule heating was more pronounced in the larger capillary, especially when concentrated buffers were employed. As a result μ_{eo} increased markedly with electric field strength.

The Joule heating observed in Figs. 13 and 14 make it difficult to determine the optimum experimental conditions for CZE, not only because of the interdependence of μ_{eo} and electric field strength, but also due to the influence that both μ_{eo} and Joule heating have on separation efficiency. A reduction in μ_{eo} reduces the net solute velocity and therefore efficiency (eqn. 15). Joule heating adds an additional source of band broadening to

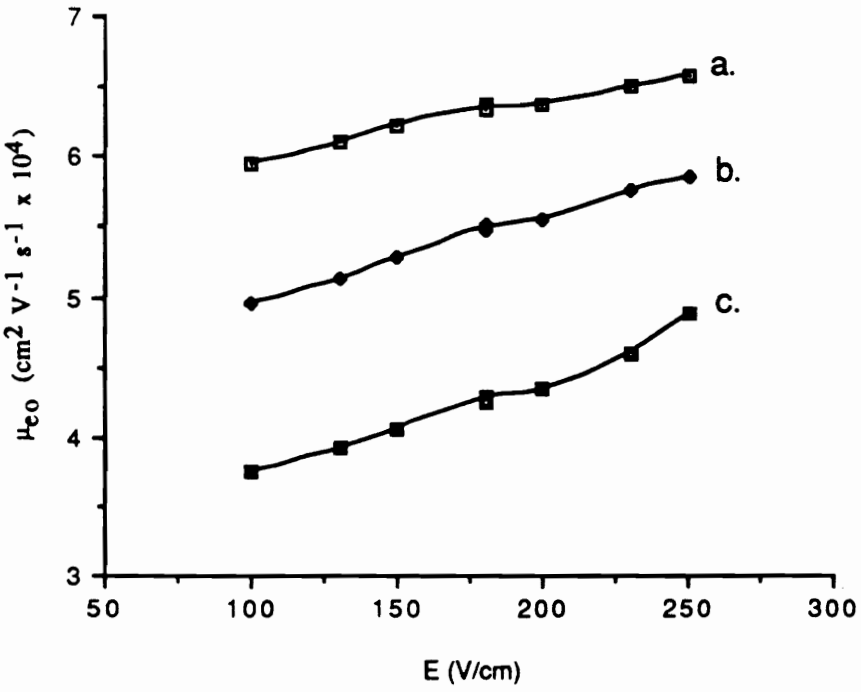

Figure 13. Influence of buffer concentration and electric field strength (E) on the coefficient of electroosmotic flow (μ_{eo}) in 50 μm fused silica capillaries. Na_2HPO_4 concentrations: a. 0.01 M b. 0.02 M c. 0.05 M.

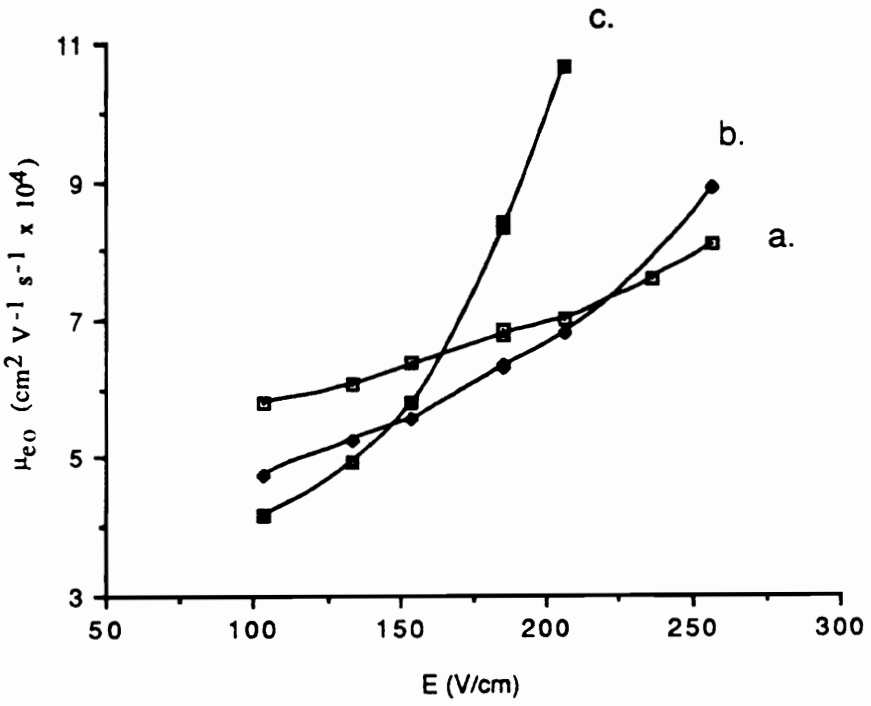

Figure 14. Influence of buffer concentration and electric field strength (E) on the coefficient of electroosmotic flow (μ_{eo}) in 100 μm fused silica capillaries. Na_2HPO_4 concentrations: a. 0.01 M b. 0.02 M c. 0.05 M.

decrease efficiency from the diffusion limited case. As shown by the curvature in a plot of efficiency as a function of electric field strength (Fig. 15), the influence of Joule heating on efficiency was noticeable even when 50 μm capillaries were employed.

To better understand the influence of μ_{eo} and Joule heating on resolution, the various operating parameters were evaluated with respect to both separation efficiency and the relative velocity difference. As shown in Fig. 16, the relative velocity difference between phenol and sodium toluene-sulfonate, $(\mu_{el,1} - \mu_{el,2})/(\mu_{el,avg} + \mu_{eo})$, was constant for a given buffer concentration, regardless of electric field strength. This was observed not only for a 0.01 M buffer in a 50 μm capillary, where Joule heating was minimal, but also for 0.02 M Na_2HPO_4 in a 100 μm capillary, where appreciable Joule heating was observed at high electric field strengths. The independence of the relative velocity difference with Joule heating is presumably attributable to both μ_{el} and μ_{eo} having the same viscosity dependence (eqns. 13 and 14).

The average values of the relative velocity difference between phenol and sodium toluenesulfonate were 0.576 and 0.661 in the 0.01 and 0.02 M buffers, respectively. Thus, on the basis of the relative velocity difference alone, resolution was improved, in 0.02 vs 0.01 M buffer, by a factor of 1.15. The influence of efficiency must, however, also be explored.

If it is assumed that no Joule heating occurs, as is presumably the case when 50 μm capillaries and low electric field strengths are employed, eqns. 13 and 29 may be combined to express resolution as a function of efficiency

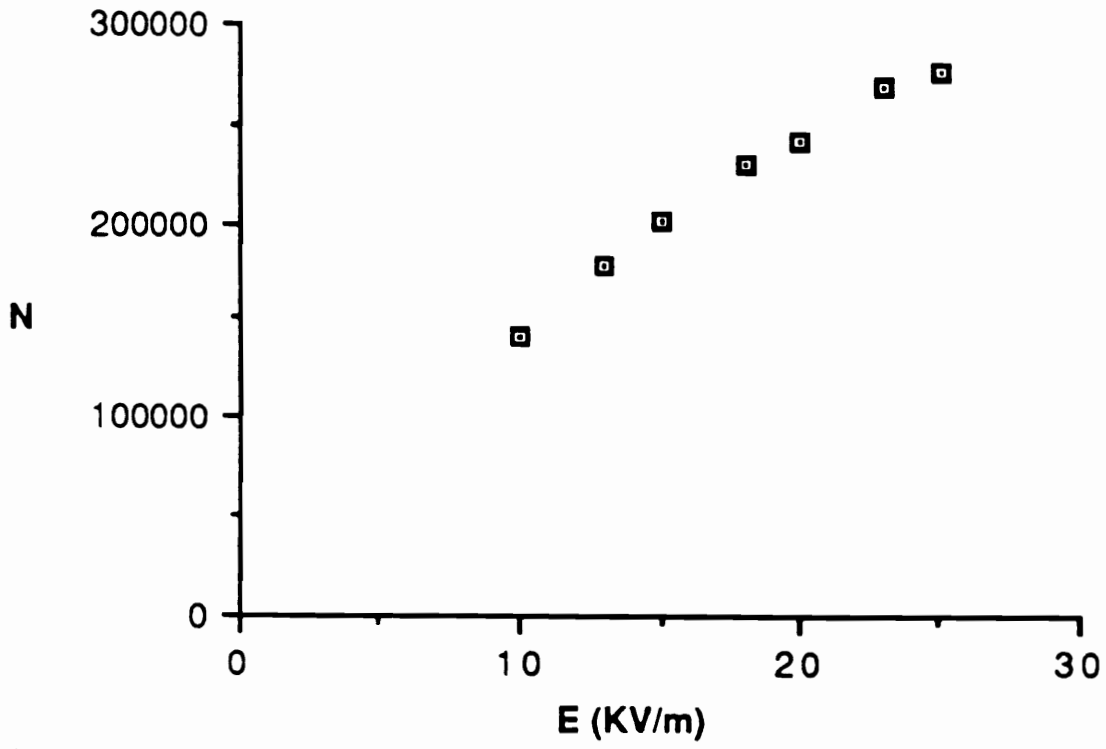

Figure 15. Efficiency (N) of phenol vs. electric field strength (E) in a 50 μm capillary. Buffer: 0.05 M Na_2HPO_4, pH 7.00.

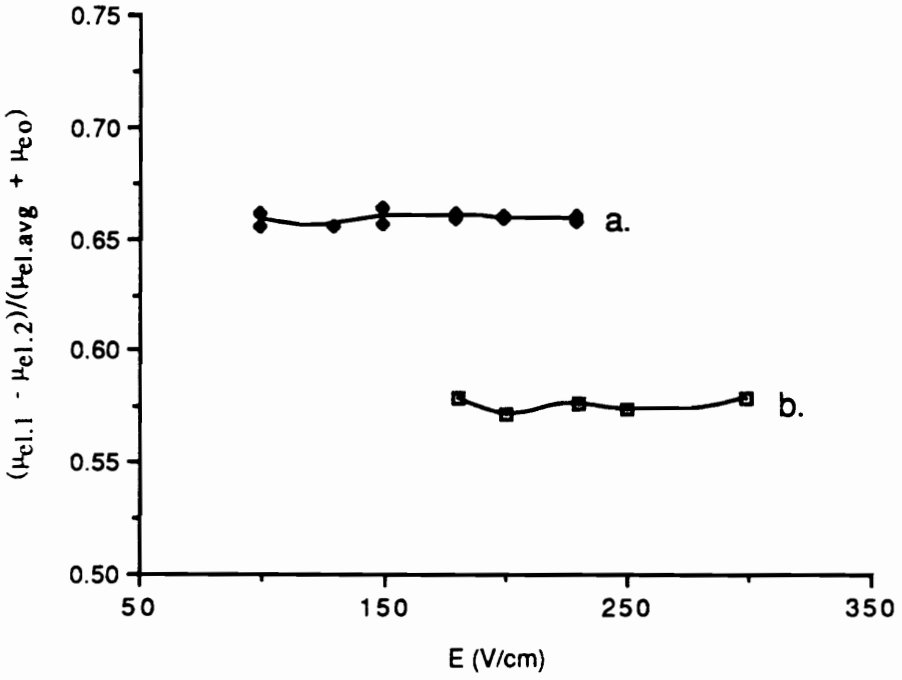

Figure 16. Influence of buffer concentration and electric field strength (E) on the relative velocity difference, $(\mu_{el.1} - \mu_{el.2})/(\mu_{el.avg} + \mu_{eo})$.
a. 0.02 M Na_2HPO_4/ 100 µm capillary.
b. 0.01 M Na_2HPO_4/50 µm capillary.

as:

$$R_S = f(v_{net}/2D_a)^{1/2} \qquad (63)$$

If it can, additionally, be assumed that diffusion coefficients are the same in each buffer (at low electric field strengths), resolution as a function of efficiency, in 0.02 vs. 0.01 M buffer, can be shown to be decreased by the ratio $(v_{0.02}/v_{0.01})^{1/2}$; where $v_{0.02}$ and $v_{0.01}$ are the net velocities in 0.02 and 0.01 M buffer, respectively. At low electric field strengths (100 V/cm), the net velocities of phenol were determined to be 4.96×10^{-2} (0.02 M) and 5.96×10^{-2} cm/sec (0.01 M). Accordingly, the resolution as a function of efficiency ratio was 0.912.

Multiplication of the relative velocity difference and efficiency ratios, yield a value of 1.05. It is thus seen that the more concentrated buffer provides a slight improvement in resolution in the diffusion limited case. When Joule heating is accounted for, however, the resolution as a function of efficiency ratio is reduced considerably and resolution is better in the less concentrated buffer.

The influence of Joule heating on efficiency in a 100 μm capillary is shown in Fig. 17. In contrast to Fig 15, the Joule heating observed in a 100 μm capillary is so severe that separation efficiency reaches a maximum at a relatively low electric field strength (approximately 175 V/cm). To maximize resolution, the capillary internal diameter should, therefore, be minimized regardless of the buffer concentration used.

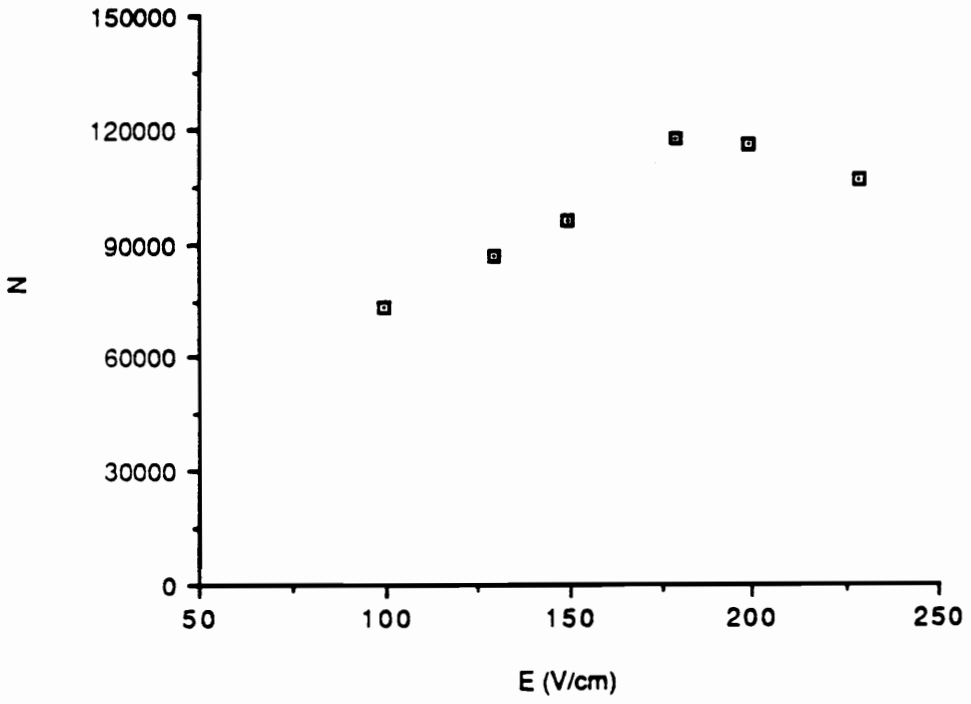

Figure 17. Efficiency (N) of sodium toluenesulfonate vs. electric field strength (E) in a 100 μm capillary. Buffer: 0.02 M Na_2HPO_4, pH 7.00.

It may, however, be undesirable to use small diameter capillaries in applications where detectability is a problem. Using eqn. 22 to compare the allowable sample volumes in 50 vs. 100 μm capillaries, it is seen that 16 times more sample may be introduced into the 100 μm capillary to yield the same H_S. As a result poorer concentration detection limits are predicted in the smaller capillaries. To provide a viable comparison, the concentration of the solute zone as it reaches the detector, the detector cell path length, and the specific values of N and t_R in 100 vs 50 mm capillaries must, however, also be examined.

Assuming equal efficiencies and migration times, and that the same amount of sample is introduced, the zone concentration in 50 μm capillaries is four times that obtained in 100 μm capillaries. By Beer's law this should result in a a four-fold improvement in sensitivity. For on-capillary UV detection, the detection limits are improved in the larger capillary as the result of a longer pathlength. As an approximation the improvement observed in 100 vs. 50 μm capillaries should be by a factor of two. (The specific noise levels in each capillary, the detector slit width and the position of each capillary in the light path are not considered).

The influence of t_R and N on the detection limit may be evaluated by rearrangement of eqn. 45. Expressed in terms of the peak height (the maximum signal) eqn. 45 becomes:

$$h = N^{1/2}A/2.51t_R \qquad (64)$$

It is seen from eqn. 64, that the improved efficiency obtained in 50 μm capillaries should result in a larger peak height for a peak of unit area. In practice, however, the efficiency enhancement observed in 50 vs. 100 μm capillaries is, as will be shown, fairly minimal. As a result, the improved efficiency obtained in 50 μm capillaries does not offset the sample volume advantage obtained in 100 μm capillaries. Furthermore, as illustrated in Figs. 13 and 14, the decrease in efficiency resulting from Joule heating is countered by a smaller t_R value by virtue of increased electroosmotic flow. In agreement with the above, approximately 8 times the sensitivity may be expected in 100 vs. 50 μm capillaries.

From the foregoing it is clear that it may in many instances be necessary to find a compromise between resolution and detectability. This may trivially be achieved by ignoring the sample volume and sample concentration limitations prescribed. Alternatively, means may be found of improving efficiency in 100 μm capillaries by reducing Joule heating. The theoretical work of Knox [24] has predicted that the Joule heat generated may be dissipated by forced convection. This prediction is supported by the experimental work of Foret et al. [25] and Karger et al. [68] and by our results [113], as shown in Fig. 18. When forced air convection at 3.5 L/min., was applied to 50 cm of the 100 μm capillary (see Fig. 9), μ_{eo} as a function of electric field strength was reduced, and separation efficiency was improved. In a 100 μm capillary, using a 0.05 M buffer and an electric field strength of 22.7 kV/m, efficiency was improved from 191,000 +/- 3.1% RSD to 226,000 +/- 3.3% RSD theoretical plates (based on 4 determinations). For comparison, the efficiency obtained in 50 μm capillaries, under the same

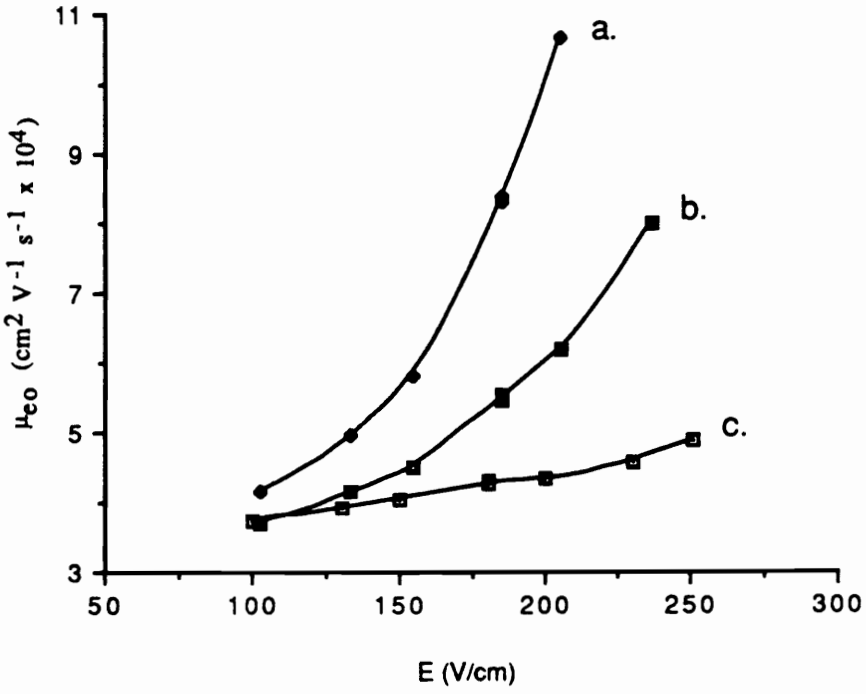

Figure 18. Influence of forced convection on the coefficient of electroosmotic flow (μ_{eo}) in 0.05 M Na_2HPO_4.
Capillaries: a. 100 μm b. 100 μm with convection c. 50 μm.

operating conditions was approximately 264,000 theoretical plates (Fig. 15).

While the use of forced air convection increases the resolution possible in 100 μm capillaries, it is notable that the improved efficiencies were obtained at the expense of analysis time. As shown in Fig. 18, electroosmotic flow was reduced in 100 μm capillaries when convection was employed. It, therefore appears that CZE is analogous to chromatography in that sample capacity, analysis time and resolution cannot be optimized simultaneously. The interrelationship between these goals, as developed for HPLC [114], is shown in Fig. 19. In practice, separation can be performed at any point within the triangle. However, in choosing an operating point towards one of the corners, thereby optimizing that goal, the additional goals are sacrificed. The choice of a suitable point, therefore, involves a compromise as dictated by the requirements of the separation.

From the interrelationship between sample capacity (sample volume and concentration), resolution and analysis time, described above, it is seen that resolution can be optimized by using small i. d. capillaries. The improvement in resolution is, however, achieved at the expense of longer analysis times and, under the constraints of eqn. 22, smaller sample sizes. Alternatively, sample size and analysis time may be improved by using a larger capillary, but at the expense of resolution. Optimization of CZE is contingent on choosing the appropriate compromise between each goal, using the guidelines developed above.

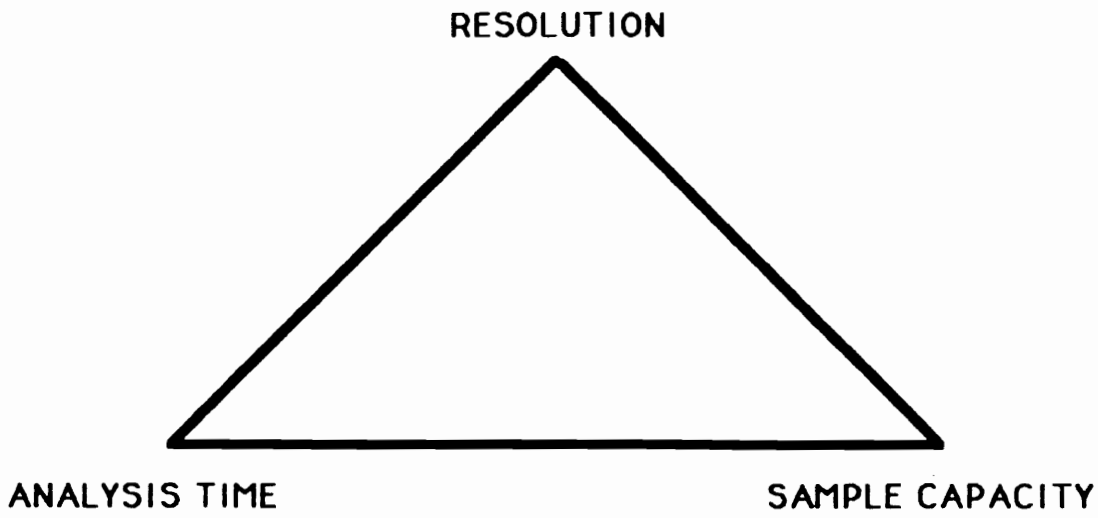

Figure 19. Interrelationship between resolution, analysis time and sample capacity.

4.3 Micellar Electrokinetic Chromatography

In comparing two analyses in which the sample capacity and analysis time are constant but in which resolution differs, the analysis providing the better resolution is more favorable since resolution can always be reduced to optimize the other goals. It is therefore desirable to develop methods which provide the maximum resolution per unit time, and then to adjust the operating parameters. In HPLC, this is achieved by maximizing selectivity (α).

Selectivity may be viewed as the difference in the velocity of two zones which arises from the variability in interaction of each sample component with a secondary phase. It follows that if a micellar phase is added to the buffer used in CZE (as in MEKC), the resolution obtained per unit time may increase, and a more favorable interrelationship between the separation goals may be obtained. In this respect the addition of suitable micellar phases to the CZE buffer becomes an important parameter.

The influence of various micellar phases on selectivity and the other parameters governing resolution are examined here to provide general guidelines for MEKC. To simplify the theory of separation in micellar media, the guidelines are developed for the analyses of neutral solutes which do not display electrophoretic mobilities. The implications may, however, in many cases be extended to the analyses of charged species.

4.3.1 Criteria for Suitable Micellar Phases

While many surfactants are worthy of investigation as micellar phases for MEKC, several criteria must be met. The surfactant must: 1) form micelles in the aqueous buffer; 2) dissolve the sample to be separated; 3) cause minimal Joule heating; 4) provide for a reasonable difference in the velocity of the micellar and aqueous phases (small t_0/t_{mc}); 5) provide different distribution coefficients (selectivity) for each sample component; 6) provide reasonable retention (capacity factors) for the sample components of interest; and 7) minimize band broadening during the separation process.

4.3.2. An Evaluation of Sodium Alkyl Sulfates as Micellar Phases for MEKC

In light of these micellar phase criteria, sodium alkyl sulfates with alkyl chain lengths of 8, 10, 12 and 14 carbons were evaluated as micellar phases. To compare MEKC to reversed phase HPLC, ASTM test mix LC-79-2 [108-109] was used as the sample.

The separation of the test mix obtained in 0.05 M SDS is shown in Fig. 20a. Column efficiency was approximately 150,000 theoretical plates. Nevertheless, benzene and benzaldehyde coeluted, indicating that SDS provides similar selectivity for each of these species and, therefore, that the distribution of solute between the aqueous and micellar phases is not governed exclusively by the hydrophobicity of the solute.

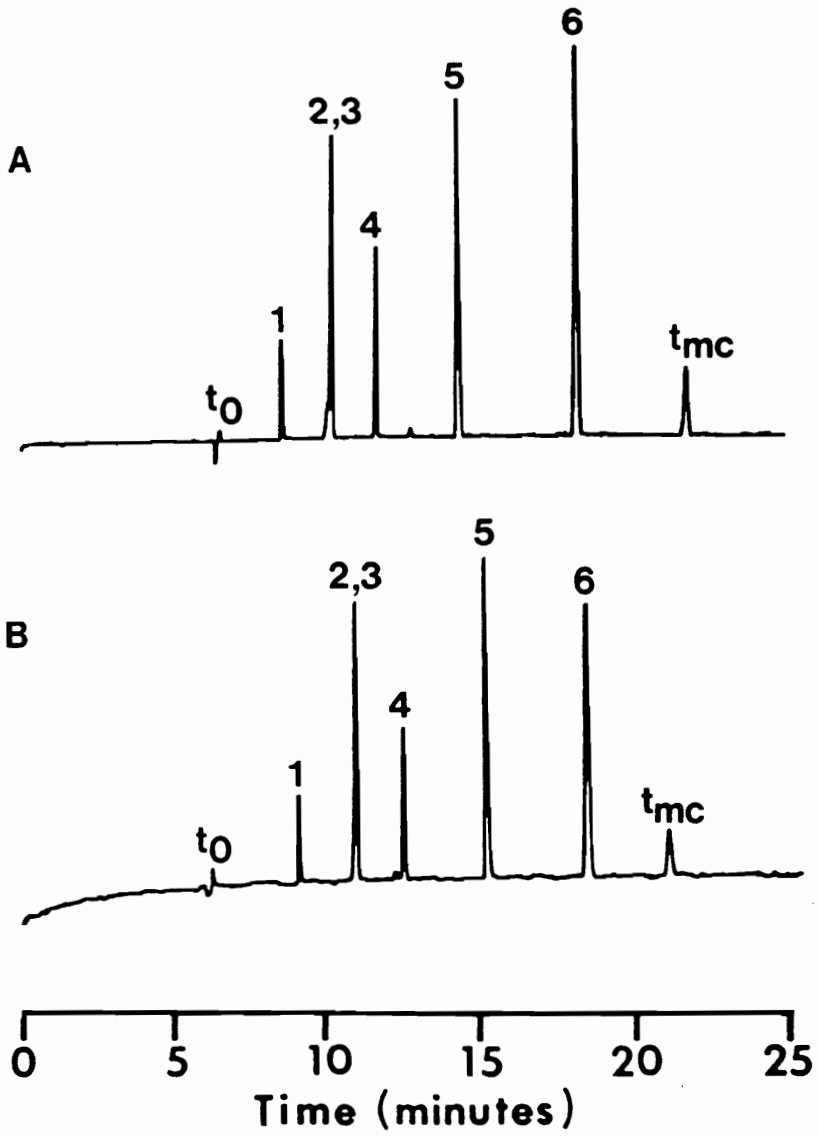

Figure 20. MEKC Separation of ASTM test mix LC-79-2 in:
A. 0.05 M SDS/0.01 M Na_2HPO_4, pH 7.00.
B. 0.075 M SDS/0.01 M Na_2HPO_4, pH 7.00
Conditions: 100 µm x 80 cm capillary (L = 50 cm); +15 kV applied voltage; siphoning injection at 3.8 cm/10 s; detection wavelength = 254 nm. Order of elution: 1. benzyl alcohol 2,3. benzene and benzaldehyde 4. acetophenone 5. methyl benzoate 6. dimethyl terephthalate (DMT).

To resolve the coeluting components, optimization in accordance with the master resolution equation for MEKC (eqn. 33) was attempted using an approach similar to that applied in conventional HPLC [115]. Thus, initial efforts focused on changing the SDS concentration to effect a more favorable capacity factor for the separation of the critical pair. As seen in Fig. 20b, and from the coefficients of correlation in Table IV, linear increases in the capacity factors of each solute were observed with an increase in the micellar/aqueous phase ratio. Solute capacity factors were therefore readily adjusted. However, for the range of concentrations utilized (0.025-0.075 M), it was not possible to effect the separation of benzene and benzaldehyde.

This observation is in agreement with the master resolution equation as expressed in terms of the capacity factor dependent terms (eqn. 34). For a t_0/t_{mc} value of 0.291 +/- 0.003, as observed for 0.05 M SDS, the $R_S = f(k')$ maximum of 0.3 occurs at a capacity factor of approximately 1.85. However, f(k') is constant to within 1% from k' = 1.6 to 2.2; the capacity factor is, therefore, essentially optimized in 0.075 M SDS (k' = 1.63). This maximum provides an enhancement in resolution by a factor of only 1.08, compared to 0.05 M SDS (k' = 1.03). It is, therefore, not surprising that resolution was not effected by increasing the micellar concentration.

In an attempt to further optimize the separation, by decreasing the t_0/t_{mc} ratio, 0.05 M sodium decyl sulfate (STS) was used instead of SDS as the micellar phase. By virtue of a larger charge to mass ratio, STS should possess a larger electrophoretic mobility, and as a consequence provide a larger value for t_{mc}. Furthermore, as a result of the decreased alkyl chain

Table IV. Solute capacity factors as a function of SDS concentration. (All values are based on 4 determinations).

Solute	SDS Concentration			r
	0.025 M	0.050 M	0.075 M	
benzyl alcohol	0.28 +/- .01	0.55 +/- .02	0.85 +/- .01	0.99985
benzene	0.54 +/- .02	1.09 +/- .02	1.63 +/- .03	0.99998
acetophenone	0.84 +/- .02	1.71 +/- .03	2.52 +/- .03	0.99980
methyl benzoate	1.67 +/- .04	3.47 +/- .05	5.16 +/- .03	0.99984
DMT	5.38 +/- .08	10.7 +/- .3	15.7 +/- .5	0.99982

length, with respect to SDS, selectivity differences may exist between the two surfactants.

Experimentally, STS provided an extended elution range (t_o/t_{mc} = 0.235 +/- 0.006), as shown in Fig. 21a. However, differences in the selectivity of STS and SDS were minor, as summarized in Table V. As a result the separation of benzene and benzaldehyde was not effected. Attempts to improve resolution by employing STS of different concentrations were not feasible. The sample was insoluble in 0.025 M STS, and 0.075 M STS caused an appreciable decrease in the detector signal to noise ratio. This is, tentatively, attributed to excess Joule heating. Joule heating can, at sufficiently high electric field strengths, disrupt a separation by elevating the temperature above the boiling point of the buffer. At temperatures approaching the boiling point it is logical that microbubbles are formed, and that the microbubbles increase detector noise.

Additional studies showed that other sodium alkyl sulfates were not suitable for MEKC, under the conditions employed. Sodium octyl sulfate at a concentration of 0.075 M did not dissolve the sample, presumably because this concentration is below the surfactant's CMC [116]. Due to the Joule heating observed in 0.075 M STS, the use of larger surfactant concentrations were not investigated. Sodium tetradecyl sulfate was insoluble in the operating buffer at the 0.025 M level, which was considered be the minimum surfactant concentration required to provide a reasonable phase ratio. The solubility was, however, noted to increase markedly with an increase in temperature, indicating that sodium tetradecyl sulfate can be employed in MEKC at elevated temperatures [12].

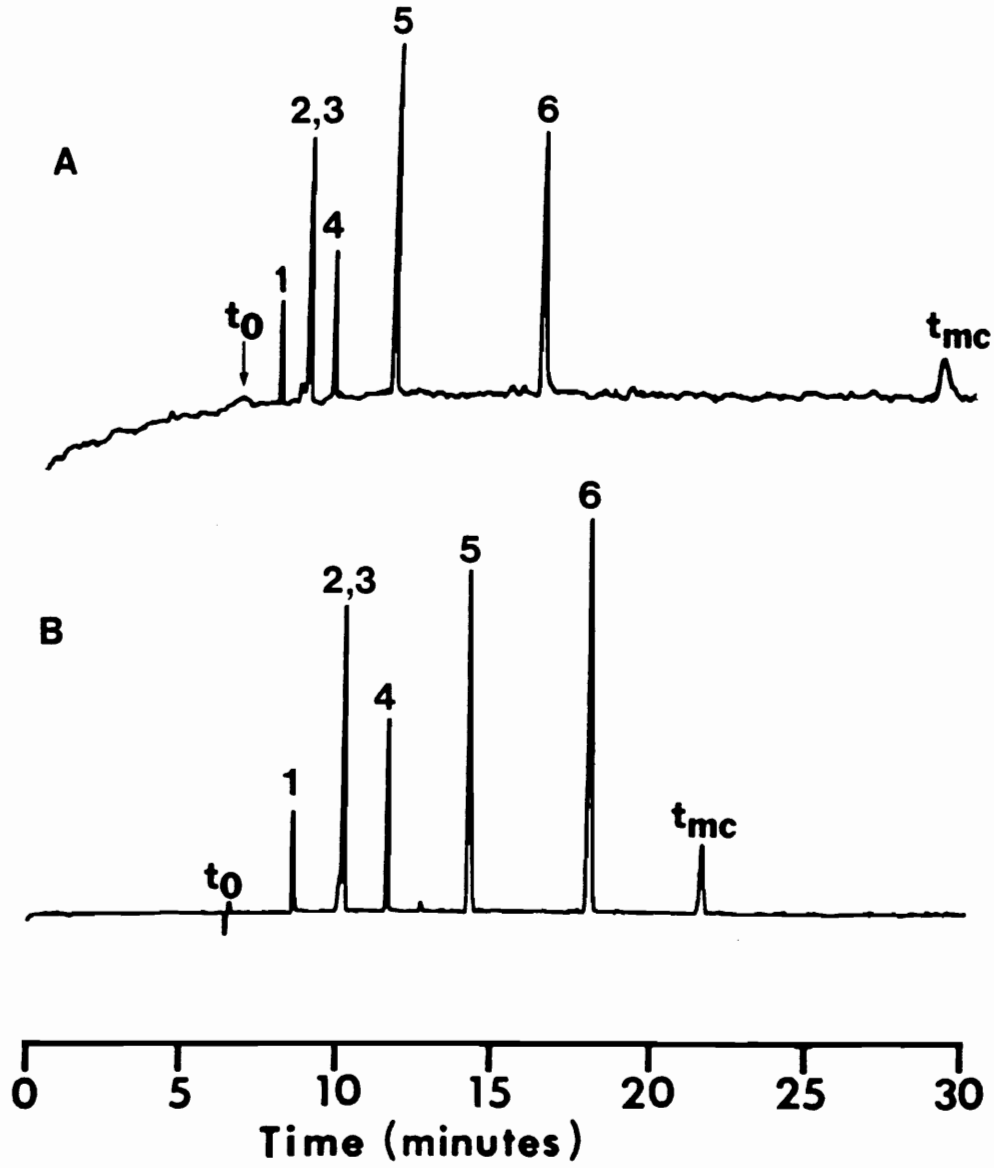

Figure 21. MEKC Separation of ASTM test mix LC-79-2 in:
A. 0.05 M STS/0.01 M Na_2HPO_4, pH 7.00.
B. 0.05 M SDS/0.01 M Na_2HPO_4, pH 7.00
Conditions and the order of elution are as described in Fig. 20.

Table V. Selectivity (α) between selected solute pairs in 0.05 M SDS and 0.05 M STS. (All values are based on 4 determinations).

Solute Pair	α in 0.05 M SDS	α in 0.05 M STS
benzyl alcohol/ benzene	1.97 +/- .03	1.92 +/- .01
benzene/acetophenone	1.569 +/- .003	1.48 +/- .02
acetophenone/methyl benzoate	2.03 +/- .02	1.91 +/- .02
methyl benzoate/DMT	3.09 +/- .04	2.73 +/- .04

4.3.3. A Comparison of MEKC and HPLC

Due to the nonzero value of the t_0/t_{mc} ratio, it is interesting to compare the MEKC resolution with that obtainable in HPLC. Rewriting eqn. 33 as:

$$R_s = \frac{N^{1/2}}{4}\left(\frac{\alpha - 1}{\alpha}\right) f(k') \qquad (65)$$

and requiring the same resolution of each separation procedure, it follows that:

$$\frac{N_H^{1/2}}{4}\left(\frac{\alpha_H - 1}{\alpha_H}\right) f(k')_H = \frac{N_M^{1/2}}{4}\left(\frac{\alpha_M - 1}{\alpha_M}\right) f(k')_M \qquad (66)$$

where the subscripts H and M denote HPLC and MEKC respectively.

When SDS was used as the micellar phase the maximum of $f(k')_M$ was 0.3, and the efficiency (N_M) obtained in a capillary with an effective length of 50 cm was approximately 150,000 plates. Assuming that a similar separation can be achieved by HPLC at a capacity factor of 10, $f(k')_H = 0.91$. Thus if selectivity is the same in each system (i.e. $\alpha_H = \alpha_M$), the resolution obtained by MEKC is similar to the resolution provided by an HPLC column generating only16,000 theoretical plates. To obtain an advantage of using MEKC over HPLC, it is therefore necessary to find micellar phases which provide better selectivity or to establish a means of reducing the t_0/t_{mc} ratio.

4.3.4. The Use of Brij 35 ® as a Modifier for MEKC

In light of the selectivity requirement of the micellar phase, it is interesting to compare the selectivity obtained by MEKC using SDS, with that obtained by conventional reversed phase HPLC, and by reversed phase HPLC employing Brij 35 as the mobile phase [109]. The orders of elution are listed in Table VI. Notably, benzene elutes at different relative times in each separation mode.

Since solvent/micelle partitioning is responsible for part of the selectivity mechanism in micellar chromatography, and under the premise that the polar head group influences selectivity in MEKC [14] (i.e. selectivity is not governed exclusively by solute hydrophobicity) it is logical to explore the use of Brij 35, as a micellar phase for MEKC [100].

Brij 35 is a nonionic surfactant, best described as a mixture of ethoxylated alcohols with an average alkyl chain length of 12 carbons and an average degree of ethoxylation of 23 oxyethylene units. Since Brij 35 is nonionic, it cannot migrate electrophoretically. To be a viable surfactant for MEKC, it must therefore be added to a charged micellar phase as a modifier.

Separations performed by modifying 0.025 M SDS with 0.01, 0.03 and 0.05 M Brij 35, are shown in Figs. 22 a-c. Benzene was selectively retained in the modified system. However, as shown in Table VII, the t_0/t_{mc} ratio was increased in the modified systems and solute capacity factors were generally reduced with respect to unmodified SDS. The decrease in solute capacity factors is consistent with a decreased solute solubility in nonionic

Table VI. Order of elution of ASTM LC-79-2 sample components under various separation conditions

	From Ref. 109	From Ref. 109	This work
"Stationary Phase":	RP-18	RP-18	SDS and STS
Mobile Phase:	30/70 (v/v) acetonitrile/water	6 % Brij® 35	0.01 M Na_2HPO_4 pH 7.00
Elution Order:	1. benzyl alcohol	1. benzyl alcohol	1. benzyl alcohol
	2. benzaldehyde	2. benzaldehyde	2,3. benzaldehyde and benzene
	3. acetophenone	3. acetophenone	
	4. methyl benz.	4. benzene	4. acetophenone
	5. benzene	5. methyl benz.	5. methyl benz.
	6. DMT	6. DMT	6. DMT

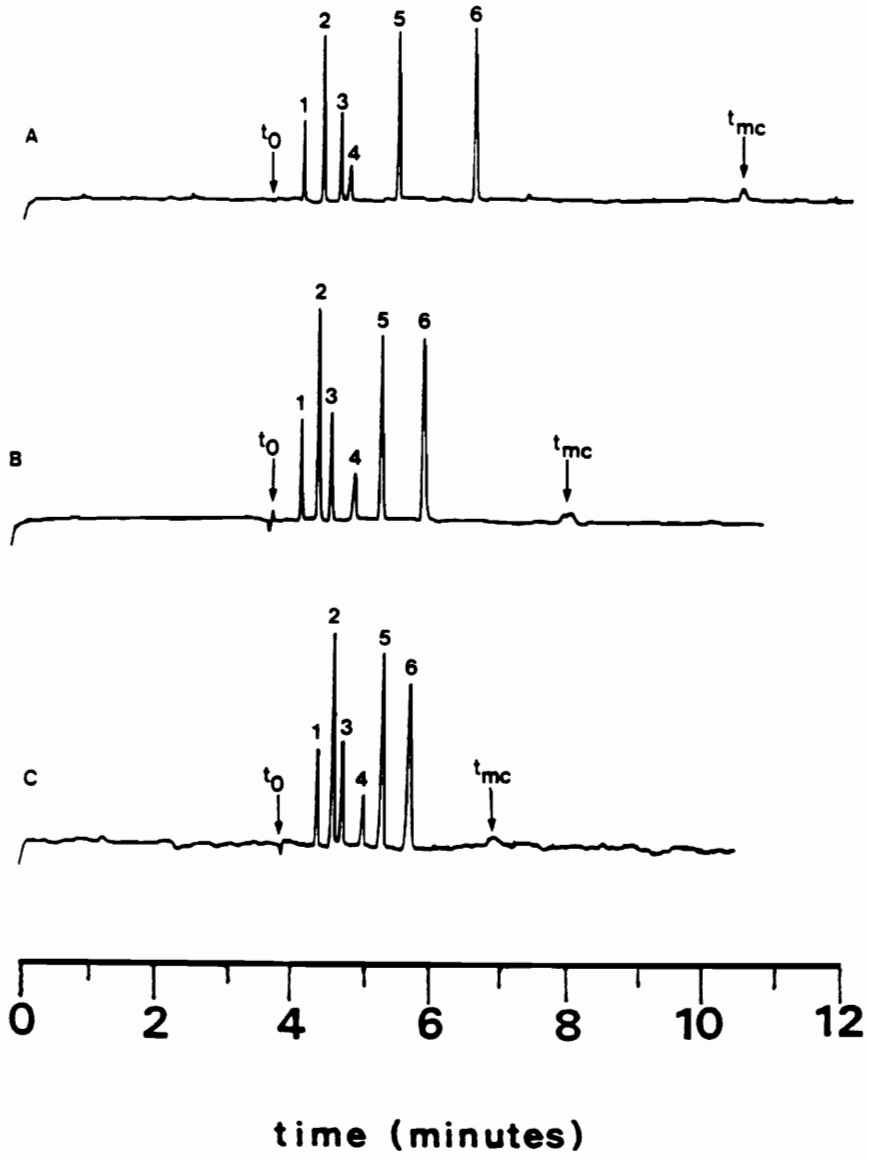

Figure 22. MEKC Separation of ASTM test mix LC-79-2 in 0.025 M SDS/0.01 M Na_2HPO_4 (pH 7.00) modified with: A. 0.01 B. 0.03 and C. 0.05 M Brij 35. Conditions: 100 µm x 70 cm capillary (L = 48 cm); +20 kV applied voltage; siphoning injection at 3.8 cm/10 s; detection wavelength = 254 nm. Order of elution: 1. benzyl alcohol 2. benzaldehyde 3. acetophenone 4. benzene 5. methyl benzoate 6. dimethyl terephthalate (DMT).

Table VII. Solute capacity factors (k') and t_0/t_{mc} ratios as a function of Brij 35 Concentration.

Solute	Micellar phase		
	0.025 M SDS/ 0.01 M Brij 35 (n = 3)*	0.025 M SDS/ 0.03 M Brij 35 (n = 4)*	0.025 M SDS/ 0.05 M Brij 35 (n = 5)*
Benzyl alcohol	0.177	0.257	0.38
+/- std. dev.	0.002	0.002	0.02
Benzaldehyde	0.309	0.419	0.58
+/- std. dev.	0.003	0.006	0.03
Acetophenone	0.437	0.552	0.73
+/- std. dev.	0.005	0.008	0.03
Benzene	0.517	0.86	1.15
+/- std. dev.	0.005	0.02	0.04
Methyl benzoate	0.98	1.27	1.64
+/- std. dev.	0.01	0.03	0.06
DMT	2.04	2.26	2.8
+/- std. dev.	0.04	0.02	0.1
t_0/t_{mc}	0.349	0.463	0.546
+/- std. dev.	0.002	0.001	0.003

* n = number of determinations.

vs. anionic surfactants. The change in selectivity supports the theory that the nature of the surfactant's polar head group plays an important role in solute retention [14]. It is unclear, however, specifically why selectivity was changed; several different models for the solubilization of benzene in micelles have been proposed [117].

While the increase in the t_0/t_{mc} ratio observed with Brij affects resolution adversely, Brij 35 has several desirable attributes as a micellar modifier. A major advantage of using neutral, as opposed to charged additives, is that they may be added to the micellar phase without an increase in Joule heating. Additionally, as noted previously [109], Brij 35 has a high cloud point temperature (approximately 100 °C) and low molar absorptivity values in the low UV region. These properties allow for Brij 35 to be used at the high temperatures which may result from Joule heating, and at the low wavelengths which may be required to effect the detection of many compounds. For this reason, and due to the Joule heating observed with surfactants with large charge to size ratios, it may be desirable to find means of decreasing t_0/t_{mc} by changing the electroosmotic flow, rather than by choosing a surfactant which provides the desirable electrophoretic mobility.

4.3.5. Influence of pH on the Elution Range in MEKC

As discussed in section 4.2.2, electroosmotic flow may be reduced by decreasing the pH of the operating buffer. As shown in Fig. 23, when 0.01 M phosphate/ 0.05 M SDS, pH 6.75, was used as the separation buffer, the

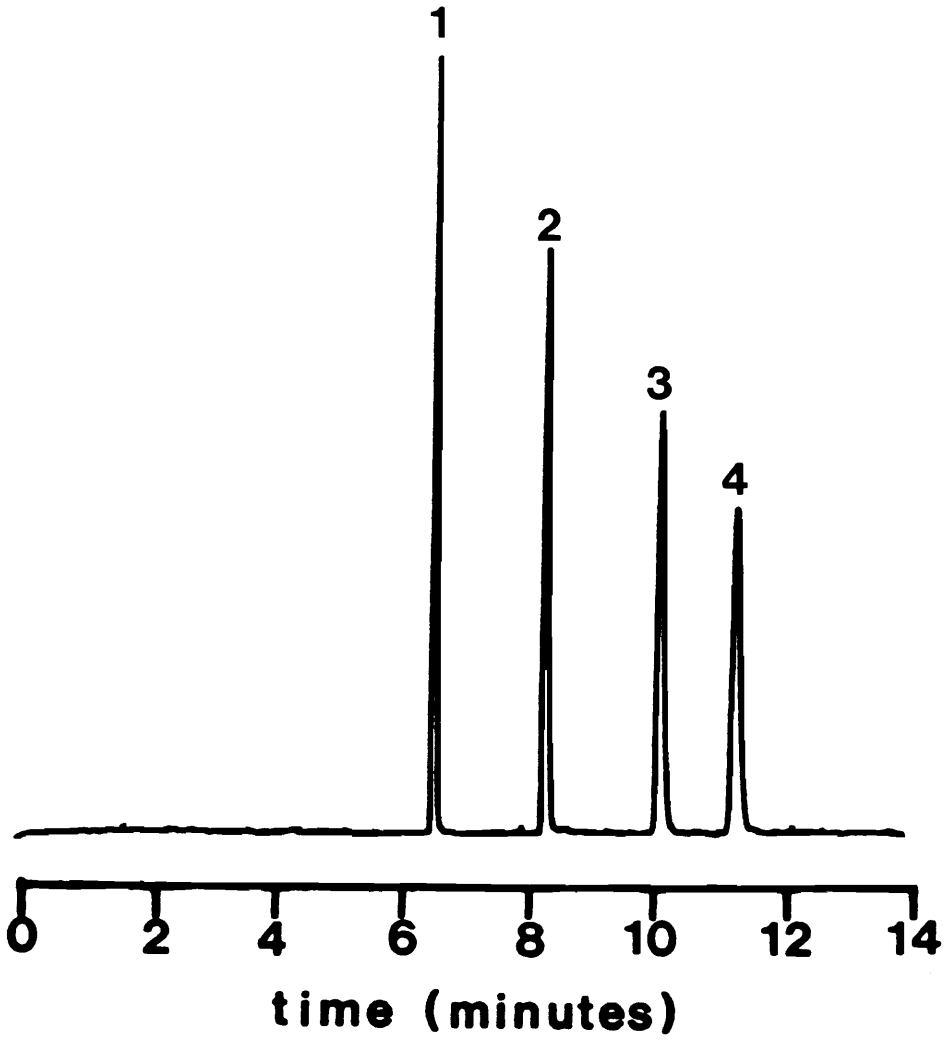

Figure 23. Separation of alkyl parabens at pH 6.75. Conditions: 100 μm x 100 cm capillary (L = 50 cm); +25 kV applied voltage; 0.05 M SDS/ 0.01 M Na_2HPO_4, pH 6.75, buffer; +5 kV/5 s electrokinetic injection; detection wavelength = 254 nm. Order of elution: 1. methyl 2. ethyl 3. propyl 4. butyl paraben.

electroosmotic flow exceeded the electrophoretic migration of SDS micelles. Accordingly, the sample was introduced at the anodic end of the capillary. The order of elution of a homologous series of alkyl parabens, as monitored at the cathodic end, was in order of increasing alkyl chain length. At a pH of 3.37 (Fig. 24) the electroosmotic flow was decreased to such an extent that the electrophoretic velocity of the SDS micelles was the dominant electrokinetic effect. As a result, sample had to be introduced into the cathodic end of the capillary, and the separation monitored towards the anodic end. In this case homologs with the greater affinity for the micellar phase eluted first.

Since the injection to detector distance was the same in each system, solute elution times are readily compared. Solutes with shorter alkyl chains (methyl, ethyl and propyl paraben) eluted faster when a pH of 6.75 (Fig. 23) was employed. Butyl paraben eluted more rapidly at a pH of 3.37 (Fig. 24), indicating that low pH buffers may provide for a more rapid analysis of solutes with a large affinity for the micellar phase. More importantly, however, if there is a pH at which the electroosmotic flow is the dominant electrokinetic effect and a pH at which electrophoresis is the dominant effect, it follows that there must be a pH at which the micellar phase is stationary. Under this constraint, eqn. 33 is reduced to the counterpart used in conventional chromatography. This suggests that if separation efficiency is maintained, the resolution obtainable in MEKC is far superior to that obtainable in HPLC (eqn. 66).

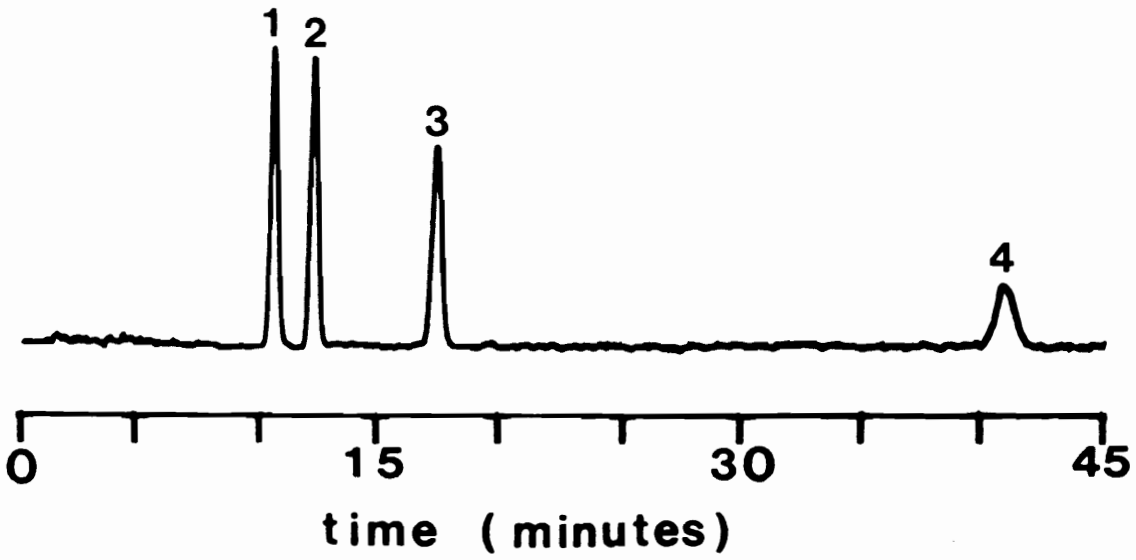

Figure 24. Separation of alkyl parabens at pH 3.37. Conditions: 100 µm x 100 cm capillary (L = 50 cm); -25 kV applied voltage; 0.05 M SDS/0.01 M Na_2HPO_4, pH 3.37, buffer; -10 kV/10 s electrokinetic injection; detection wavelength = 254 nm. Order of elution: 1. butyl 2. propyl 3. ethyl 4. methyl paraben.

4.3.6. Optimization of Capacity Factor Related Terms

It is clear from the foregoing that the relative magnitudes of the electrokinetic effects are critical parameters in the optimization of MEKC separations. To more closely examine the influence of electroosmosis and electrophoresis on resolution, the fundamental equations for MEKC (eqns. 31-34) are expressed here in terms of the electroosmotic flow velocity (v_{eo}) and the electrophoretic velocity (v_{el}).

The velocities of the aqueous and micellar phases, v_0 and v_{mc}, respectively, are given as:

$$v_0 = v_{eo} \tag{67}$$

and

$$v_{mc} = v_{eo} + v_{el} \tag{68}$$

t_0 and t_{mc} may be related to v_0 and v_{mc} as:

$$t_0 = L/v_0 = L/v_{eo} \tag{69}$$

and

$$t_{mc} = L/v_{mc} = L/(v_{eo} + v_{el}) \tag{70}$$

It follows from eqns. 67-70, that eqn. 31 may be rewritten as:

$$k' = \frac{t_R - L/v_{eo}}{L/v_{eo} - t_R (v_{eo} + v_{el})/v_{eo}} \tag{71}$$

and that eqn. 32 becomes:

$$t_R = \frac{(1 + k')(L/v_{eo})}{1 + [(v_{eo} + v_{el})/v_{eo}]\, k'} \qquad o)k' \qquad (72)$$

The master resolution equation (eqn. 33) may, in turn, be expressed as:

$$R_s = \frac{N^{1/2}}{4}\left(\frac{\alpha - 1}{\alpha}\right)\left(\frac{k'_2}{1 + k'_2}\right)\left(\frac{1 - [(v_{eo} + v_{el})/v_{eo}]}{1 + [(v_{eo} + v_{el})/v_{eo}]\, k'_1}\right) \qquad (73)$$

which may be rewritten, as a function of the capacity factor dependent terms, as:

$$f(k') = \left(\frac{k'}{1 + k'}\right)\left(\frac{1 - [(v_{eo} + v_{el})/v_{eo}]}{1 + [(v_{eo} + v_{el})/v_{eo}]\, k'}\right) \qquad (74)$$

Assuming that it is possible to adjust the electrophoretic mobility of SDS micelles to -0.5 mm s^{-1} via use of an appropriate electric field strength, and that the electroosmotic flow velocities may be adjusted to values of 0.2, and 0.4 and 0.5 mm s^{-1} by controlling pH [81-82] and/or using a coated capillary, f(k') may be plotted as a function of k' as shown in Fig. 25. In contrast to Fig. 6, Fig. 25 shows that it is actually possible for f(k') to exceed unity [82]. At the appropriate capacity factors, f(k') is actually infinite. This corresponds to a situation in which the distribution of the solute between each phase is such that its net migration velocity is zero.

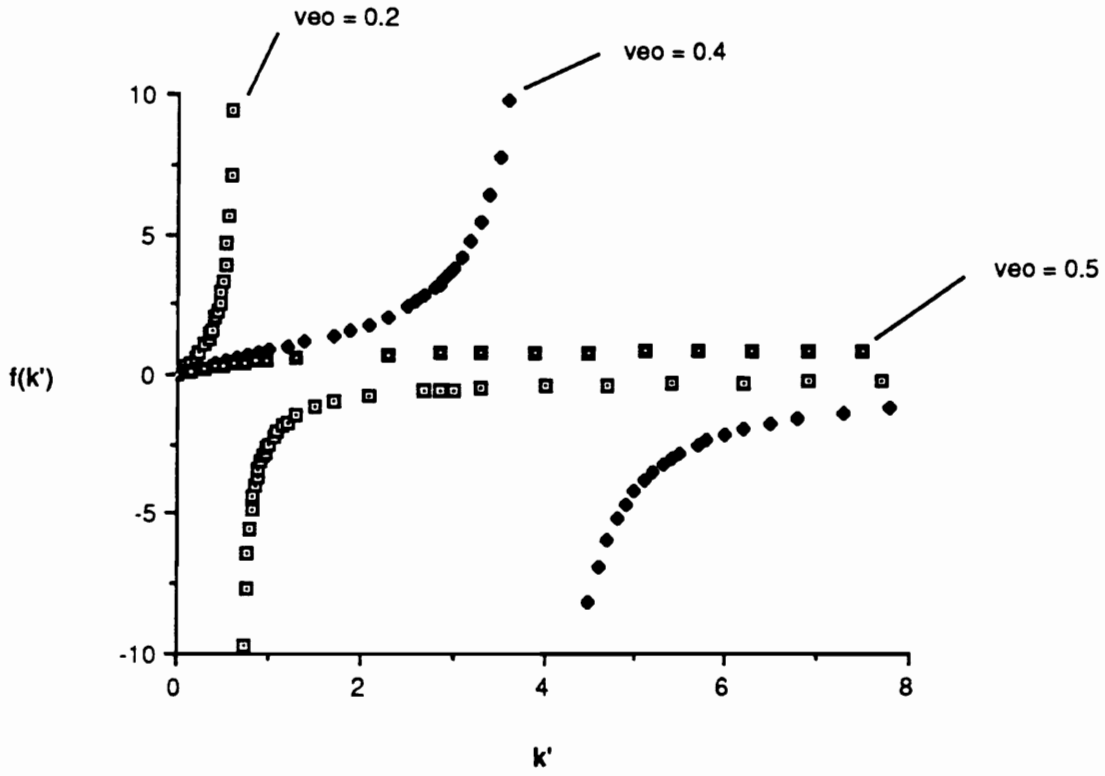

Figure 25. Influence of k' on f(k') for electroosmotic velocities (v_{eo}) of 0.2, 0.4 and and 0.5 mm s^{-1}. (Assumes v_{el} = -0.5 mm s^{-1}).

At capacity factors larger than the asymptote, f(k') becomes negative. This corresponds to the case shown in Fig. 24, where the solute distributes into the micellar phase to such an extent that it is transported against the electroosmotic flow. As noted, separation is still effected, but must be monitored at the anodic end of the capillary.

4.3.7. Optimization of Resolution in MEKC

The improvement in resolution predicted as a result of the decreased t_0/t_{mc} ratio must, however, also be examined with respect to the accompanying reduction in the linear migration velocity of the solutes. Since infinite resolution is possible for MEKC, under the constraint that the solute does not migrate, near infinite resolution should be possible at low net migration velocities. However, for a capillary of unit length, L, the analysis time will be correspondingly longer. It is, therefore, important to address not only resolution, but the resolution obtained as a function of time.

Expressing efficiency in terms of H (eqn. 16), and assuming that H_A, the total height equivalent of a theoretical plate, is independent of the solute's net velocity (for the purpose of illustration) allows for resolution at constant selectivity to be expressed as:

$$R_s = L^{1/2} f(k') \qquad (75)$$

Under the criterion that the same resolution is required at electroosmotic velocities of 0.6 and 0.4 mm s^{-1}, eqn. 75 may be rewritten as:

$$L^{1/2}_{0.6}\, f(k')_{0.6} = L^{1/2}_{0.4}\, f(k')_{0.4} \qquad (76)$$

where the subscripts denote the respective electroosmotic velocities.

Eqn. 76 may be used to calculate the fractional length of capillary required to achieve the same resolution at an electroosmotic velocity of 0.4 mm s^{-1} as attainable at 0.6 mm s^{-1}. Substituting the result into eqn. 72, it can be seen that as shorter capillaries are employed, the analysis time is decreased, despite the decrease in the solute's net velocity. Assuming equal values of H_A for each electroosmotic velocity, it is therefore possible to achieve unit resolution more rapidly at an electroosmotic velocity of 0.4 mm s^{-1} than at 0.6 mm s^{-1}. The specific improvement in analysis time is, as shown in Fig. 26, predicted to be appreciable.

However, for the the magnitude of improvement in analysis times predicted in Fig. 26 to be valid, the assumption that H_A is independent of velocity must be upheld. As noted by Terabe et al. [101], this assumption is not valid. Assuming that H_A is the product of the two primary contributions: diffusion, H_D, and mass transfer in the micellar phase, H_{mc}, (see section 2.3), H_A may be written as [101]:

$$H_A = H_D + H_{mc} \qquad (77)$$

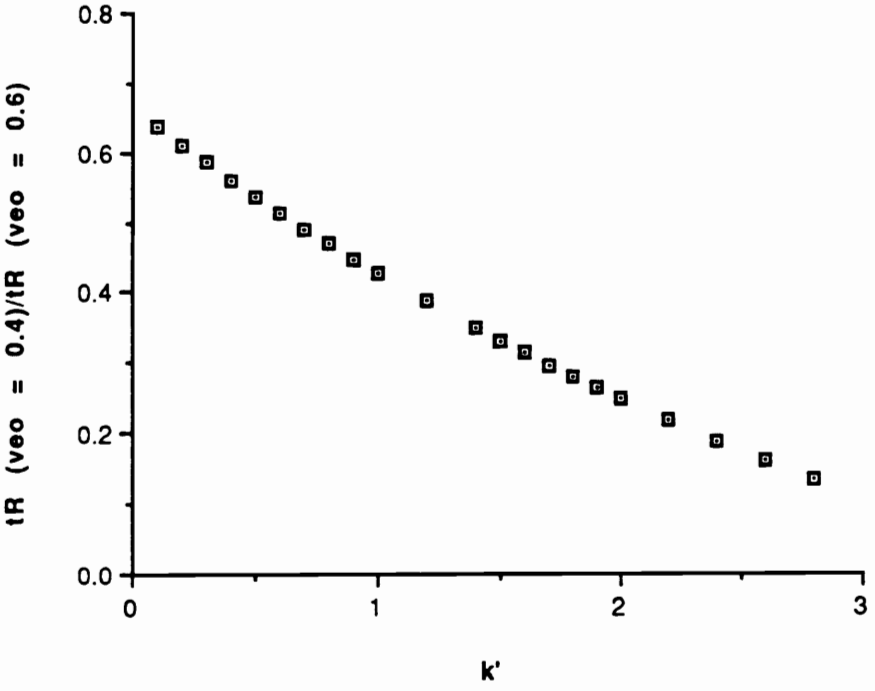

Figure 26. Fractional analysis time required to achieve unit resolution at electroosmotic velocities of 0.4 vs. 0.6 mm s^{-1}. (Assumes H is independent of electroosmotic velocity and that v_{el} = -0.5 mm s^{-1}).

Expressions for H_D and H_{mc} were given by eqns. 37-38. Combined with eqns. 69-70, eqns. 37-38 may be expressed in terms of v_{el} and v_{eo} as:

$$H_D = \frac{2\,(D_m + k'\,D_{mc})}{1 + [(v_{eo} + v_{el})/v_{eo}]\,k'} \quad \frac{1}{v_{eo}} \qquad (78)$$

and

$$H_{mc} = \frac{2\,[1 - (v_{eo} + v_{el})/v_{eo}]^2\,k'}{[1 + k'\,(v_{eo} + v_{el})/v_{eo}]\,(1 + k')^2} \quad \frac{v_{eo}}{k_d} \qquad (79)$$

In accordance with the above, for unit resolution, a comparison of different electroosmotic velocities is better written as:

$$(L/H_A)_{0.6}\, f(k'_1)^2_{0.6} = (L/H_A)_{0.4}\, f(k'_2)^2_{0.4} \qquad (80)$$

Assuming that H_A in each case is diffusion limited (described by eqn. 78), the fractional length of capillary required to effect the same resolution at an electroosmotic velocity of 0.4 as at 0.6 mm s^{-1} may be calculated from eqn. 80. Substituting the resultant value into eqn. 72, provides a comparison of the relative analysis time at each electroosmotic velocity. Interestingly, the ratio of the relative retention times is unity for the entire range of capacity factors studied (0-3). Thus equal resolution is achieved in equal time at both electroosmotic velocities, despite the disparity in the length of capillary required for the separation. For resolution to be improved time effectively at the lower electroosmotic velocity, H_{mc} must therefore be more favorable.

The ratios of H_{mc} at each velocity (Fig. 27) actually show mass transfer to be poorer at the lower electroosmotic velocity. The analysis time required to achieve unit resolution is, therefore, less at the higher electroosmotic velocity (in contrast to Fig. 26). Accordingly, resolution is improved more time effectively, by increasing capillary length, than by decreasing the electroosmotic velocity.

However, since the applied voltage is limited to 50 kV (due to corona discharge [24]), it may not always be possible to create a strong enough electric field in long capillaries. The use of slower electroosmotic flows may therefore prove favorable when the selectivity is poor, and adequate resolution must be obtained by cooptimization of efficiency and the capacity factor dependent terms. When adequate selectivity is possible, it should be possible to develop rapid separations in short capillaries. The choice of an suitable micellar phase, therefore, appears to be the critical step in the development of MEKC analyses.

4.4 Applications

Due to the inherent charge/hydrodynamic radius selectivity and high efficiency of CZE, many separations require no optimization of operating conditions beyond those prescribed as generally suitable in the preceding sections: a 50-100 μm x 50-100 cm fused silica capillary; a 0.01-0.05 M phosphate buffer; an operating voltage of 15 -30 KV; and a limited sample size and concentration as dictated by the efficiency requirement of the separation. For illustration, the separation of sodium cumenesulfonate and

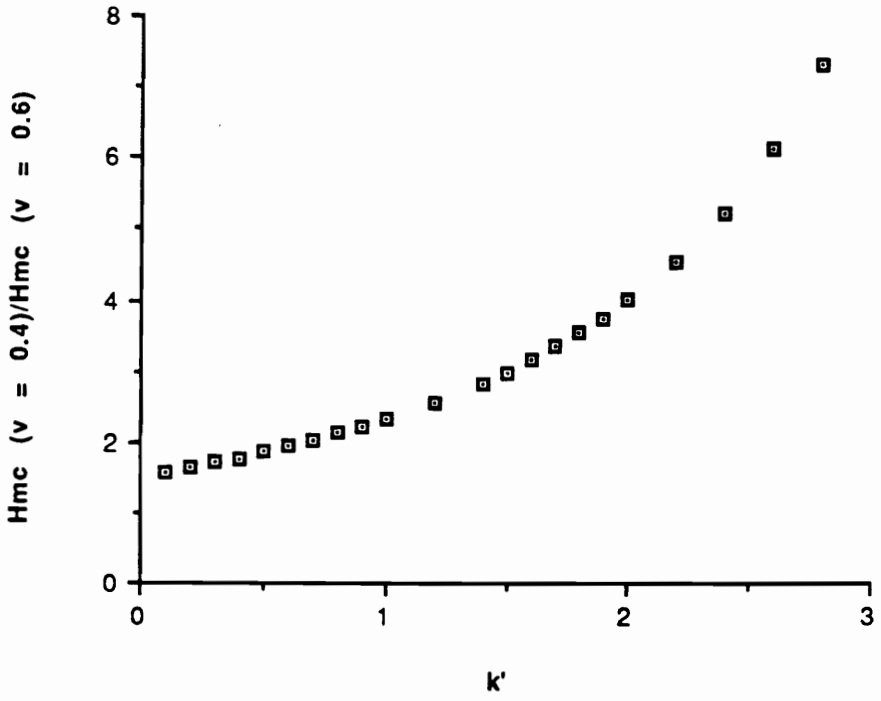

Figure 27. Relative H_{mc} values at electroosmotic velocities of 0.4 vs. 0.6 mm s^{-1}. (Assumes v_{el} = -0.5 mm s^{-1}).

sodium toluenesulfonate, which are used commercially as detergent hydrotopes, is shown in Fig. 28.

4.4.1. Separations of Bipyridinium Salts

The separation of disubstituted bipyridinium salts (Fig. 29 i, iii and v) from their monosubstituted impurities (Fig. 29 ii, iv and vi) was not as straightforward. The separation of a synthetic mixture of 1,1'-bis(2-hydroxyethyl)-4,4'-bipyridinium dibromide and 1-(2-hydroxyethyl)-4,4'-bipyridinium bromide (structures i and ii), obtained in 0.01M Na_2HPO_4, pH 7.00, is shown in Fig. 30. The separation is characterized by severe peak tailing, which was attributed to solute adsorption on the wall of the fused silica capillary.

To minimize solute adsorption, the analysis was repeated in a 0.01 M Na_2HPO_4, pH 3.00, buffer modified with 5.0 mM tetramethylammonium chloride (TMAC). As documented in section 4.2.2., decreasing buffer pH reduces the capillary surface charge and therefore decreases solute/capillary interaction. Quaternary ammonium salts have been shown to adsorb strongly to ionized silanol groups, and should reduce the number of surface sites available for solute adsorption. The electropherogram obtained in the modified pH 3.00 buffer is shown in Fig. 31.

On the basis of five replicate determinations, the ratio of disubstituted to monosubstituted salt was determined to be 16.6 :1 +/-1.62% RSD. Analyses of the same sample, performed under the same conditions in a different capillary yielded a peak ratio of 17.5 :1 +/- 0.98% RSD (n = 4),

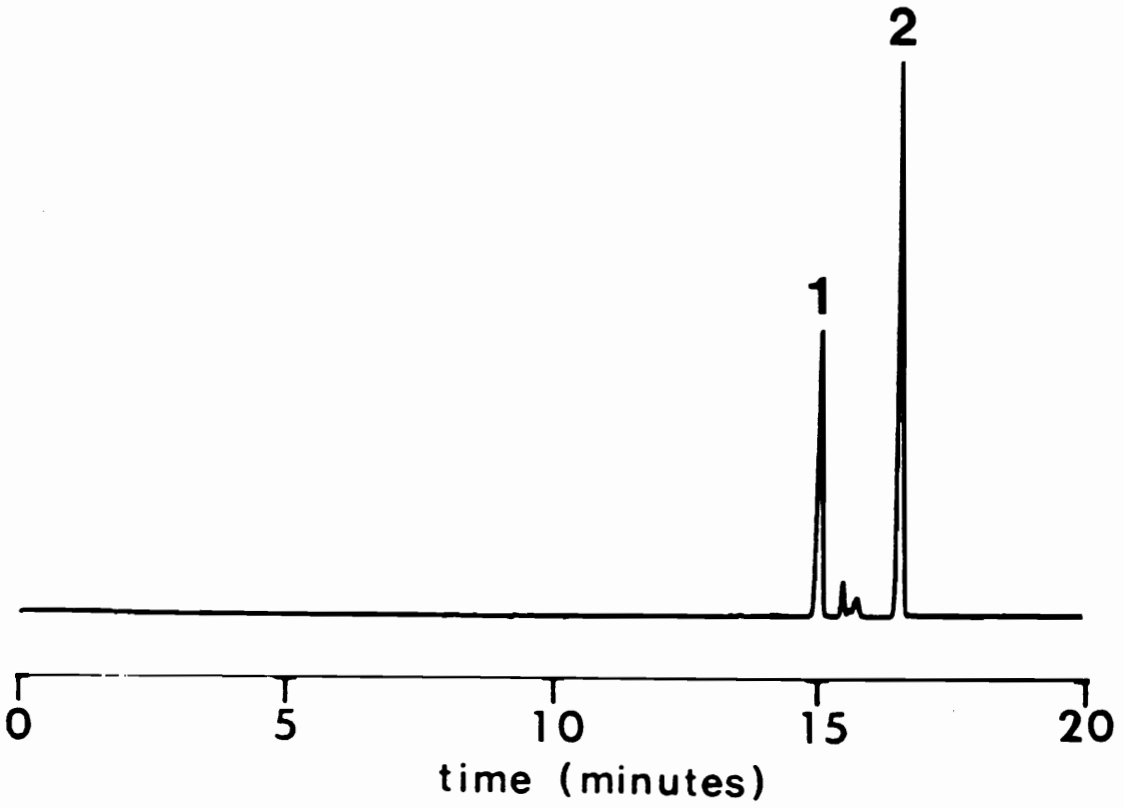

Figure 28. Separation of sodium cumenesulfonate and sodium toluene-sulfonate. Conditions: 100 μm x 100 cm capillary (L = 80cm); 0.01 M Na_2HPO_4, pH 7.00, buffer; + 20 kV applied voltage. 3 kV/ 7 s electrokinetic injection; detection wavelength = 230 nm. Order of elution: 1. sodium cumenesulfonate 2. sodium toluene-sulfonate.

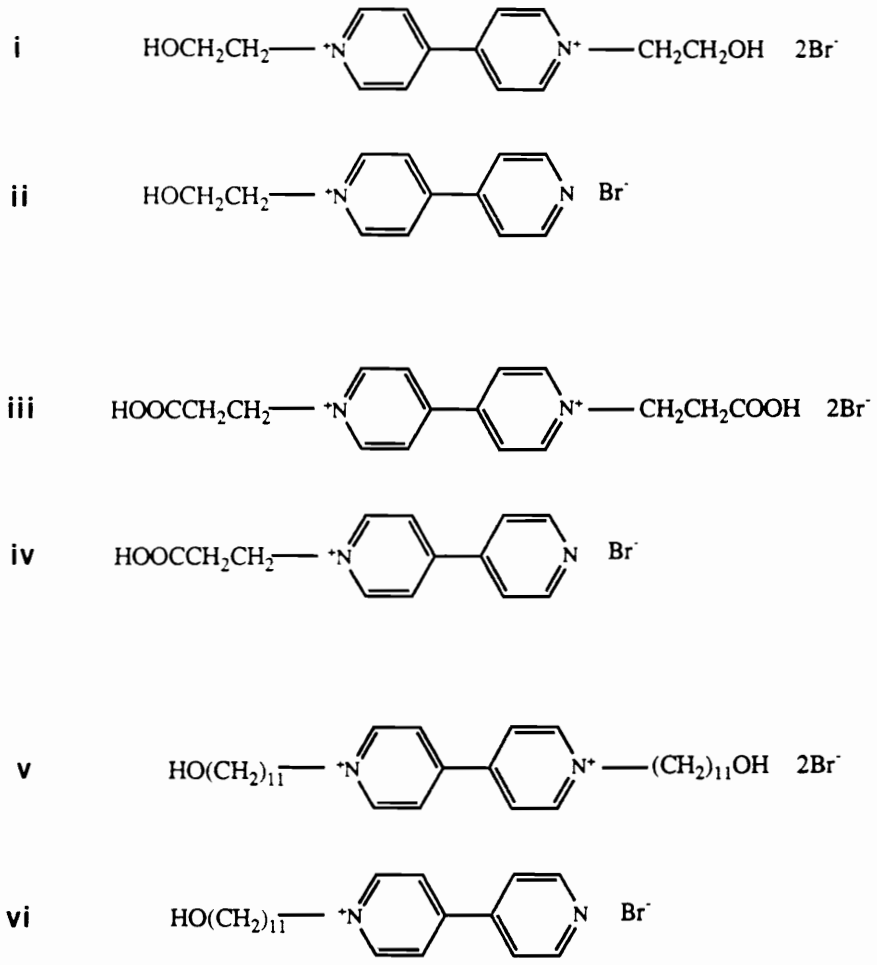

Figure 29. Structures of bipyridinium salts separated in Figs. 30-33.

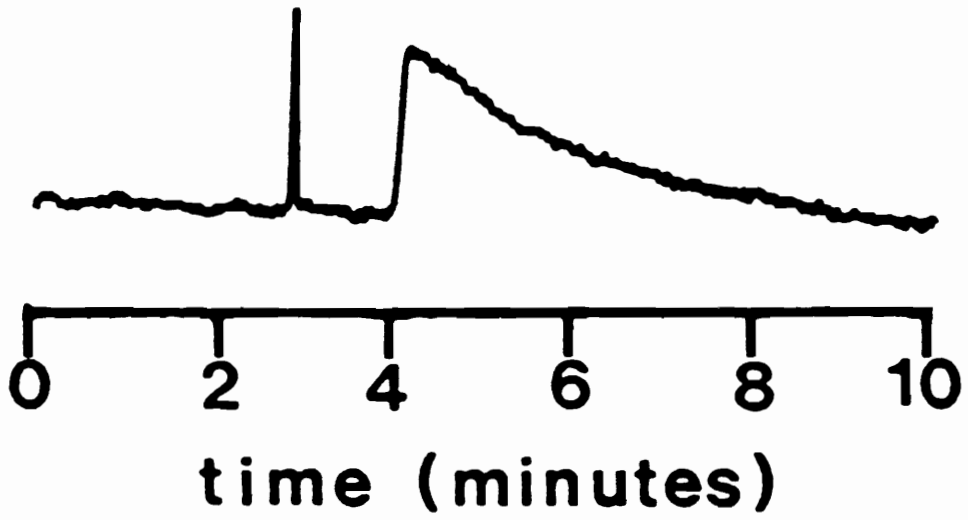

Figure 30. Separation of 1,1'-bis(2-hydroxyethyl)-4,4'-bipyridinium dibromide and 1-(2-hydroxyethyl)-4,4'-bipyridinium bromide (structures i and ii in Fig 29). Conditions: 100 μm x 71 cm capillary (L = 48 cm); 0.01 M Na_2HPO_4, pH 7.00, buffer; + 20 kV applied voltage; injection by siphoning at 3.8 cm/7 s; detection wavelength = 254 nm.

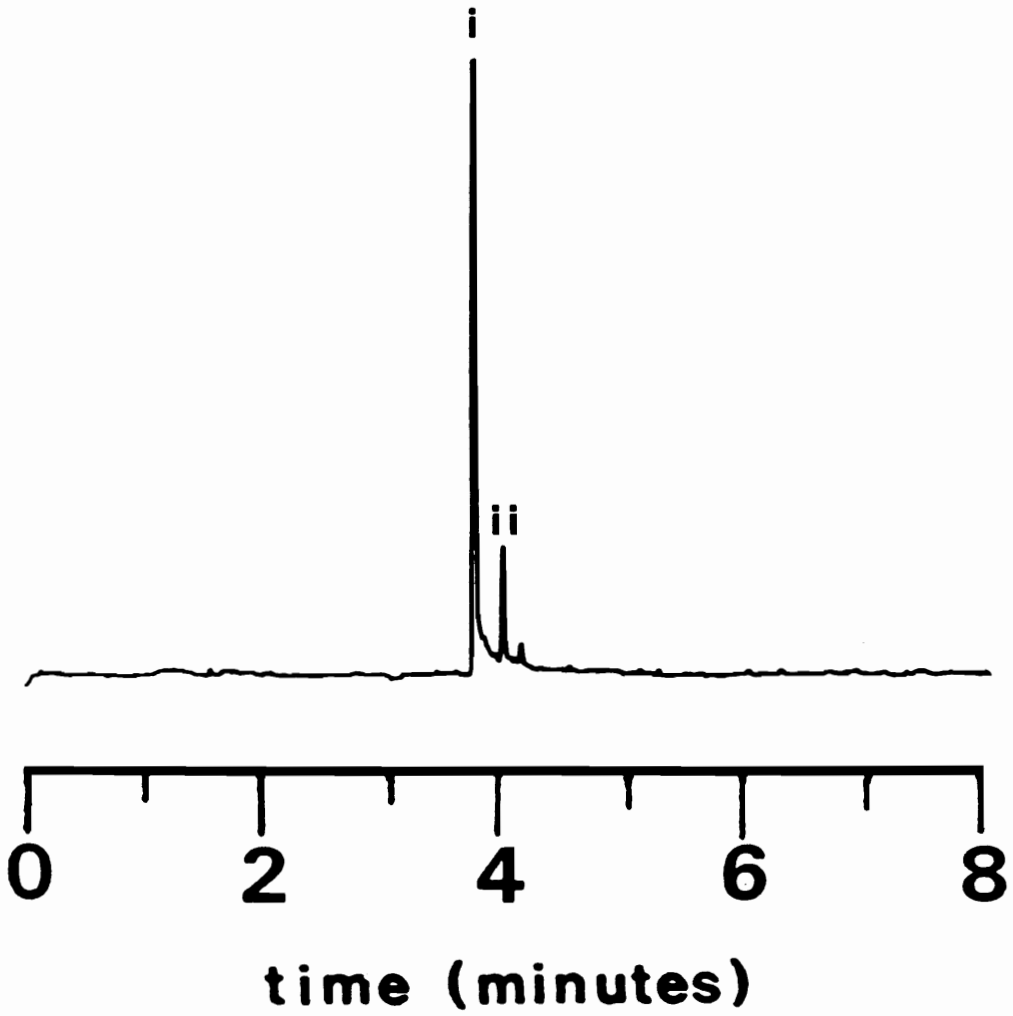

Figure 31. Separation of 1,1'-bis(2-hydroxyethyl)-4,4'-bipyridinium dibromide and 1-(2-hydroxyethyl)-4,4'-bipyridinium bromide (structures i and ii in Fig 29) in a modified buffer. Conditions: 100 μm x 75 cm capillary (L = 50cm); 0.01 M Na_2HPO_4/0.005 M TMAC, pH 3.00, buffer; + 20 kV applied voltage; injection by siphoning at 3.8 cm/7s; detection wavelength = 254 nm.

indicating fairly good capillary to capillary reproducibility. The quantitative data are in good agreement with results obtained by NMR [118], and indicate that the method may be used for the rapid evaluation of monomer purity. Obtaining pure disubstituted 4,4'-bipyridinium dibromides is a prerequisite for efficient step growth polymerization. It is, therefore, desirable to be able to monitor monomer purity prior to polymerization. Analyses performed following recrystalization in acetonitrile/ethanol resulted in a peak ratio of 34:1 +/- 8.3% RSD (n = 4), indicating that such purification was of limited efficacy.

The same buffering system was additionally applied to the separation of 1,1'-bis(2-carboxyethyl)-4,4'-bipyridinium dibromide/1-(2-carboxyethyl)-4-4'-bipyridinium bromide (compounds iii and iv), as shown in Fig. 32. On the basis of two sets of five replicate determinations, performed in different capillaries, the ratio of disubstituted to monosubstituted salt was determined to be 2.04 +/-1.53% RSD and 1.89 +/- 1.91% RSD, respectively.

For the analysis of 1,1'-bis(11-hydroxyundecyl)-4,4'-bipyridinium dibromide/1-(11-hydroxyundecyl) 4,4'-bipydinium bromide (compounds v and vi), the sample was insoluble in the aqueous buffer, and it was necessary to modify the buffer with methanol. The electropherogram obtained in 50/50 (v/v) 0.01 M Na_2HPO_4, 5.0 mM (TMAC), pH 3.00/ methanol is shown in Fig. 33. The use of methanol indicates that CZE is not limited to strictly aqueous buffers [40,77]. This is an important attribute, since it effectively extends the applicability of CZE to more hydrophobic samples.

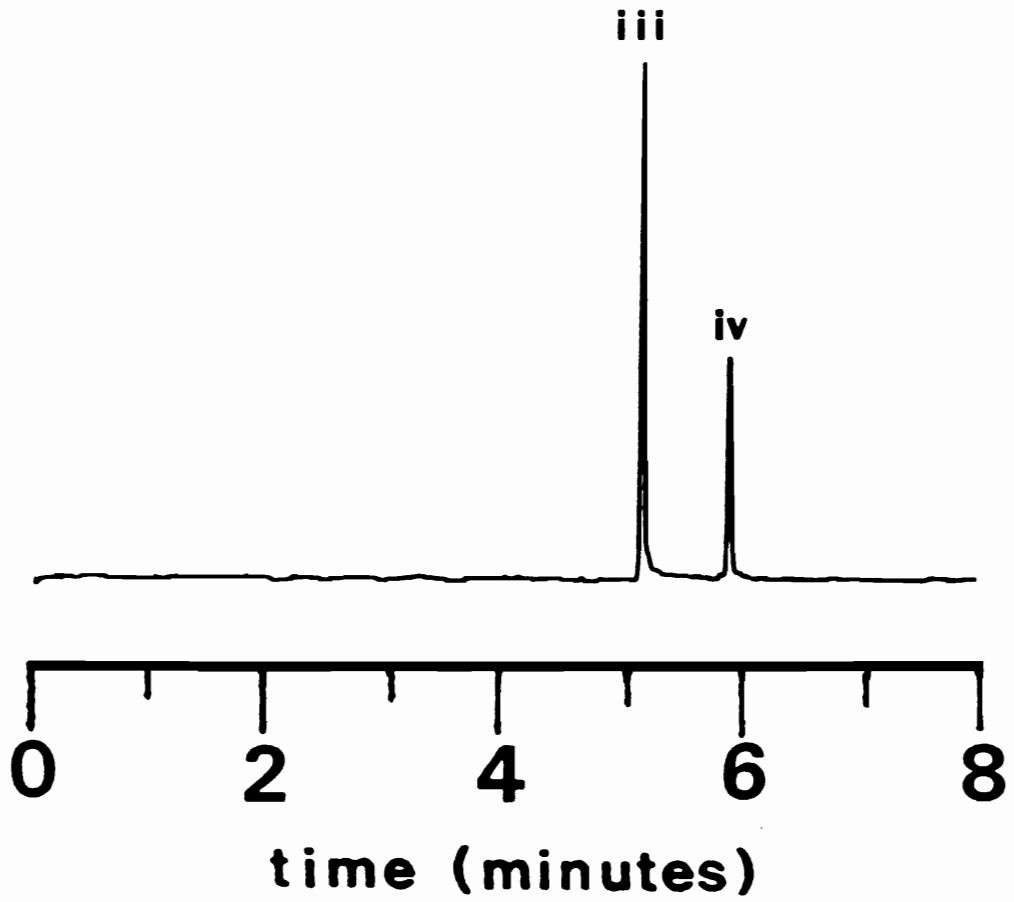

Figure 32. Separation of 1,1'-bis(2-carboxyethyl)-4,4'-bipyridinium dibromide and 1-(2-carboxyethyl)-4,4'-bipyridinium bromide (structures iii and iv in Fig 29). Conditions are as in Fig. 31.

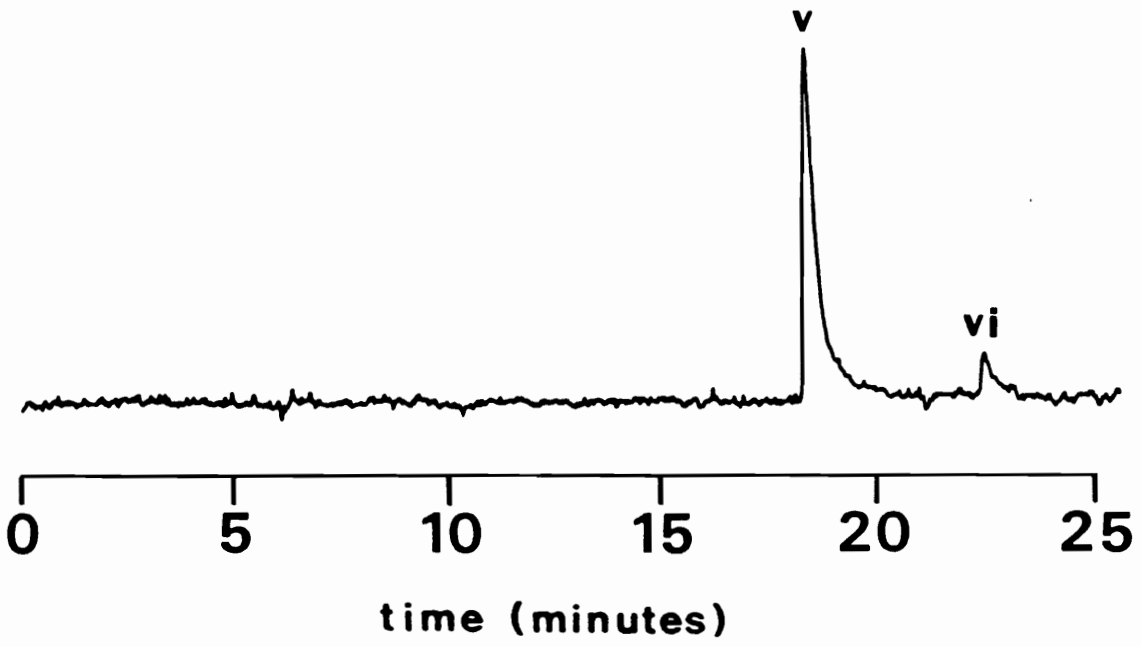

Figure 33. Separation of 1,1'-bis(11-hydroxyundecyl)-4,4'-bipyridinium dibromide and 1-(11-hydroxyundecyl)-4,4'-bipyridinium bromide (structures v and vi in Fig 29). Conditions are as in Fig. 31, except that the buffer was 50/50 (v/v) methanol/0.01 M Na_2HPO_4, 0.005 M TMAC, pH 3.00.

4.4.2. Separations of Pharmaceuticals.

CZE was also used for the analyses of structurally similar pharmaceuticals. The separation of Zidovudine and Trifluridine is shown in Fig. 34. In the pH 7.00 buffer, Trifluridine (pKa = 7.85) is partially ionized and therefore migrates at a slower net velocity than Zidovudine (pKa = 9.68).

MEKC was used for the separation of Allopurinol, Thioguanine, Acyclovir and Mercaptopurine. As shown in Table VIII, these are chemically similar pharmaceuticals with different pKas. Separation (Fig. 35) is based on both variability in the charge to size ratio of each species and on differences in the partition coefficients of each species between micellar SDS and the aqueous phase.

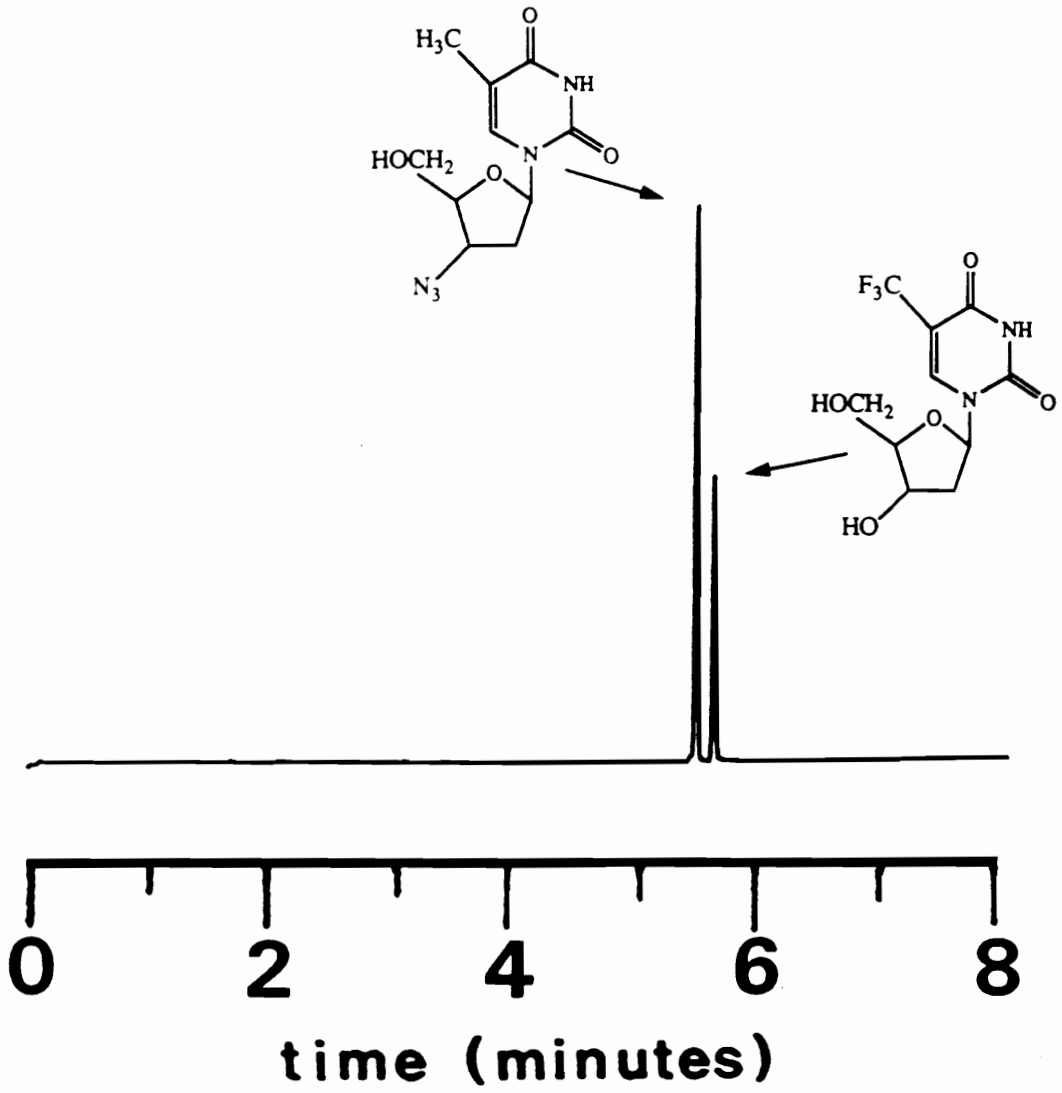

Figure 34. Separation of Zidovudine and Trifluridine. Conditions: 100 µm x 70 cm capillary (L = 50 cm); 0.01 M Na_2HPO_4, pH 7.00, buffer; + 20 kV applied voltage; injection by siphoning at 3.8 cm/7 s; detection wavelength = 254 nm. Order of elution: 1. Zidovudine 2. Trifluridine.

Table VIII. Structures and pKas of pharmaceuticals separated in Fig. 35.

Compound	Structure	pKa(s)
Allopurinol	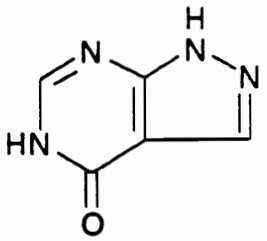	10.2
Thioguanine	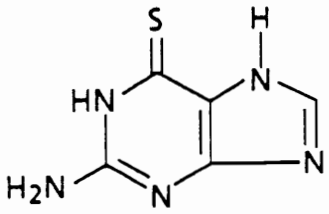	8.0
Acyclovir	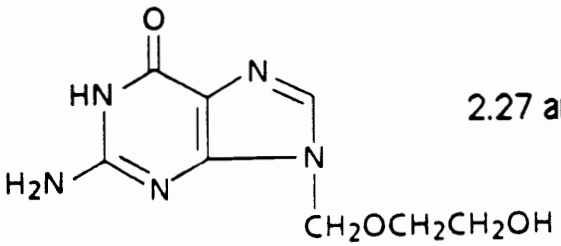	2.27 and 9.25
Mercaptopurine	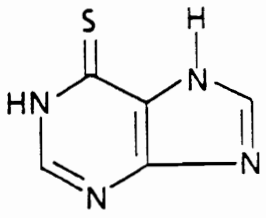 • H_2O	7.8

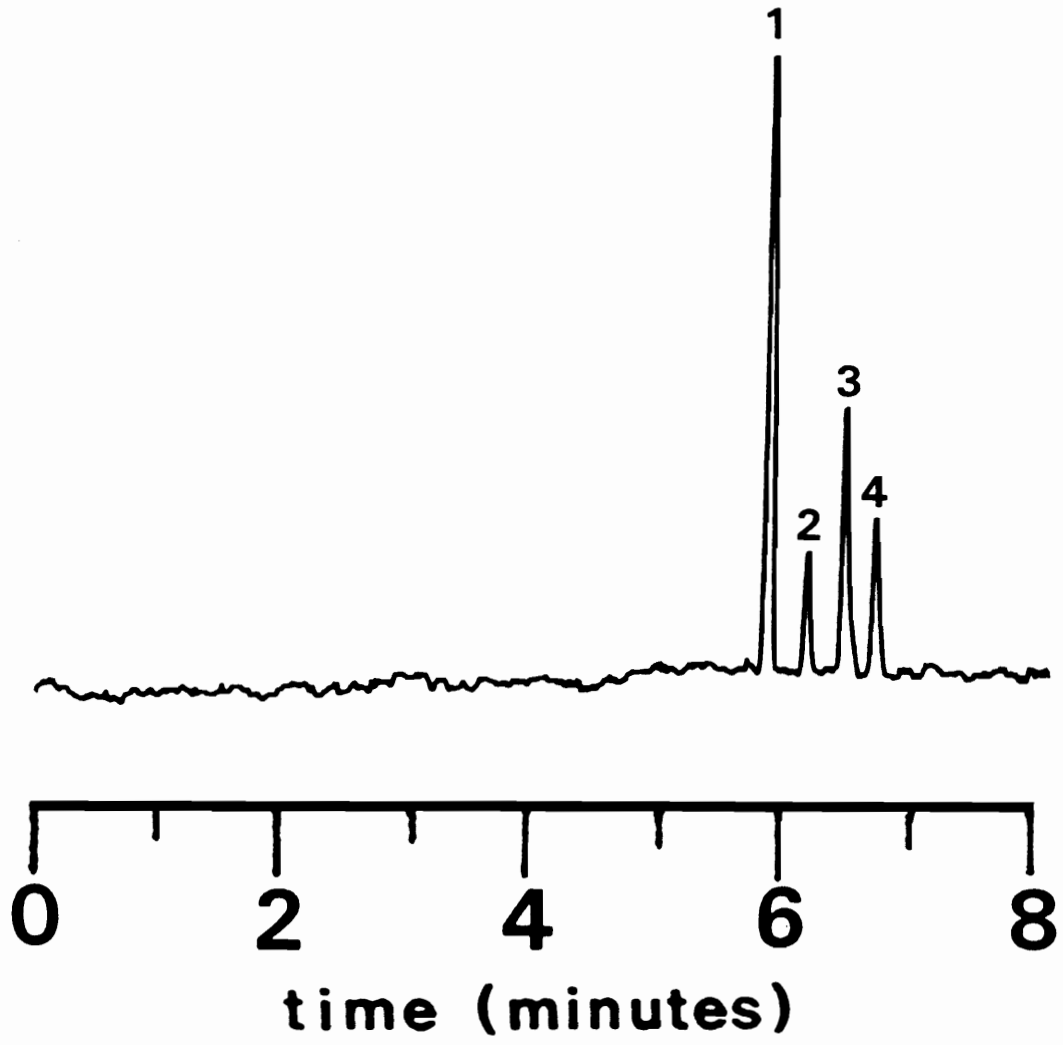

Figure 35. MEKC separation of Allopurinol, Thioguanine, Acyclovir and Mercaptopurine. Conditions: 100 µm x 70 cm capillary (L = 50 cm); 0.075 M SDS/0.01 M Na_2HPO_4, pH 7.00, buffer; + 20 kV applied voltage; injection by siphoning at 3.8 cm/7 s; detection wavelength = 220 nm. Order of elution: 1. Allopurinol 2. Thioguanine 3. Acyclovir 4. Mercaptopurine.

CHAPTER V

CONCLUSIONS

Separations based on the electrokinetic phenomena of electrophoresis and electroosmosis have been shown to provide excellent separation efficiencies. For small solutes such as phenol and caffeine, analyzed by CZE, efficiencies in excess of 250,000 theoretical plates were obtained in analysis times of less than 5 minutes. The high efficiencies are attributed to the transport properties of electroosmosis and electrophoresis. In contrast to pumped flow, electrokinetic processses provide a flat flow profile, and thereby minimize band broadening stemming from mass transfer.

To obtain high efficiencies additional sources of variance must, however, be minimized. In practice this dictates minimizing the diameter of the capillary employed for the separation, and limiting both the sample size and sample concentration. These latter criteria limit detectability of many species. It is therefore important in many applications to either cooptimize efficiency and detectability or to reduce the efficiency requirement of a separation by increasing resolution through the relative velocity difference.

The use of forced air convection, to dissipate the Joule heat generated in larger capillaries, has been shown here to minimize the losses in efficiency incurred as larger capillaries are employed, and may be used to effect a more favorable relationship between efficiency and detectability. The relative velocity difference between two zones may be increased by decreasing the electroosmotic flow velocity. This may achieved experimentally by either increasing the buffer concentration or decreasing

buffer pH. Decreasing the electroosmotic flow, however, reduces the net solute velocity and therefore separation efficiency. As a result, the improvement in total resolution may be insignificant.

A further detriment of decreasing the relative velocity difference or employing forced air convection is that the improved resolution is obtained at the expense of analysis time. To overcome this limitation, and thereby optimize electrokinetic separations with respect to both resolution and analysis time, the use of secondary equilibria with charged micelles was also evaluated. The MEKC studies conducted here focused primarily on the separation of neutral species. However, applicability to the separation of ionic compounds (pharmaceuticals) was also demonstrated (Fig. 35).

A particularly attractive property of micellar systems is illustrated by the selectivity differences between SDS and SDS modified with Brij 35. The difference in retention behavior in each system, shows that selectivity may be changed by changing the nature of the surfactant's polar head group. This suggests that if a suitable micellar phase can be found for a given separation problem, rapid analyses should be possible. In the optimized separation of ASTM test mix LC-79-2 (Fig. 22.c), complete resolution between the six sample components was achieved in less than 6 minutes.

Typical separation efficiencies for MEKC were in the order of 150,000 theoretical plates/50 cm. The favorable mass transfer observed in CZE is thus essentially maintained in micellar media. On the basis of efficiency MEKC appears to be a favorable alternative to conventional HPLC. Replacing the conventional HPLC stationary phase with a secondary phase which is itself mobile, however, introduces an additional term (t_0/t_{mc}) into the

master resolution equation. Using SDS in 0.01 M Na_2HPO_4, pH 7.00, as the separation media, the t_0/t_{mc} ratio is 0.291. As a result the resolution obtainable in MEKC, generating 150,000 theoretical plates, is roughly equivalent to the resolution provided by a 15 cm HPLC column packed with 5 μm particles.

To improve resolution in MEKC the electroosmotic flow may be reduced, by decreasing buffer pH, to provide a more favorable t_0/t_{mc} ratio. Alternatively longer capillaries may be employed. While both of these procedures increase the total analysis time, the use of longer capillaries is shown here to be the more time effective means of improving separation when resolution beyond that provided by selectivity is required.

Using the guidelines for CZE and MEKC outlined in this work separations were developed for model analytes, as well as for several industrial samples. For CZE, method development is generally simpler than for HPLC due the abscence of a secondary equilibrium. For MEKC, method development is contingent on choosing the appropriate concentration of a suitable micellar phase. The methods developed showed excellent run to run reproducibility (< 1% RSD); quantitative reproducibility using an internal standard was typically about 3% RSD. Larger variations in migration times were observed on different days or in different capillaries. This indicates that it is important to control both the temperature and the surface characteristics of the fused silica capillaries employed for the analysis.

REFERENCES

1. O. Vesterberg, *J. Chromatogr.*, 480 (1989) 3.

2. J. W. Jorgenson, *Anal. Chem.*, 58 (1986) 743 A.

3. F. E. P. Mikkers, F. M. Everaerts and Th. P. E. M. Verheggen, *J. Chromatogr.*, 169 (1979) 11.

4. J. W. Jorgenson and K. D. Lukacs, *Anal. Chem.*, 53 (1981) 1298.

5. J. W. Jorgenson and K. D. Lukacs, *Science*, 222 (1983) 266.

6. P. W. Atkins, *Physical Chemistry*, 2nd ed., W. H. Freeman and Co., San Francisco (1982), Chapter 26.

7. G. H. Bolt, *J. Phys. Chem.*, 61 (1957) 1166.

8. D. J. Shaw, *Introduction to Colloid and Surface Chemistry*, 3rd ed., Butterworths, London, England (1980), Chapter 7.

9. C. L. Rice and R. Whitehead, *J. Phys. Chem.*, 69 (1965) 4017.

10. M. Martin, G. Guiochon, Y. Walbroehl and J. W. Jorgenson, *Anal. Chem.*, 57 (1985) 559.

11. S. Terabe, K. Otsuka, K. Ichikawa, A. Tsuchiya and T. Ando, *Anal. Chem.*, 56 (1984) 111.

12. S. Terabe, K. Otsuka and T. Ando, *Anal. Chem.*, 57 (1985) 834.

13. K. Otsuka, S. Terabe and T. Ando, *J. Chromatogr.*, 332 (1985) 219.

14. D. E. Burton, M. J. Sepaniak and M. P. Maskarinec, *J. Chromatogr. Sci.*, 25 (1987) 514.

15. J. Liu, J. F. Banks and M. Novotny, *J. Microcolumn Sep.*, 1 (1989) 136.

16. R. A. Wallingford and A. G. Ewing, *J. Chromatogr.*, 441 (1988) 299.

17. S. A. Swedberg, *J. Chromatogr.*, 503 (1990) 449.

18. J. R. Sargent and S. G. George, *Methods in Zone Electrophoresis*, 3rd ed., BDH Chemicals Ltd., Poole, England (1975), Chapter 1.

19. A. Tiselius, *Trans. Faraday Soc.*, 33 (1937) 524.

20. S. Hjerten, *Chromatogr. Rev.*, 9 (1967) 122.

21. P. H. Rhodes in *Electrophoresis '81*, R. C. Allen and P. Arnaud (Eds.), deGruyter, Berlin (1981), pp. 919-932.

22. Th. P. E. M. Verheggen, F. E. P. Mikkers and F. M. Everaerts, *J. Chromatogr.*, 132 (1977) 205.

23. J. C. Giddings, *Sep. Sci.*, 4 (1969) 181.

24. J. H. Knox, *Chromatographia*, 26 (1988) 329.

25. F. Foret, M. Deml and P. Bocek, *J. Chromatogr.*, 452 (1988) 601.

26. E. Grushka, R. M. McCormick and J. J. Kirkland, *Anal. Chem.*, 61 (1989) 241.

27. J. C. Sternberg, *Adv. Chromatogr.*, 2 (1966) 205.

28. Y. Walbroehl, *Ph. D. Dissertation*, University of North Carolina, Chapel Hill (1986).

29. F. E. P. Mikkers, F. M. Everaerts and Th. P. E. M. Verheggen, *J. Chromatogr.*, 169 (1979) 1.

30. K. D. Lukacs and J. W. Jorgenson, *J. High Resolut. Chromatogr. Chromatogr. Commun.*, 8 (1985) 407.

31. J. C. Giddings, *J. Chromatogr.*, 5 (1961) 46.

32. J. C. Giddings, *Dynamics of Chromatography*, Marcel Dekker, New York (1965), Chapters 2-4.

33. S. Hjerten, *J. Chromatogr.*, 347 (1985) 191.

34. G. J. M. Bruin, J. P. Chang, R. H. Kuhlman, K. Zegers, J. C. Kraak and H. Poppe, *J. Chromatogr.*, 471 (1989) 429.

35. D. J. Rose, *Ph. D. Dissertation*, University of North Carolina, Chapel Hill (1988).

36. R. M. McCormick, *Anal. Chem.*, 60 (1988) 2322.

37. H. H. Lauer and D. McManigill, *Anal. Chem.*, 58 (1986) 166.

38. J. S. Green and J. W. Jorgenson, *J. Chromatogr.*, 478 (1989) 63.

39. M. M. Bushey and J. W. Jorgenson, *J. Chromatogr.*, 480 (1989) 301.

40. Y. Wahlbroehl and J. W. Jorgenson, *J. Chromatogr.*, 315 (1984) 135.

41. F. Foret, M. Deml, V. Kahle and P. Bocek, *Electrophoresis*, 7 (1986) 430.

42. I. H. Grant and W. Steuer, *J. Microcol. Sep.*, 2 (1990) 74.

43. J. S. Green and J. W. Jorgenson, *J. Chromatogr.*, 352 (1986) 337.

44. B. Nickerson and J. W. Jorgenson, *J. High Resolut. Chromatogr. Chromatogr. Commun.*, 11 (1988) 878.

45. Y. F. Cheng and N. J. Dovichi, *Science*, 242 (1988) 562.

46. M. C. Roach, P. Gozel and R. N. Zare, *J. Chromatogr.*, 426 (1988) 129.

47. B. W. Wright, G. A. Ross and R. D. Smith, *J. Microcol. Sep.*, 1 (1989) 85.

48. X. Huang, T. K. J. Pang, M. J. Gordon and R. N. Zare, *Anal. Chem.*, 59 (1987) 2747.

49. X. Huang, J. A. Luckey, M. J. Gordon and R. N. Zare, *Anal. Chem.*, 61 (1989) 766.

50. R. A. Wallingford and A. G. Ewing, *Anal. Chem.*, 59 (1987) 1762.

51. R. A. Wallingford and A. G. Ewing, *Anal. Chem.*, 60 (1988) 1972.

52. R. A. Wallingford and A. G. Ewing, *Anal. Chem.*, 61 (1989) 98.

53. S. L. Pentoney, R. N. Zare and J. F. Quint, *Anal. Chem.*, 61 (1989) 1642.

54. J. A. Olivares, N. T. Nguyen, C. R. Yonker, and R. D. Smith, *Anal. Chem.*, 59 (1987) 1230.

55. R. D. Smith, C. J. Barinaga and H. R. Udseth, *Anal. Chem.*, 60 (1988) 1948.

56. E. D. Lee, W. Muck, J. D. Henion and T. R. Covey, *J. Chromatogr.*, 458 (1988) 313.

57. M. Jansson, A. Emmer and J. Roeraade, *J. High Resolut. Chromatogr. Chromatogr. Commun.*, 12 (1989) 797.

58. W. H. Wilson, H. T. Rasmussen and H. M. McNair, presented at the *1990 Pittsburgh Conference and Exposition on Analytical Chemistry and Applied Spectroscopy, New York, NY, March 1990,* paper No. 1041.

59. M. M. Bushey and J. W. Jorgenson, *Anal. Chem.*, 62 (1990) 978.

60. D. J. Rose and J. W. Jorgenson, *J. Chromatogr.*, 447 (1988) 117.

61. S. L. Pentoney, X. Huang, D. S. Burgi and R. N. Zare, *Anal. Chem.*, 60 (1988) 2625.

62. S. Honda, S. Iwasa and S. Fujiwara, *J. Chromatogr.*, 404 (1987) 313.

63. D. J. Rose and J. W. Jorgenson, *Anal. Chem.*, 60 (1988) 642.

64. J. Tehrani, L. Day and R. Macomber in *Proc. of the Eleventh International Symposium on Capillary Chromatography,* P. Sandra and G. Redant, eds., Huethig Verlag, Heidelberg, FRG (1990). pp 899-912.

65. S. E. Moring, J. C. Colburn, P. D. Grossman and H. H. Lauer, *LC-GC,* 8 (1990) 34.

66. D. J. Rose and J. W. Jorgenson, *J. Chromatogr.*, 438 (1988) 23.

67. X. Huang and R. N. Zare, *Anal. Chem.*, 62 (1990) 443.

68. R. J. Nelson, A. Paulus, A. S. Cohen, A. Guttman and B. L. Karger, *J. Chromatogr.*, 480 (1990) 111.

69. B. B. VanOrman and G. L. McIntire, *J. Microcol. Sep.*, 1 (1989) 289.

70. P. D. Grossman, K. J. Wilson, G. Petrie and H. H. Lauer, *Anal. Biochem.*, 173 (1988) 265.

71. W. G. Kuhr and E. S. Yeung, *Anal. Chem.*, 60 (1988) 1832.

72. Y. Walbroehl and J. W. Jorgenson, *J. Microcolumn Sep.*, 1 (1989) 41.

73. P. D. Grossman, J. C. Colburn, H. H. Lauer, R. G. Nielsen, R. M. Riggin, G. S. Sittampalam and E. C. Rickard, *Anal. Chem.*, 61 (1989) 1186.

74. T. Tsuda, Y. Kobayashi, A. Hori, T. Matsumoto and O. Suzuki, *J. Microcol. Sep.*, 2 (1990) 21.

75. A. Zhu and Y. Chen, *J. Chromatogr.*, 470 (1989) 251.

76. W. M. Muck and J. D. Henion, *J. Chromatogr.*, 495 (1989) 41.

77. S. Fujiwara and S. Honda, *Anal. Chem.*, 59 (1987) 487.

78. P. Gozel, E. Gassmann H. Michelsen and R. N. Zare, *Anal. Chem.*, 59 (1987) 44.

79. E. Gassman, J. E. Kuo and R. N. Zare, *Science*, 230 (1985) 813.

80. S. Fanali, L. Ossicini, F. Foret and P. Bocek, *J. Microcolumn Sep.*, 1 (1989) 190.

81. H. T. Rasmussen and H. M. McNair, *J. High Resolut. Chromatogr. Chromatogr. Commun.*, 12 (1989) 635.

82. S. Otsuka and S. Terabe, *J. Microcolumn Sep.*, 1 (1989) 150.

83. S. Terabe, H. Otsumi, K. Otsuka, T. Ando, T. Inomata, S. Kuze and Y. Hanaoka, *J. High Resolut. Chromatogr. Chromatogr. Commun.*, 9 (1986) 666.

84. A. T. Balchunas and M. J. Sepaniak, *Anal. Chem.*, 59 (1987) 1466.

85. J. A. Lux, H. Yin and G. Schomburg, *J. High Resolut. Chromatogr.*, 13 (1990) 145.

86. K. Otsuka, S. Terabe and T. Ando, *J. Chromatogr.*, 348 (1985) 39.

87. D. F. Swaile, D. E. Burton, A. T. Balchunas and M. J. Sepaniak, *J. Chromatogr. Sci.*, 26 (1988) 406.

88. D. E. Burton, M. J. Sepaniak and M. P. Maskarinec, *J. Chromatogr. Sci.*, 24 (1986) 347.

89. S. Fujiwara, S. Iwase and S. Honda, *J. Chromatogr.*, 447 (1988) 133.

90. R. A. Wallingford and A. G. Ewing, *Anal. Chem.*, 60 (1988) 258.

91. T. Saitoh, H. Hoshino and T. Yotsuyanagi, *J. Chromatogr.*, 469 (1989) 175.

92. A. Dobashi, T. Ono, S. Hara and J. Yamaguchi, *Anal. Chem.*, 61 (1989) 1984.

93. H. Nishi, N. Tsumagari, T. Kakimoto and S. Terabe, *J. Chromatogr.*, 465 (1989) 331.

94. H. Nishi, N. Tsumagari, T. Kakimoto and S. Terabe, *J. Chromatogr.*, 477 (1989) 259.

95. H. Nishi, N. Tsumagari and S. Terabe, *Anal. Chem.*, 61 (1989) 2434.

96. M. M. Bushey and J. W. Jorgenson, *Anal. Chem.*, 61 (1989) 491.

97. J. Gorse, A. T. Balchunas, D. F. Swaile and M. J. Sepaniak, *J. High Resolut. Chromatogr. Chromatogr. Commun.*, 11 (1988) 554.

98. A. S. Cohen, S. Terabe, J. A. Smith and B. L. Karger, *Anal. Chem.*, 59 (1987) 1021.

99. R. A. Wallingford, P. D. Curry and A. G. Ewing, *J. Microcolumn Sep.*, 1 (1989) 23.

100. H. T. Rasmussen, L. K. Goebel and H. M. McNair, *J. Chromatogr.*, 516 (1990) 223.

101. S. Terabe, K. Otsuka and T. Ando, *Anal. Chem.*, 61 (1989) 251.

102. M. J. Sepaniak and R. O. Cole, *Anal. Chem.*, 59 (1987) 472.

103. J. M. Davis, *Anal. Chem.*, 61 (1989) 2455.

104. T. Tsuda, T. Mizuno and J. Akiyama, *Anal. Chem.*, 59 (1987) 799.

105. M. Deml, F. Foret and P. Bocek, *J. Chromatogr.*, 320 (1985) 159.

106. X. Huang, M. J. Gordon and R. N. Zare, *Anal. Chem.*, 60 (1988) 375.

107. T. Tsuda, K. Nomura and G. Nakagawa, *J. Chromatogr.*, 264 (1983) 385.

108. Subcommittee E-19.08 Task Group on Liquid Chromatography of the American Society for Testing and Materials, *J. Chromatogr. Sci.*, 19 (1981) 338.

109. M. F. Borgerding and W. L. Hinze, *Anal. Chem.*, 57 (1985) 2183.

110. K. D. Altria and C. F. Simpson, *Chromatographia*, 24 (1987) 527.

111. W. J. Lambert and D. L. Middleton, *Anal. Chem.*, 62 (1990) 1585.

112. K. D. Altria and C. F. Simpson, *Anal. Proc.*, 23 (1986) 453.

113. H. T. Rasmussen and H. M. McNair, *J. Chromatogr.*, in press.

114. J. J, DeStefano and J. J. Kirkland, *Anal. Chem.*, 47 (1975) 1193 A.

115. L. R. Snyder, J. L. Glajch and J. J. Kirkland, *Practical HPLC Method Development*, John Wiley and Sons, Inc., New York, 1988, Ch. 4.

116. M. J. Rosen, *Surfactants and Interfacial Phenomena*, John Wiley and Sons, Inc., New York, 2nd ed., 1989, Ch. 3.

117. R. Nagarajan, M. A. Chaiko and E. Ruckenstein, *J. Phys. Chem.*, 88 (1984) 2916.

118. *Personal Communication* P. T. Engen, Virginia Tech.

APPENDIX

Summary of Abbreviations

A	peak area
a	radial distance from the capillary axis
C	electrolyte concentration
CMC	Critical Micelle Concentration
CZE	Capillary Zone Electrophoresis
D_a	diffusion coefficient of a solute in an aqueous phase
D_{mc}	diffusion coefficient of a solute in a micellar phase
d	intermicelle distance
d_c	capillary internal diameter
DMT	dimethyl terephthalate
E	electric field strength
e	charge of an electron (-1.60219×10^{-19} C)
F	force
g	gravitational acceleration constant
GC	Gas Chromatography
H	height equivalent of a theoretical plate
H_A	total height equivalent of a theoretical plate
H_C	height equivalent of a theoretical plate contribution from mass transfer at the capillary wall
H_D	height equivalent of a theoretical plate contribution from solute diffusion
H_I	height equivalent of a theoretical plate contribution from intermicelle mass transfer
H_i	an independent contribution to the total height equivalent of a theoretical plate
H_L	height equivalent of a theoretical plate contribution from mass transfer in the aqueous phase
H_M	height equivalent of a theoretical plate contribution from mass transfer
H_{mc}	height equivalent of a theoretical plate contribution from micelle sorption-desorption kinetics
H_P	height equivalent of a theoretical plate contribution from micelle polydispersity
H_S	height equivalent of a theoretical plate contribution from sample volume

H_T	height equivalent of a theoretical plate contribution from Joule heating
h	peak height
Δh	height difference between buffer reservoirs
HPCE	High Performance Capillary Electrophoresis
HPLC	High Performance Liquid Chromatography
I_0	zero order Bessel function of the first kind
i. d.	capillary internal diameter
K	partition coefficient
k'	capacity factor
k_d	solute desorption rate constant from the micellar phase
L	length of solute migration
L_T	total capillary length
MEKC	Micellar Electrokinetic Chromatography
N	number of theoretical plates (efficiency)
n	number of determinations
n_{aq}	number of moles of solute in the aqueous phase
n_{mc}	number of moles of solute in the micellar phase
R_s	resolution
r	capillary internal radius
r_h	hydrodynamic radius of a solvated ion
RSD	Relative Standard Deviation
S	sample volume
SDS	sodium dodecyl sulfate
STS	sodium decyl sulfate
t	time
t_a	relative time the solute spends adsorbed to the capillary wall
t_b	breakthrough time
t_c	relative time the solute spends in the aqueous phase
t_d	mean adsorption time of an analyte on the capillary wall
t_{mc}	retention time of a solute which distributes exclusively into the micellar phase
t_R	solute retention time or solute migration time
t_s	sampling time
t_0	retention time of a solute which distributes exclusively into the aqueous phase
V	applied voltage
V_s	sampling voltage

V_0	separation voltage
v_{el}	electrophoretic velocity
v_{eo}	electroosmotic flow velocity
v_{mc}	velocity of the micellar phase
v_{net}	net solute velocity
v_{sf}	velocity resulting from hydrodynamic flow
v_0	velocity of the aqueous phase
W	detector slit width
x	length of sample plug introduced
y	fraction of H_A stemming from H_S
z	charge of a species
α	selectivity
B	ratio of the volume of the aqueous phase to the volume of micellar phase
ε	dielectric constant
ζ	zeta potential
η	viscosity
κ	thermal conductivity
κ_d	reciprocal of the electric double layer thickness
λ	molar conductivity
μ_{el}	coefficient of electrophoretic migration
μ_{eo}	coefficient of electroosmotic flow
ρ	density
σ_x^2	spatial variance of a solute band
ϕ	fractional change in net migration velocity per Kelvin
ω	polydispersity constant

VITA

Henrik Torstholm Rasmussen was born in Copenhagen, Denmark, on February 18, 1965 . In 1974 he moved to Buckinghamshire, England, and in 1981 emmigrated to the United States of America with his family. In the United States, the author attended Delaware Valley College of Science and Agriculture (Doylestown, PA), graduating in May, 1986, with a Bachelor of Science degree in chemistry. He entered the graduate program at Virginia Polytechnic Institute and State University in September, 1986, and received his Doctor of Philosophy degree in chemistry in October, 1990. During college and graduate school, he held summer internships at Merck Sharp and Dohme, Colgate-Palmolive, and Johnson Wax. Following graduation he will be employed by the National Institute of Standards and Technology (Gaithersburg, MD) as a postdoctoral fellow.

Henrik Rasmussen